DEVELOPMENT OF GPS AND OBSTACLE AVOIDANCE BASED LOW ALTITUDE NAVIGATION SYSTEM FOR A POWERED PARACHUTE AERIAL VEHICLE

By
VINDHYA DEVALLA
COLLEGE OF ENGINEERING STUDIES
DEPARTMENT OF AEROSPACE ENGINEERING

Submitted

IN PARTIAL FULFILLMENT OF THE REQUIREMENT OF THE DEGREE OF DOCTOR OF PHILOSOPHY

To

UNIVERSITY OF PETROLEUM AND ENERGY STUDIES
Dehradun
June, 2015

UNIVERSITY OF PETROLEUM
AND ENERGY STUDIES
UPES
www.upes.ac.in
THE NATION BUILDERS UNIVERSITY

THESIS COMPLETION CERTIFICATE

This is to certify that the thesis on **"Development of GPS and Obstacle Avoidance Based Low Altitude Navigation System for A Powered Parachute Aerial Vehicle"** by Vindhya Devalla in Partial completion of the requirements for the award of the Degree of Doctor of Philosophy is an original work carried out by her under my supervision and guidance.

It is certified that the work has not been submitted anywhere else for the award of any other diploma or degree of this or any other University.

12/06/2015

Dr. Om Prakash
Thesis Supervisor
Associate Professor & Head
Department of Aerospace Engineering (COES)
University of Petroleum and Energy Studies, Dehradun

ACKNOWLEDGEMENTS

I, first and foremost, would like to express my deepest gratitude to Dr. Om Prakash, my supervisor, for encouraging me to take up a project on Parafoil UAVs as the topic of research. Dr. Om Prakash has been a source of inspiration and a monument of motivation to me throughout this work. Without him, this work would never have been completed. I am thankful to Dr Kamal Bansal, Dean, College of Engineering Studies for the motivational and administrative support throughout.

My heartfelt thanks to Dr. Parag Diwan, Chancellor Dr. S J Chopra, Vice Chancellor Dr. Shrihari, President Prof. Utpal Ghosh for motivating me with seed fund, space and environment in this serene campus of University of Petroleum and Energy Studies, Dehradun, in India to carry out this work. I would also like to thank Science and Engineering Research Board - Department of Science and Technology (DST - SERB) for granting me initial fund for understanding the feasibility of the project. I would like to mention a special thanks to team R&D, UPES for providing constant guidance and support in getting the sponsored project from DST SERB.

I should mention my gratitude to Mr. Amit Kumar Mondal, who is there with me throughout the journey especially when I had tough times, measuring it by word of thanks is not adequate/appropriate. Also, I thank Dr. Manish Prateek, Mr. A J Arun Jeya Prakash and Mr. Karthik Reddy for supporting me during the last leg of this work. I am thankful to each and every faculty colleague of Aerospace Engineering department for their support and cooperation.

Finally, I must express my very profound gratitude to my parents and my sister for providing me with unfailing support and continuous encouragement throughout my years of study and through the process of researching and writing this thesis. This accomplishment would not have been possible without them. Thank you.

Vindhya Devalla
University of Petroleum and Energy Studies
June 2015

DEDICATED TO

MY PARENTS

& ALMIGHTY

DECLARATION

I do hereby declare that this submission is my own work and that, to the best of my knowledge and belief, it contains no material previously published or written by another person nor material which has been accepted for the award of any other degree or diploma of the university or other institute of higher learning, except where due acknowledgment has been made in the text.

Vindhya Devalla

Doctoral Research Fellow, Department of Aerospace Engineering

University of Petroleum and Energy Studies

Dehradun-248007

CONTENTS

Contents	Page No.

EXECUTIVE SUMMARY

Unmanned Aerial Vehicle is an aircraft with no on board pilot. UAVs can be controlled with remote or autonomously. They are used for number of different missions depending upon the application. There are different types of UAVs available like fixed wing, multi copter and Parafoil UAV. Certain characteristics like low speed, high payload carrying capability, etc. makes Parafoil UAV a versatile platform for various applications.

Parafoil is entirely made of fabric and is a non- rigid wing. A Parafoil get inflated just like a parachute when dropped from a height. The wing has a low aspect ratio with an elliptical or a rectangular plan form when inflated. To act as an airfoil, the upper membrane and the lower membrane are sewn together with a gap between both. The leading edge is kept open so as to allow the air inside the cells creating air pressure, which maintains the shape of the Parafoil as a wing. The vents in the ribs allow the air pass from one cell to another which helps in maintaining uniform air pressure in the wing. To avoid the air loss the fabric is made of non-porous material. The suspension lines are used to connect the Parafoil to the payload. Addition of a Propulsion unit on the payload makes the Paraglider a Parafoil UAV. This Vehicle has a “Fly-bar” to which the Parafoil is connected and a motor on the Payload.

Directional control is achieved by pulling the fly-bar either side, which changes the direction of the lift making the aircraft turn. The Powered Parafoil has a tendency to fly at constant airspeed. These systems have pendulum stability and oscillations, because of the mass of the airframe suspended significantly below the canopy, which allows the system to have a yaw motion rather than roll motion. Lateral control is obtained by the propulsion system which is attached to

the payload. The thrust of the propulsion system is controlled to maintain the altitude, take-off or landing.

Modeling of Parafoil UAV has been studied in detail in this work. A new direction control scheme was developed using a 9 DOF model with a single servo which is connected to “fly-bar” and tilts the Parafoil left and right. Complete Parafoil payload system performance has been studied by open loop simulation and open loop flight test results. These results are then used to develop a closed loop control system for autonomous way point navigation. The Parafoil UAV has inherent pendulum stability due to which simple controller schemes were designed. A Single servo is used for direction control and a Single BLDC motor is used for takeoff, landing and level flight, due to which, the control system design became simpler.

This work focusses on developing a GPS and Obstacle avoidance based low altitude navigation system for a Parafoil UAV. The vehicle would follow a planned trajectory for following the path effectively. This work presents guidance, navigation and control of a Parafoil UAV. Lateral heading and longitudinal altitude hold controller has been designed. A path planning algorithm is also designed for following a trajectory using way point navigation. The lateral heading and longitudinal altitude hold controllers have been verified by the actual flight parameters.

Parafoil UAV being a low speed UAV can be widely used for remote sensing, aerial surveillance and precision delivery applications. The Aerial photographs taken using this system would be precise and very clear. Such a system with autonomous navigation capability can be used for low altitude remote sensing especially oil and gas pipeline monitoring. A benefit of the Parafoil UAV for unmanned aircraft use is their unique ability to glide to the ground in a relatively safe manner, even if all control systems are disabled. This is particularly desirable in urban environments where a failure of any large UAV would likely result in collateral damage to structure on the ground. Powered Parafoils, on the other hand, would be unlikely to land with a vertical speed above 10mps, without making severe damage to any ground edifice or even the airframe itself is unlikely.

NOMENCLATURE

- A,B,C = apparent mass terms
- A^* = canopy aspect ratio
- b = canopy span
- d = diameter of a suspension line
- C_D = drag coefficient
- C_L = lift coefficient
- C_Y = side force coefficient
- C_{lp},C_{lr} = rolling moment damping coefficient
- $C_{mc/4}$ = pitching moment coefficient at quarter chord
- C_{mq} = pitching moment damping coefficient
- C_{nr},C_{np} = yawing moment damping coefficients
- c = canopy chord length
- F = force
- g = acceleration due to gravity
- h,h* = canopy span wise camber height, and h/c ratio, respectively
- I = inertia matrix
- I_A,I_B,I_C = apparent inertia terms
- M = mass matrix
- L = length of control line pulled
- m = mass
- q(bar) = dynamic pressure
- p,q,r = roll, pitch and yaw rates
- R = link length

LIST OF FIGURES

LIST OF TABLES

CHAPTER 1

INTRODUCTION

Unmanned Aerial Vehicles commonly known as drones are aircrafts without human pilot on-board. In past the high resolution remote sensing images were taken by manned airplanes or helicopters. But there are some disadvantages, e.g. under special weather conditions (e.g. low clouds) or when airstrip is blocked, the airplanes cannot be used. Technological advances have allowed engineers to develop unmanned aerial vehicles which have an increasing demand in military, remote sensing, surveillance, etc.

1.1 UNMANNED SYSTEMS

The U.S Department of Defense (DOD) defines an unmanned aircraft as follows [1]:

"A powered vehicle that does not carry a human operator, can be operated remotely or autonomously, can be expendable or recoverable and can carry a lethal or non-lethal payload. Ballistic or semi ballistic vehicle, cruise missiles, artillery projectiles, torpedoes, mines, satellites and unattended sensors are not considered unmanned vehicles. Unmanned vehicles are the primary component of unmanned system."

This definition covers multiple forms of unmanned systems including Unmanned Air Systems (UASs), unmanned ground vehicles (UGV), unmanned surface vehicles (USVs), and unmanned underwater vehicles (UUVs).

The definition excludes sensors with no form of propulsion. This exclusion is likely intended to eliminate son buoys and unattended ground sensors (UGS).

Non-powered aircraft, known as gliders, can perform many useful missions and are generally considered to be UAS. They have flight controls which are capable of navigation, and carry payloads. One could argue that a glider's propulsion is the conversion of potential to kinetic energy [2]. UASs have taken many names and forms over their long history can be called in many ways:

- Remotely piloted vehicle
- Unmanned aerial vehicle
- Uninhabited combat aerial vehicle
- Organic aerial vehicle
- Aerial robotics
- Micro aerial vehicle

General attributes of unmanned aircraft are following:

- Smaller size potential
- High versatility
- Greater performance than manned aircraft
- Uninhabited combat aircraft system
- Remotely piloted aircraft
- Remotely piloted helicopter

1.2 TYPES OF UNMANNED AERIAL VEHICLES

A Short Overview of different types of Unmanned Aerial vehicles (UAV) is given. The first remote controlled UAV was developed for military use called drones. UAV generally consist two systems namely, Unmanned Aircraft and Control Station. There is a wide range of UAVs available from small vehicles with less than 0.8kg (e.g. Sensefly) to very large vehicles with the flight weight more than 900kg (e.g. B-Hunter). The different types of UAVs can be classified as: multi-rotor, fixed wing and Parafoil UAV [3].the classification can be done on weight, height and construction

1.2.1 Multi-copter types

Helicopters or multiple copter type UAVs come into this category, which have vertical rotors without any airstrip. The lift is created actively by the whole body which consumes lot of battery having limited flight time and height [4]. Payload constraints are most common in these UAVS.

Figure 1.1. A Multi- Copter UAV [2]

The characteristics of these systems are given below:

- Vertical takeoff and landing (VTOL).
- Equipped with vertical rotor, No runway is needed.
- No dynamic lift is created by wings, the whole lift has to be created actively, which consumes much battery, therefore the flight time and height is limited.
- Heavy payload cannot be carried.
- Need advanced gyro compass and sensors which assist the flight.

1.2.2 Fixed wing types

Figure 1.2. A Fixed Wing UAV [2]

These aircrafts are similar to the traditional aircraft design. Most of the lift is created by the wings leading to long flight time [5]. These UAVs can carry good payload compared to multi copter types

The characteristics of these systems are given below:

- Design similar to classical aircrafts
- Runway is needed for landing
- Dynamic lift created by wing, therefore, long flight time
- Can carry higher payload
- High speed
- Can operate under strong wing conditions
- Advanced autopilots are needed
- High landing speed, therefore slight mistake during landing cause severe damage
- Higher expertise needed to operate compared to multi copter

1.2.3 Parafoil UAV

These type of UAVs are very robust and easy to fly due to the design as Parafoil as the wing and very safe in case of system crash. Due to the low speed, the images taken using this UAV are very clear [6].

Figure 1.3. A Powered Parafoil UAV [2]

The characteristics of these systems are given below:

- Can carry high payloads
- Long flight time
- Low flight speed
- Very robust
- Easy to fly
- Very safe in the case of system failure
- Cannot be operated in rainy conditions sensitive to wind condition

1.3 PARAFOIL UNMANNED AERIAL VEHICLE

The Powered Parafoil is an aircraft which derives lift from a ram-air inflated canopy, under which the fuselage is suspended. The Parafoil is inflated by the dynamic pressure of the air flowing into the canopy which has a cross section in the shape of an airfoil. This process helps the vehicle to create lift. This feature differentiates these Parafoils from conventional Parafoils which are used to simply create drag. Powered Parafoils have been utilized mostly for recreation activities, but some of the special properties make them a suitable platform for unmanned aerial vehicle (UAV) and remote sensing applications. Powered Parafoils have existed since 1981 [7]. The concept was introduced at the Sun & Fun aviation event by the ParaPlane Corporation as seen in figure 1.4.

Figure 1.4. ParaPlane Corporation first model [7]

They represent aircraft that are somewhere between balloons and fixed wing aircraft when control is considered as shown in figure 1.5. The direction of a powered Parafoil is controlled by the pilot rotating on either a left or right steering bar that pulls down a line attached to the trailing edge of the canopy. The increased drag causes the aircraft to turn. The control lines connected to the canopy are pulled down together, which will drop both trailing ends of the canopy at a time and cause a sudden increase in lift.

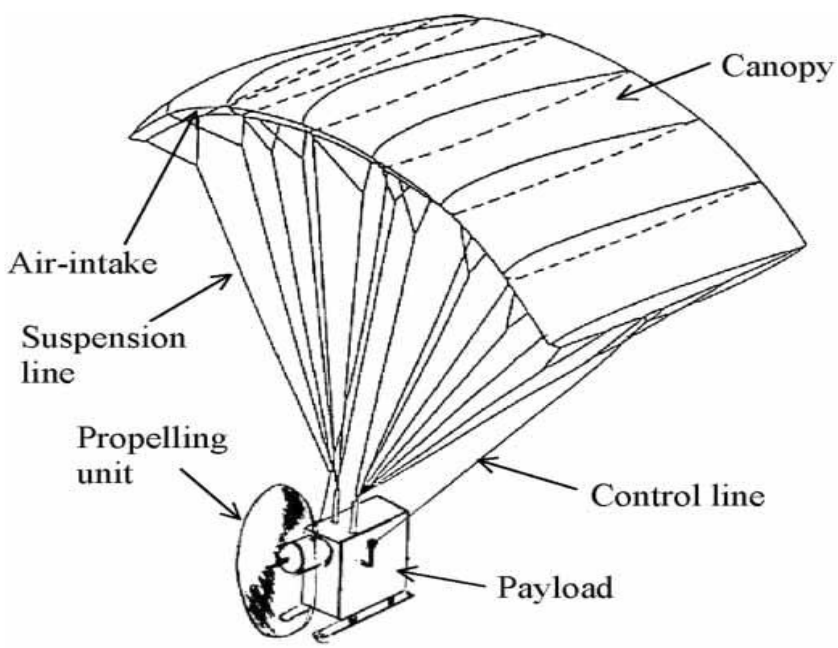

Figure 1.5. Control Surfaces of Powered Parafoil UAV [8]

This maneuver is done during landing, when the pilot wants a smooth touchdown. A different steering configuration which is used on some small-scale aircraft is known as a “fly-bar.” In this design, the Parafoil is connected to the ends of a bar and the bar is tilted, tilting the Parafoil, as seen in figure 1.6.

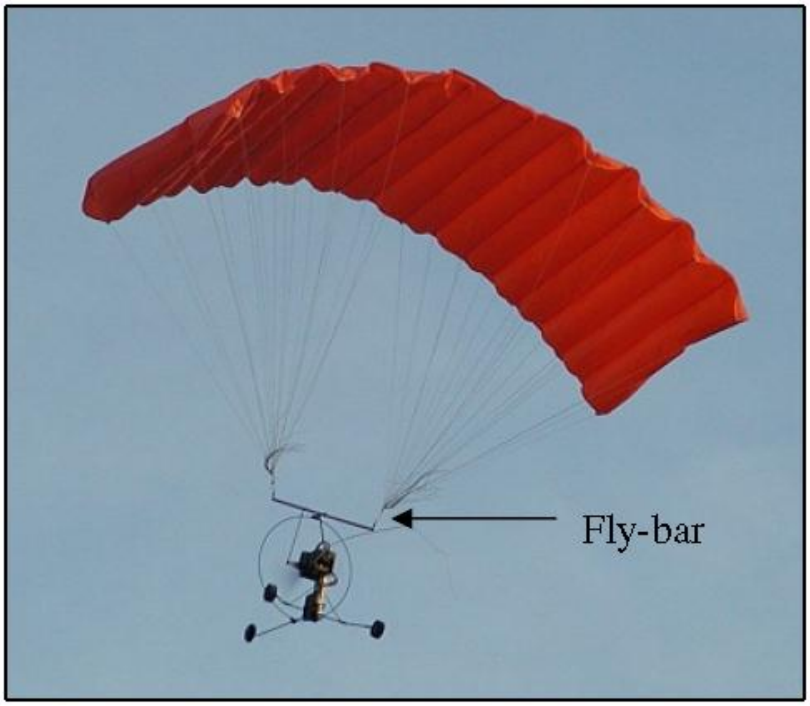

Figure 1.6. Alternate steering in Powered Parafoil [8]

This bar can be tilted either side of the aircraft, changing the direction of the lift and making the aircraft turn. Aircraft using each of the two steering systems behave identically in response to thrust inputs. Powered Parafoils have the tendency to fly at a constant airspeed [8]. A powered Parafoils will climb, cruise and descend somewhere around the speed of 26 – 32 MPH. These Aircrafts have pendulum stability and oscillations as shown in the figure 1.7, because of the mass of the airframe suspended significantly below the canopy. The applications powered Parafoil in surveillance and imaging has benefit of a low-speed, low-cost, and stable platform which is capable of lifting payloads of up to 600 lbs. These platforms are very stable and must only get disturbed with gusts that would change the flight trajectory.

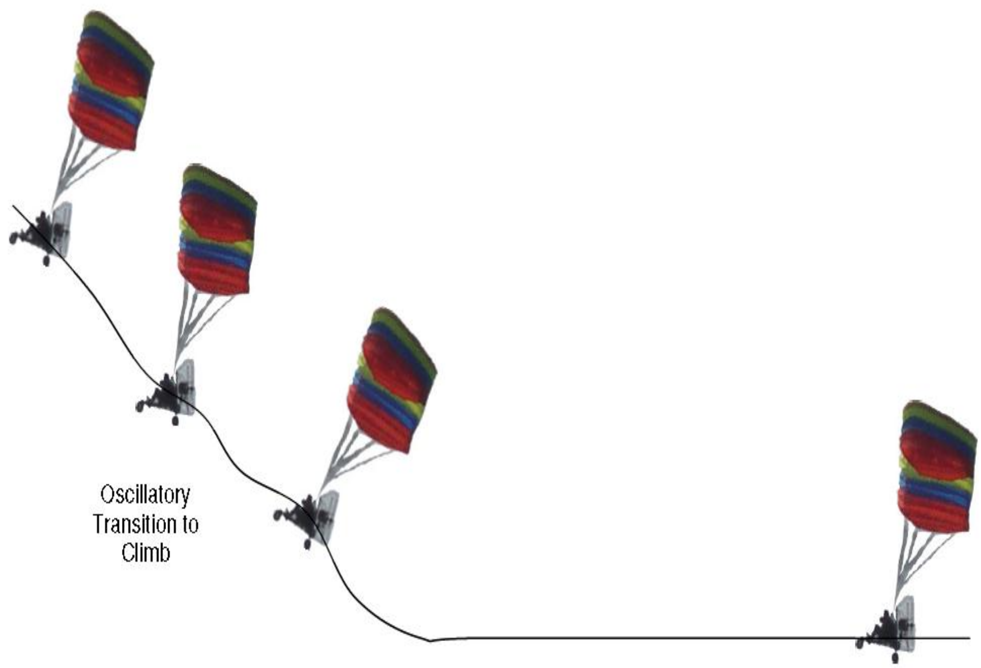

Figure 1.7. Oscillations in Powered Parafoil while takeoff [8]

The addition of a propelling unit makes the paraglider an Unmanned Aerial Vehicle (UAV). A Powered Parafoil consists of a Parafoil and a payload equipped with an engine or motor and a propeller. From the view of dynamics and control, the configuration provides the following unique characteristics, as compared to traditional wing aircraft [8].

- The separation between the centers of gravity of the canopy and the payload produces a swinging motion.
- Changing the thrust induces a considerable pitching motion.
- Relative pitching and yawing motions exists between the canopy and the payload.
- Canopy is a tailless flying wing.

- Directional control is mainly achieved through yawing motion, rather than through rolling motion.
- The apparent mass of the canopy must be taken into account, as in case of an airship.

1.4 TERMS USED IN POWERED PARAFOIL AERIAL VEHICLE

1.4.1 Airfoil

The Surface of the Parafoil which is used to produce lift, typically, the canopy itself is called as airfoil [9].

1.4.2 Camber

The curvature of the wing is called as camber. A Parafoil has two cambers namely upper camber and lower camber [9].

1.4.3 Leading edge

Leading edge refers to the forward edge of the Parafoil [9].

1.4.4 Trailing edge

Trailing edge refers to the rear edge of the Parafoil [9].

1.4.5 Chord line

Chord line is the imaginary line joining trailing edge and the leading edge [9].

1.4.6 Relative wind

Relative wind is the direction of airflow with respect to the wing, which is generally opposite and parallel to the flight path of the Parafoil [9].

1.4.7 Angle of attack

Angle between the relative wind and the chord line is known as Angle of attack [9].

1.4.8 Longitudinal axis

Longitudinal Axis is the vertical axis of a powered Parafoil Aerial vehicle; it is also called as roll axis [9].

1.4.9 Angle of incidence

Angle between the chord line and the longitudinal axes is known as angle of incidence [9].

1.4.10 Trim angle

Trim angle is the angle between the Chord line and the horizontal plane of the powered Parafoil when the vehicle is in unpowered condition [9].

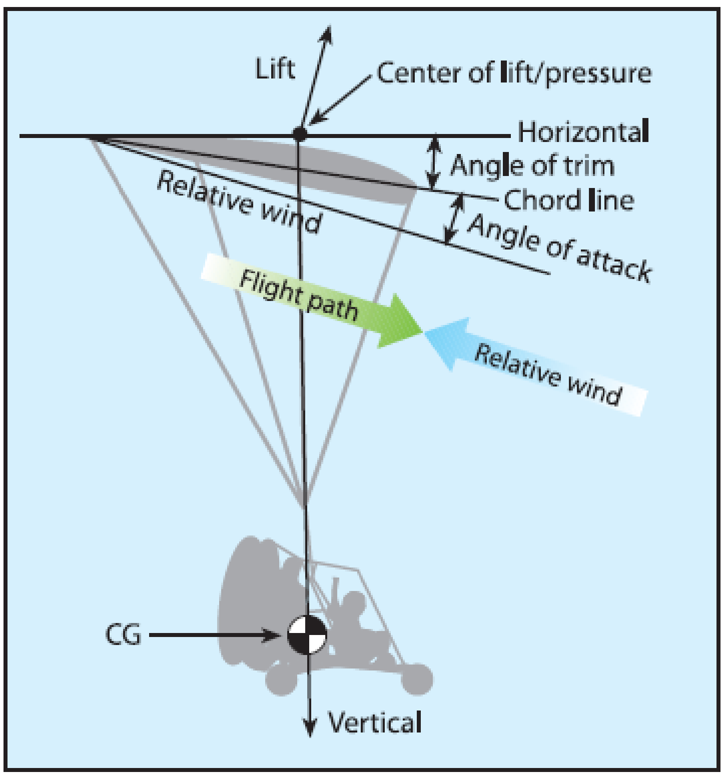

Figure 1.8. Angle of Attack [9]

1.4.11 Pitch angle

Pitch angle is the angle between wing chord to the horizontal plane [9].

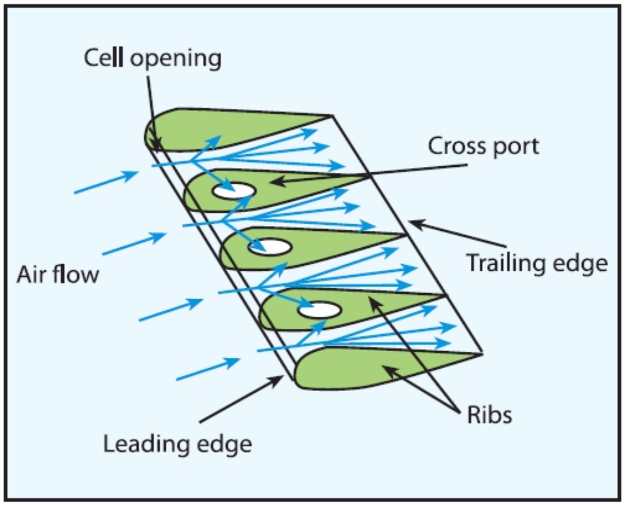

Figure 1.9. Air Flow into the Wing [9]

1.4.12 Aspect ratio

Ratio of wing span by average chord line gives the aspect ratio. More the aspect ratio more will be lift with less induced drag [9].

1.4.13 Wing loading

The total weight the wing can support is known as Wing loading, this can be found by dividing the total weight of the aircraft by the total area of the wing [9].

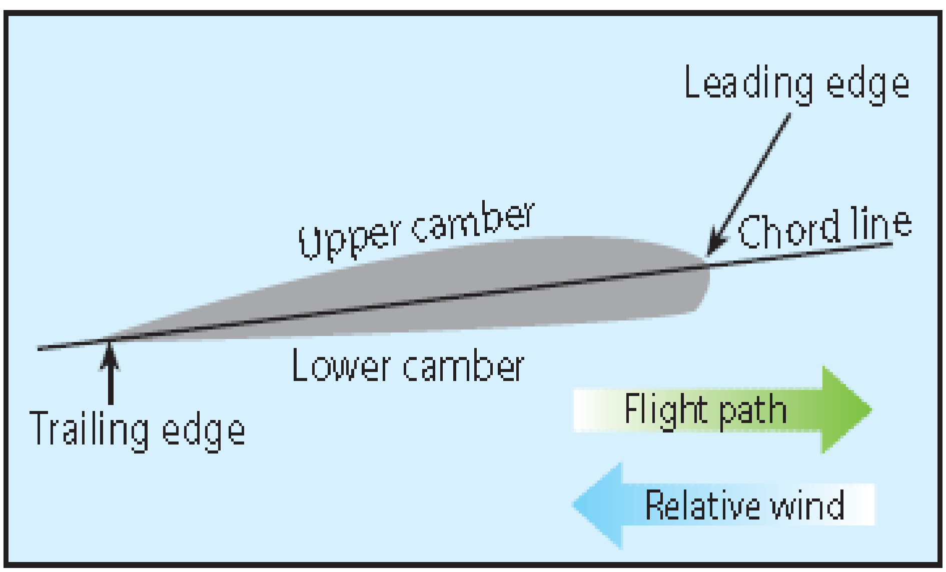

Figure 1.10. Aerodynamic terms of an Airfoil [9]

1.5 AERODYNAMICS OF A POWERED PARAFOIL AERIAL VEHICLE

1.5.1 Ram Air Parafoil

The powered Parafoil wing retains the rigid shape during the flight because of air pressure. These aircrafts are no different from the conventional aircrafts as both of them have top skin, bottom skin, leading edge and trailing edge. Also they have upper surface curved and lower comparatively flatter. The only difference is fabric and opening in the leading edge. The fabric prevents the air from escaping as it is made of zero porosity material. Once the canopy is filled with air, excess outside air cannot enter the pressurized wing. This results in forming aerodynamically correct and stiff wing

1.5.2 Lift, Weight, Thrust, Drag

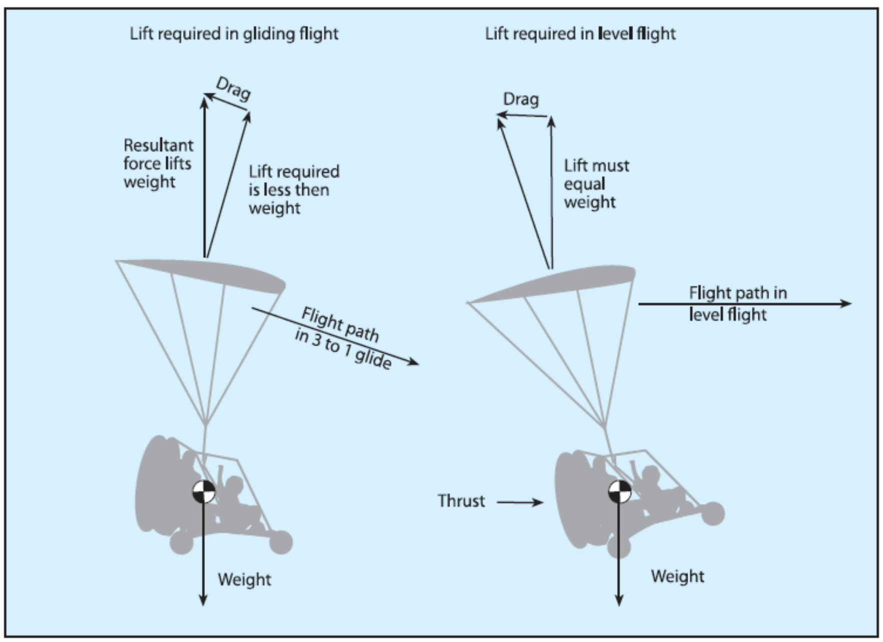

Figure 1.12. Different forces for gliding and level flight [9]

In a level and straight flight condition lift is equal to weight and thrust is equal to drag. With the curved upper surface and flat lower surface moves through the air, it forces the air to flow around it resulting in faster air flow on the upper surface and lower airflow at the lower surface. Air travelling with high velocity creates low pressure and low velocity cerates high pressure. Therefore, high pressure at the lower surface generates lift.

Weight is produced by the gravity equal to weight of the instruments on board and the craft's weight.

When lift is greater than weight and thrust is greater than drag the vehicle will climb up. When lift is less than weight and thrust is less than drag, vehicle will descend down. The thrust is produced by the propulsion system attached to the vehicle. Drag is produced by the resistance due to the chute, lines, vehicle and the steering bar.

1.5.3 Throttle Control

Throttle controls the climb and descend of the vehicle by changing the angle of attack of the wind. The rate of climb is controlled by the throttle setting.

1.5.4 Pendulum Stability

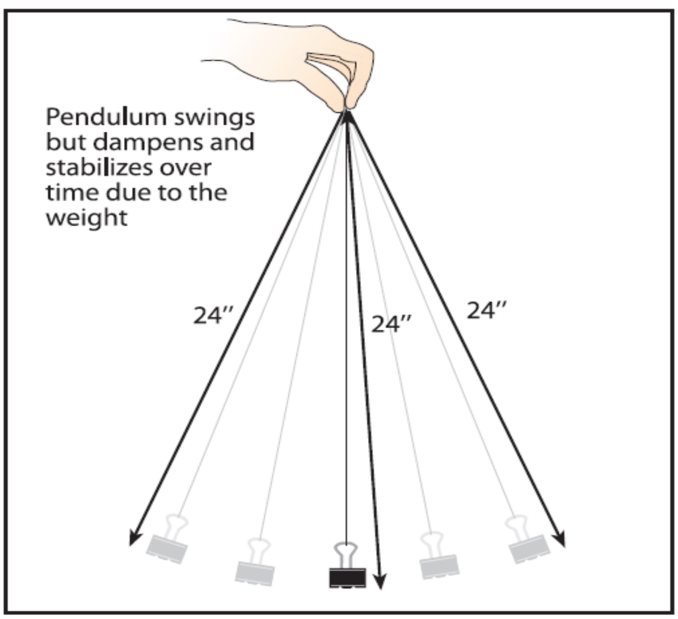

Figure 1.13. Pendulum Effect [9]

A pendulum consists of a suspension point with the weight attached to other end. In case of a powered Parafoil vehicle the canopy acts as a suspension point and the vehicle act as the weight. When the weight is moved to and fro it tries to swing to get back to its original stable point. An object is said to be stable when it get backs to its original point after subjected to disturbances. When the controls are released the stable aircraft tries to return back to the level flight. Likewise, whenever a wind gust moves the powered Parafoil due to payload weight it tries to get back to the original position which can be called as natural stability.

1.5.5 Effect of Wind Gusts on Pendulum Stability

A side gust will move the canopy to side first and vehicle will move back to the center due to pendulum stability.

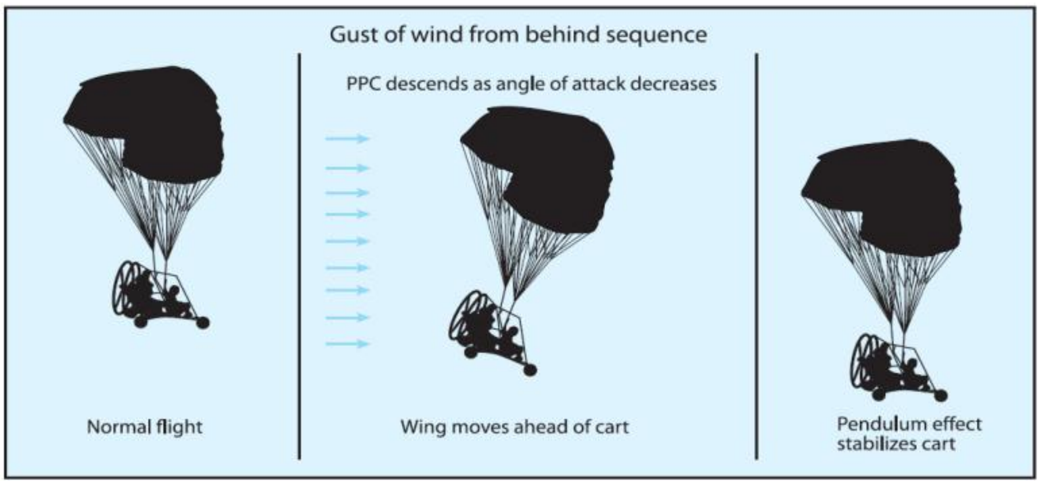

Figure 1.14. Powered Parafoil Stability after backward Wind Gust [9]

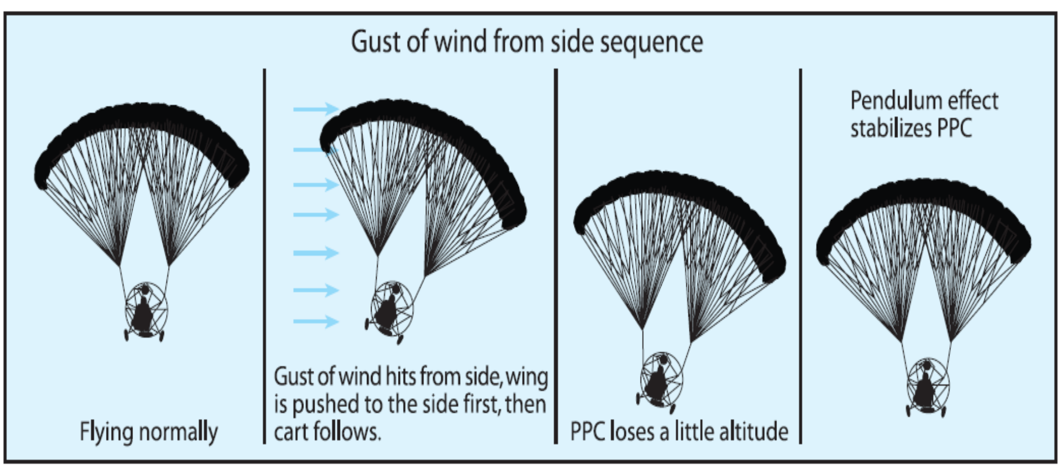

Figure 1.14. Powered Parafoil Stability after Side Wind Gust [9]

A gust of wing will move the canopy backward resulting in lift and after some time the vehicle will come back to the center resulting in reduced angle of attack, which tends to descend the vehicle down again the vehicle, will try to relocate to center of the suspension resulting in level flight.

A gust of wing from backside tries to descend the vehicle, but due to the pendulum effect the when vehicle tries to come back to the stable state angle of attack is increased resulting in lift and vehicle centers itself again and level flight is continued.

1.5.6 Axes of movement: Yaw Pitch and Roll

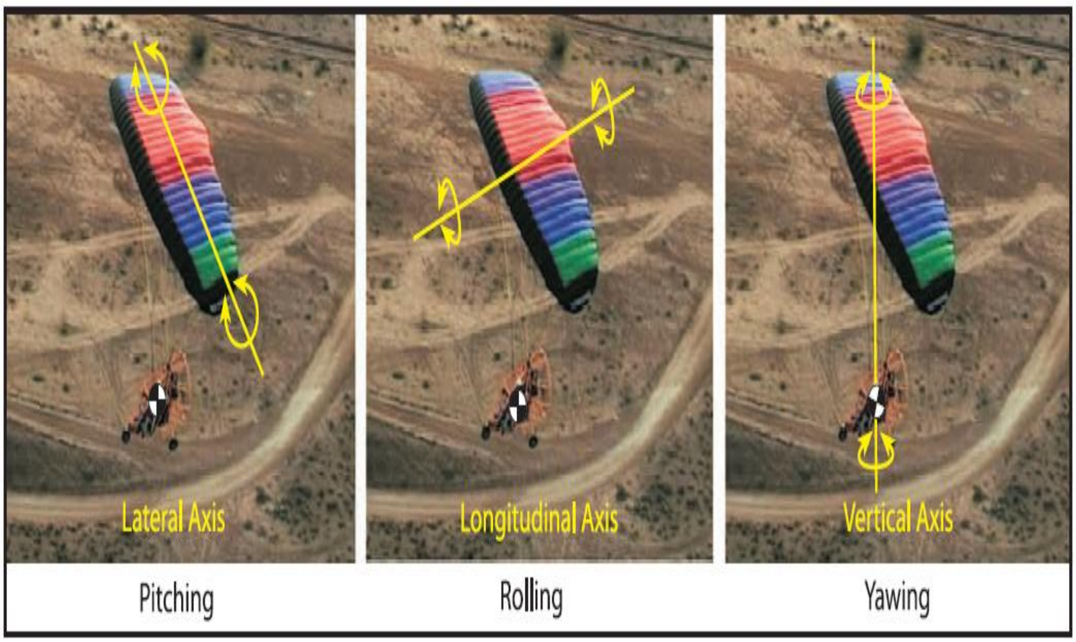

Figure 1.15. Powered Parafoil Axes of Rotation [9]

The Pendulum effect control the longitudinal and lateral or pitch and roll axes, the vehicle must be only programmed to control vertical or yaw axes. To turn the steer bar is pulled down to one of the side. The pitch movement is automatically controlled by the wind gusts. The throttle control can also control pitch moments for climb and descent. This simple control makes the Parafoil easy to fly.

1.5.7 Steering Controls

The steering is accomplished by pulling the control string using the steering bar connected to a servo motor.

Whenever the servomotor is controlled by the pilot one side of the steering bar goes down resulting in pulling the side of the canopy connected to it.

Left String	Right String	Result
Pulled down	No Action	Left Turn
No Action	Pulled down	Right Turn
Pulled Down (less angle)	Pulled Down (less angle)	Lift
Pulled down (high angle)	Pulled Down (high angle)	Descend

Table 1.1. Asymmetric brake deflection

The more the trailing edge deflected the faster will be the turn and shorter the radius more altitude is lost. As the drag increases there is a loss of lift, which can be minimized by increasing the throttle.

1.5.8 The effects of wind direction

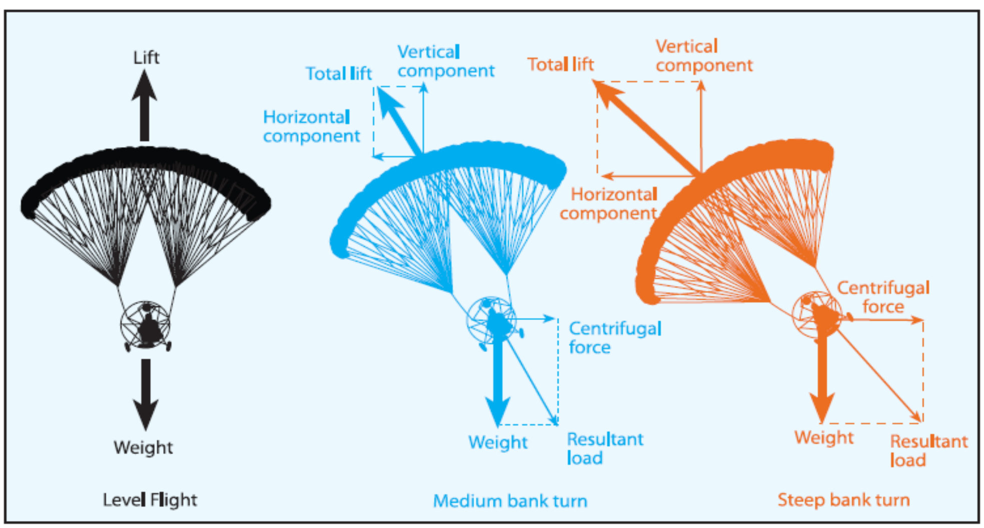

Figure 1.16. Powered Parafoil Loads and Turning Forces [9]

The canopy has to be faced towards the wing when on ground called weather vaning which helps in easy takeoff. Ground steering is accomplished by pulling the control strings either left or right. The difference between wind direction and takeoff roll direction will not allow the canopy to take off properly. Therefore the takeoff and landing must be done directly into the wind.

1.6 THESIS OUTLINE

The further organization of thesis is given in the following manner.

Chapter 2 goes with the brief description of literature review, research outcomes, objectives and methodology. The literature review covers two types of systems namely autonomous unpowered Parafoil systems and Powered Parafoil Systems.

Chapter 3 discusses in detail about the experimental design, which deals with the Basic System Performance calculations, structure of the payload, electronic components installed, detailed description of each component, hardware design. The chapter also explains the data acquisition system. The planned flight tests plan is also given in detail.

The mathematical model is discussed in chapter 4. A 9 DOF nonlinear model has been developed and explained in detail. A new control strategy is also discussed which helps in understanding the turn performance, by pulling one side of the Parafoil, this technique would help in understating the radius of turn and turn rate of the system. The tilt mechanism would help in developing the lateral heading direction control system. A thrust vector is also added to the payload. This helps us understating the amount of thrust required for level flight, take off and gliding flight. This helps in designing the longitudinal altitude hold auto pilot design.

Chapter 5 discusses the control system design for a Powered Parafoil Aerial Vehicle. Before the control system design, the vehicle was first stabilized Roll, pitch and yaw later heading controller and longitudinal altitude hold controller was designed. A waypoint algorithm was then designed and burned into the controller. Two algorithms steer to target and path restoration algorithms are discussed. The controller gains are also calculated. The flight test closed loop results are then plotted.

Chapter 6 deals with the conclusion and future scope.

CHAPTER 2

LITERATURE REVIEW AND METHODOLOGY

2.1 INTRODUCTION

This Chapter deals with the literature review and methodology used. The first half of the chapter deals with the literature review. The review is divided into two parts that is on autonomous unpowered gliding Parafoils and the Powered Parafoil Aerial vehicles. The later section gives the detailed description about methodology used, objectives and the research focus.

2.2 LITERATURE REVIEW

In various designs, the ballistic and Parafoil configurations are more advantageous than other configurations, as they are simple in developing. During the last decade many efforts were made to replace the uncontrolled circular Parachute with maneuverable autonomously guided Ram Air Parafoils that assure more accurate delivery of variety of payloads from high altitudes and standoff distances. Parafoils have proven good in many situations as they are stable and have slow decent rate. This can be more advantageous in surveying as they have long flight duration. Maneuvering is normally achieved by deflecting the trailing edge of the canopy asymmetrically, while some degree of glide slope control is offered with symmetric flap deflection. Dropped from sufficient altitude, a Parafoil controlled vehicle is capable of reaching a much larger area. These attributes offer a great deal of flexibility to precision delivery systems. The rear section housing the arrestor chute for the precision delivery system can be replaced with a module containing the Parafoil and necessary actuators and other components such as computer and avionics would be the same. This setup converts the unpowered Parafoil into a powered Parafoil.

2.1.1 Review on Autonomous Un-Powered Parafoil Systems

UAV systems have proven helpful in delivering payloads as well. For the precise delivery of the payload a sensor network must be established. The advantages and disadvantages of the different types of UAVs are mentioned below [10].

UAV Type	**Advantages**	**Disadvantages**
Ballistic	Simplicity Packaging	Small glide slope High impact deceleration
Parafoil	Glide slope Maneuverability Slow descent rate	Long flight duration Susceptibility to wind
Rotorcraft	Slow descent rate	Cost and complexity
Fixed Wing	Maneuverability Long range	Cost and complexity

Table 2.1. Comparison Between Different UAV Systems

These systems are in use, as the Parafoil concept is not the new one. The main functions of these systems are to deliver cargo to remote areas. The navigation subsystem of the guidance, navigation and control on onboard manages data acquisition, processes sensor data and provides guidance and control subsystems with information about Parafoil states. Using this information along with local wind profiles, the guidance subsystem plans the mission and generates the feasible trajectory to the desired landing point. Finally it is responsibility of the control system to track this trajectory using the information provided by the navigation subsystem and on board actuators.

Several approaches are currently being used by different developers for the precise landing.

- Affordable Guided Airdrop System (AGAS) – Capewell Components Co., LLC

- Controlled Aerial Delivery System (CADS) – Cobham PLC
- Dragon Train – Aerobotics, LLC
- FireFly – Airborne Systems North America
- Improved Container Delivery System (ICDS) – U.S. Army NSDREC & U.S. Air Force
- Low Cost Aerial Delivery System (LCADS) – U.S. Army PM-FSS
- MegaFly – Airborne Systems North America
- MicroFly – Airborne Systems North America
- Mosquito – Stara Technologies, Inc.
- Onyx 300 – Atair Aerospace, Inc.
- Onyx Ultra Light (UL) – Atair Aerospace, Inc.
- Panther 500 – Pioneer Aerospace Corp. / Aerazur
- Panther 2K – Pioneer Aerospace Corp. / Aerazur
- 10K Screamer – Strong Enterprises
- 2K Screamer – Strong Enterprises
- Sherpa 1200/2200 – Mist Mobility Integrated Systems Technology (MMIST), Inc.
- Système de Navigation pour Charge Accompagneè (SNCA) – NAVOCAP
- SPADES 300 – Dutch Space
- SPADES 1000 – Dutch Space

The avionics, hardware and the target accuracy of the above systems is given in detail in Table 2.2

Year	**Organization**	**System**	**Avionics used**	**Result**
2008	US SOCOM [11]	Snow Flake ADS	Three accelerometers, Three rate gyroscopes, a magnetometer,	55m target accuracy

			Global Positioning System Receiver and a Barometric Altimeter, Servo Motor	
2006	German Aerospace Center [12]	ALEX	MEMS accelerometer, Laser altimeter, absolute pressure sensor, temperature sensor, force transducer, rate gyro, 3-axis magnetometer, GPS, Pitot Tube and Camcorder	200m target accuracy
2004	DLR [13]	X-38	Embedded GPS/INS system, Optical Range sensor	Cancelled
2003	Cal poly state university [14]	ATRP	Microcontroller, digital compass, and accelerometer	
1997	US Soldier Systems[15]	GPADS - Light	single board computer, Processor, GPS Receiver, Barometric Pressure Sensor, compass and	250m Accuracy

			a servo actuator	
1994	NASA [16]	Spacew edge	GPS, rate gyro, and compass and on board data recorder	1600m accuracy

Table 2.2. Various Autonomous Gliding Parafoils

The addition of a power/ propelling unit makes the paraglider an Unmanned Aerial Vehicle (UAV) which can be used for land observation, surveillance etc. such a paraglider is called powered Parafoil system (PPS) . A PPS consists of a Parafoil and a suspended payload equipped with an engine or motor and a propeller. From the view of dynamics and control, the configuration of the PPS provides the following unique characteristics, as compared to conventional wing aircraft [17].

- The separation between the centers of gravity of the canopy and the payload produces a swinging motion.
- Changing the thrust induces a considerable pitching motion.
- Relative pitching and yawing motions exists between the canopy and the payload
- Canopy is a tailless flying wing
- Directional control is mainly achieved through rolling motion, rather than through yawing motion.
- The apparent mass of the canopy must be taken into account, as in case of an airship

There are several companies working on these kinds of models using remote control such as:

- Hi-Cam aerial and video systems [18]
- Paralight aviation ltd international [19]

- Sea breeze Parafoils [20]
- Powered Parafoil and sports flying [21]
- Really cool toys

1.6.1 Review on Powered Parafoil Aerial Vehicles

In 2011, Y Ochi and M Watanabe have designed a flight controller for a powered Parafoil system. The author discussed that the powered Parafoil having canopy, payload with a propeller unit is assumed to be having 8dof.

The same year SUSI 62 [16], a Parafoil UAV has been designed for remote sensing. SUSI 62, has a payload of about 8kg and needs a runway of about 50 m. the system is controlled by a remote control.

Figure 2.2. SUSI 62

In the year ***2007***, small scale Powered Parafoil in flight has been examined [17]. The results were simulated and modeled in MATLAB.

Figure 2.3. Small Scale Powered Parafoil

In ***2005***, A Vertical Launch Parafoil Aerial Vehicle –Flying Eye was developed [18] to follow a predetermined flight path using sensors, controllers, mechanical components and software.

Figure 2.4. Flying-Eye Project

In the same year Tommy Ike Hailey described the use of powered Parafoil [19] in Archeological aerial photography. He also worked on the performance, altitude stability, in-flight stability and drift assessment of the vehicle and proved suitable for the aerial photography. The author also discussed the limitations of this vehicle. The author also suggested that Powered Parafoil can be used by agencies responsible for the management of cultural resources for planning site development, monitoring site threats and producing aerial images that will appeal to the public.

In ***2004***, A Snowgoose [20], autonomously guided powered Parafoil based UAV that was designed for US Special Operations command. It is meant to be useful for leafleting and resupply operations today. It was designed by Mist Mobility Integrated Systems Technology Inc. (MMIST) of Canada. The developed UAV is a Remote controlled vehicle. It has an unattended ground sensor (UGS). The operator piloted the Parafoil toward the target using a push button on the remote. Later the system was made autonomous by programming the target point.

Figure.2.5. Snowgoose PPC

Papers by Yamauchi and Rudakevych [21], [22] describe the “Griffon” a man portable UAV utilizing the “PackBot” ground-mobile robotics platform and Parafoil wing. The Griffon was developed under phase 1 small business innovation research (SBIR) project. It weighs 57 pounds, and does not fly autonomously; it is remotely piloted. The Parafoil used is an extremely sports traction kite with slight modification. The default angle flight was adjusted, and the kite was converted to a four control-line configuration. The chosen kite was a “Razor”, manufactured by ozone, with a wing area 11 square meters. The authors utilized a similar approach to that which will be used in present research. A simplified free-body diagram was given as the starting point for design of the powered Parafoil fuselage. Torques was summed about the center of the gravity and the motor was placed slightly below the Parafoil attachment point, yet well above the center of mass. The aircraft thrust was measured and noted against the RPM, as will be done in current investigation. The tests presented by yamauchi were stated to be for verification of adequate thrust to lift the given payload. The Griffon was flight tested in June 2003, and achieved an altitude of 200 feet and flight speed in excess of 20 miles per hour, with a 2.2 HP engine. The author did state that the Parafoil wing limits the aircraft’s usability in windy conditions.

Figure 2.6. Griffon PPC

In ***2003***, Bukeye was developed [23]. The X-38/Crew Return Vehicle, a lifting body re-entry vehicle, has been developed as a lifeboat in case of emergency at the international space station. To simulate and verify the performance of the onboard Parafoil, guidance, navigation and control system, a commercial powered Parafoil vehicle, known as Bukeye was modified to accommodate the avionics and reduced scale Parafoil for aerodynamic similarity.

Figure 2.7. Buckeye PPC

The Powered Parafoil Systems developed in the last decade are given in detail in table 2.3.

Year	**System**	**Avionics**	**Control Surfaces**	**Operation**	**Application**
2011	SUSI 62	Sensors, Engine, Servo Motor, Gyroscope	Two Servos	Remote Control	Remote Sensing

2005	Flying Eye	Sensors, controllers, mechanical components	Two servos	Remote Control	Lab Instrument
2005	Powered Parafoil	Sensors, Engine, Servo Motor, Gyroscope	Two servos	Remote Control	Archeological Surveillance
2004	Snow Goose	Gyro, Motor, Servo Motor, Unattended Ground Sensors	Two Servos	Remote Control	US Special Operations
2004	Griffon Packbot	Sensors, Engine, Servo Motor, Gyroscope	Two Servos	Remote Control	Surveillance

Table 2.3. Powered Parafoil Systems

1.7 MOTIVATION AND NEED FOR RESEARCH

Parafoil Aerial Vehicle (PAV) can be used for applications that require accurate vertical positioning which include crop dusting, high resolution and close range imaging, proximity sensing of targets and detection of substances and organisms that are altitude specific. The below table gives the comparative study on various UAVs, and their features motivated to select PAV as a subject of research. The considered model will be controlled using a single servo and the mathematical modeling will also be done for single servo.

Factor	**Multi Copter**	**Fixed wing**	**PAV**	**Selection**
Design /Fabrication Complexity	Difficult	Difficult	Easy	PAV
Aerodynamic Efficiency	Less	More	More	Multi copter
Flight time	Less	More	More	PAV
Control over Handling	Difficult	Difficult	Easy	PAV
Payload Capacity	Fixed	Fixed	Variable	PAV
Autopilot	Advanced	Advanced	Low end	PAV
Wind effect	Less effect	Less effect	More effect	Fixed wing
Transportation of Vehicle	Easy	Difficult	Easy	PAV
Crash Impact	More damage	More damage	Less damage	PAV
Runway	Not required	Required	Less Required	Multi copter
Flight Speed	Low speed	High speed	Low speed	Depends on the application
Flight Stability	Less stable	Stable	Highly stable	PAV

Table 2.4: Comparative Study on Different Technologies

Keeping all the factors in view a Parafoil/Parachute aerial vehicle can be considered to be the most stable Aerial vehicle. A benefit of the powered parachute for unmanned aircraft use is their unique ability to glide to the ground in a relatively safe manner, even if all control systems are disabled. This is particularly desirable in urban environments where a failure of any large UAV would likely result in collateral damage to structure on the ground. Powered parachutes, on the other hand, would be unlikely to land with a vertical speed above 10mph, making severe damage to any ground edifice or even the airframe itself is unlikely.

1.8 LITERATURE RESEARCH OUTCOMES

- Various unmanned aerial systems have been analyzed and it has been observed that the Powered Parafoils have many unique capabilities such as high payload carrying capability, low speed, stabilized flight etc. that makes powered Parafoils advantageous compared to that of conventional UAS systems.
- The literature of the powered Parafoils have been studied and determined that, due to the unique structure, the features can be described only by nonlinear model for Parafoil payload coupled system.
- All the developed powered Parafoil system, use asymmetric brake deflection mechanism on either side through two servo motors to achieve yaw control.
- Measurement systems have been determined which can be used to achieve guidance and navigation control.
- The separation between the centers of gravity of the canopy and the payload produces a swinging motion.
- Changing the thrust induces a considerable pitching motion.
- Relative pitching and yawing motions exists between the canopy and the payload.
- Directional control is mainly achieved through yawing motion, apart from rolling motion.

1.9 RESEARCH FOCUS

- A 9 DOF model developed for unpowered Parafoil model has been modified by adding a thrust force vector to the payload to simulate model dynamics under thrust condition.
- The thrust provided will be utilized to increase, decrease and hold the altitude of the vehicle.
- A single servo will be used to control the direction by tilting down the Parafoil to left and right.
- A stability circuit will be developed that will reduce down the oscillations on the vehicle
- Guidance and navigation will be incorporated using way-point navigation technique which loiter and navigate the vehicle
- The mission starts by taking the vehicle to certain height and engaging the autonomous guidance and navigation mode.
- A hardware model will be developed that can be used for various applications.

1.10 OBJECTIVES

The project aims at making an Autonomous Flying Para Drone moving on pre-defined path with obstacle avoidance and path restoration technique.

- To develop a Servo motor based direction control System
- To develop a GPS Based navigation system
- To develop a Ultrasonic sensor based obstacle avoidance system
- Interfacing all the above control systems

1.11 METHODOLOGY

Task	**Testing Parameters**	**Output**
Selection of UAV	Easy to glide Good Endurance	Parafoil Aerial Vehicle

	Good Range Moderate Speed Variable payload	
Design	Endurance Range Strength Para foil size Payload calculation	Size of the Parafoil according to the weight of the Parafoil
Selection of Material (As per the comparison in next table)	Less weight More strength Easy to mold High impact strength Resistance to effect of temperature variation Corrosion resistant Cost	Aluminum Alloys, CFRP rods
Fabrication	Structural analysis Fabrication of sub - assemblies Assembly	Structure of the UAV
Power Source Selection	Variable transmission Power output Light Weight High Torque Less Fuel Consumption	2 stroke CI or SI IC Engine Li Po Battery
Modeling	3 dof 6 dof 9 dof	Controlling parameters

Control system design	Simulink model	Controlled flight parameters
Servo motor control	Decide the angle Interfacing Servo with microcontroller	Servo motor based direction changing ground robot
GPS	Study of GPS Interfacing GPS with Microcontroller Extracting the values using microcontroller	GPS navigation based ground robot
IMU	Study of IMU Interfacing IMU with Microcontroller Extracting the values using microcontroller	IMU value based direction control ground robot
Ultra Sonic Sensor	Study of ultrasonic Sensor Interfacing Ultrasonic sensor with Microcontroller Extracting the values using microcontroller	Ultrasonic sensor based obstacle avoidance ground robot
Hardware and Software Interfacing	Interfacing GPS and IMU with controller	Navigation Control
	Interfacing Ultrasonic sensors and motor controller	Obstacle avoidance and Direction control
	Interfacing controller	Complete UAV

	and Structure	
Algorithm Design	Main control loop	Left and right steering using IMU values
	Steer to target	Steering with IMU and GPS values
	Landing at the target	Using IMU and GPS and Servo
	Obstacle avoidance	Ultrasonic sensor, IMU and GPS
	Full break algorithm	Stop the Parafoil
Testing at different climatic conditions	Remote Controlled UAV	Semi-Autonomous
	Autonomous	Autonomous

Table 2.5. Methodology developed for proposed PAV

Keeping all the factors in view a Parafoil aerial vehicle is selected. Applications that require accurate vertical positioning include crop dusting, high resolution and close range imaging, proximity sensing of targets and detection of substances and organisms that are altitude specific. A benefit of the powered Parafoil for unmanned aircraft use is their unique ability to glide to the ground in a relatively safe manner, even if all control systems are disabled. This is particularly desirable in urban environments where a failure of any large UAV would likely result in collateral damage to structure on the ground. Powered Parafoils, on the other hand, would be unlikely to land with a vertical speed above 10mph, making severe damage to any ground edifice or even the airframe itself is unlikely.

CHAPTER 3
EXPERIMENT DESIGN

3.1 UNMANNED POWERED PARAFOIL AERIAL VEHICLE CONCEPT

The UPPAV is a concept which consists of a Parafoil and a powered payload. The Parafoil is connected to the payload at two joints using flexible lines. The vehicle is fully stable and requires only two controls, one for direction control and one for take-off and landing. The vehicle has numerous advantages and applications ranging from aerial delivery to remote sensing. The vehicle was developed for remote sensing purpose. The vehicle is a small unmanned powered Parafoil vehicle with payload carrying capability of 2.5 – 4.5 Kg including the electronics, battery and sensors. The vehicle was developed with only two controls. The chapter discusses in detail about the payload concept which includes various parts of the payload, Parafoil Performance which includes the Parafoil size with respect to the payload calculation and the sensors and control unit used in detail. The above mentioned systems are prime requirements to full fill the autonomous remote sensing task.

3.2 PAYLOAD COMPONENTS

The payload generally consists of the following parts

- Nose
- Main frame
- Propeller guard
- Back landing gears
- Front landing gear

- Control rod
- Sensors and control Unit

The above mentioned parts are discussed in detail in this chapter. The sensors and control unit is placed on the payload.

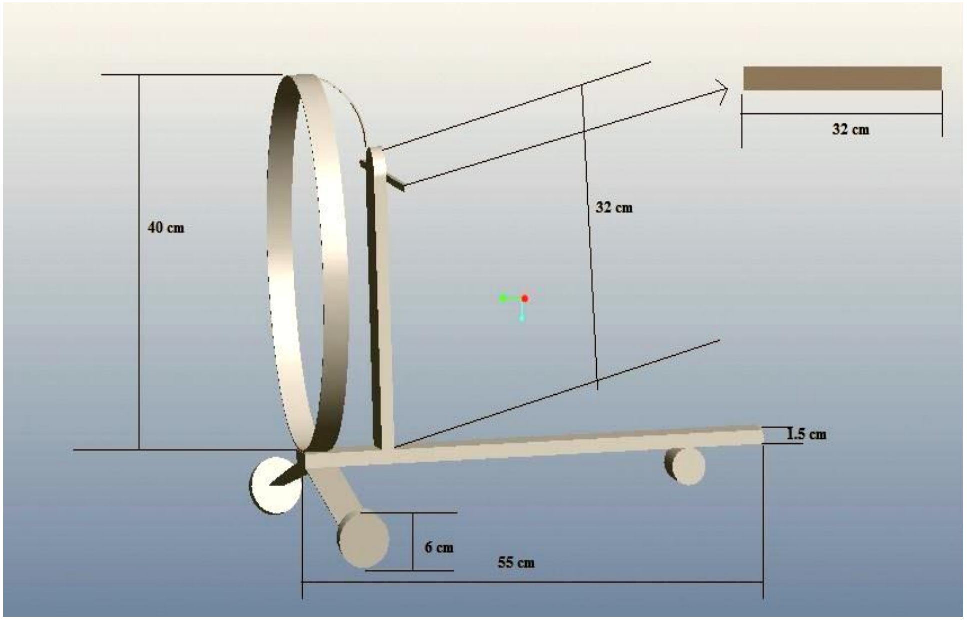

Figure 3.1: Physical Dimensions of the Vehicle

3.2.1 Nose to Main Frame Ratio

The nose is made up of balsa wood. The nose is generally considered to be long compared to the main frame in a ratio of 7:5. The length of the nose is 55cm

It is observed that if the nose is taken short the vehicle tends to stall.

3.2.2 Main Frame

The mainframe is also made up of balsa wood. The mainframe acts as a house for propulsion unit and the control unit. The propulsion system (motor and the propeller) is placed exactly at the center so that the propeller does not touch the surface of the nose when rotating.

3.2.3 Propulsion unit

The propulsion unit consists of an out-runner Brushless DC Motor (BLDC). The motor selection is done by the power calculation. The power required can be calculated by multiplying volts and amps.

- Input watts per pound gives the power requirement based on the weight of the model.
- If the model weight is considered to be x, and power required is 100 watts then then 100x input watts per pound is the minimum power required to achieve the desired performance.
- The input power the motor can handle is determined by
  Average voltage X continuous current = input watts

Therefore for a 3 kg payload, 6 Cells, Continuous Power Capability: 19.8 Volts (6 x 3.3) x 40 Amps = 792 Watts. The size propeller attached to the model depends on the motor selected.

3.2.4 Propeller Guard

The propeller guard is made of aluminum which is bent in the form of a circle to give protection to the strings. The diameter of the propeller guard is 32cm.

3.2.5 Front and Back Landing Gears

The front landing gear has one wheel and the back landing gear has two wheels giving the shape of a triac. All the wheels are made of balsa wood. Each wheel is of 6cm diameter

3.2.6 Control Rod

The control rod is hinged to the main frame at the center, and is connected to a servo through a push pull rod. The control rod made of an aluminum rod, and is 32cm.

3.2.7 Sensors and Control Unit

The complete set of electronics and the controller used is discussed in detail in the later sections of the chapter (3.6 - Data acquisitions and control system). The toal weight of the sensors system is 20 grams.

3.3 PARAFOIL SIZING

A Ram Air Parafoil comes under the category of NACA Clark Y aero-foil.

3.3.1 Size of the Parafoil

The mass of the payload may range in between 1kg to 8000kg. Change in the weight of the payload increases the size of the parachute [29] The general requirements for calculating the size of the parachute are:

Figure.3.2: Parafoil used for UPPAV

- Payload mass(W)
- Horizontal flight velocity(w)
- Vertical flight velocity(u)

- Lift(L)
- Drag(D)
- Aspect ratio(A)
- Chord length(B)
- Span (B)
- Density(d)

3.3.2 Size

The size of the parachute will be determined by the mass of the payload to be delivered. Therefore the velocity of the parachute is also calculated [29].

The wind specifications set the lower limit on wing loading.

The velocity of the parachute is square root of horizontal flight velocity and vertical flight velocity.

$$v = \sqrt{u^2 - w^2} \tag{3.1}$$

The horizontal flight velocity (w) is calculated by, the L/D is assumed to be 3.

$$w = \frac{u}{L/D} \tag{3.2}$$

Using these values the size of the parachute is calculated, which is given by:

$$S = \frac{W}{10 \times \sqrt{(C_l^2 + C_d^2) \times (0.5 \times V^2 \times d)}} \tag{3.3}$$

3.3.3 Cord

The cord of the parachute is calculated using Aspect Ratio and the Surface area of the parachute

$$C = \sqrt{S / A} \tag{3.4}$$

3.3.4 Width

The Width of the parachute is given by multiplying cord and aspect ratio

$$B = C \times A \tag{3.5}$$

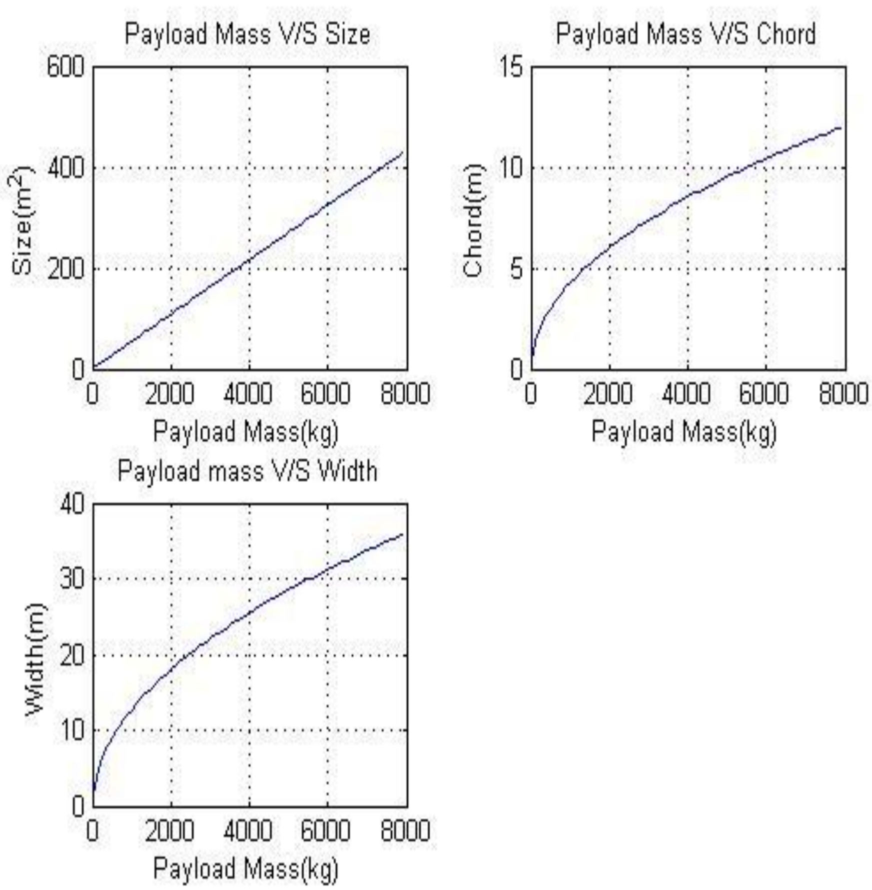

Figure 3.3: Parafoil Size to the Payload

Since our operation has to be performed using a small Parafoil the following table was again calculated to the approximate size of the Parafoil which should be capable of lifting a payload of maximum 5 Kg, which includes the discussed payload components.

S.No.	Weight (kg) (maximum)	Span (m)	Chord (m)	Area (m^2)
1	1	0.84	0.28	0.24
2	2	1.2	0.4	0.48
3	3	1.47	0.5	0.73
4	4	1.68	0.56	0.97
5	5	1.89	0.63	1.2

Table 3.1: Parafoil Payload Relationship

Keeping the Payload components, Parafoil Performance and Parafoil sizing, the Parafoil that was selected is capable of lift 5 Kgs (Maximum), the following is the specification of the vehicle.

Payload mass	3-4 kg (Including electronics)
Cord	0.65m
Span	2m
Area	1.3 m^2
velocity	10 km/h
density	1.22
Aspect Ratio	3

Table 3.2: UPPAV Specifications

3.4 PERFORMANCE PARAMETERS

Performance Parameters include the basic L/D concept and lift and drag coefficient calculation and glide performance.

3.4.1 Parafoil L/D Ratio

The L/D ratio of Parafoil changes according to the angle of attack, thereby getting different L/D ratios at different flight conditions. L/D ratio is also used to determine the drag coefficients it is taken as 3 initially.

3.4.2 Parafoil Lift and Drag Coefficient Calculation

The requirement of lift coefficient acting on UPPAV is determined as following from the estimated flight velocity [11]

$$L = \frac{1}{2}\rho V^2 S C_l \tag{3.6}$$

$$L=W \tag{3.7}$$

$$C_l = \frac{2W}{\rho A V^2} = 0.5 \tag{3.8}$$

For the drag coefficient, the lift to drag ratio can be determined by the gliding flight

$$C_d = \frac{C_l}{L/D} = 0.16 \tag{3.9}$$

The total drag that is acting on the Parafoil is given as the sums of the parasite drag and drag due to lift.

$$C_d = C_{d_p} + C_{d_i} \tag{3.10}$$

$$C_{d_i} = \frac{A C_l^2}{\Pi a b^2} = 0.046 \tag{3.11}$$

Parasite drag can be calculated by subtracting the Drag due to the lift from the total drag

$$C_{d_p} = C_d - C_{d_i} = 0.104 \tag{3.12}$$

These estimates suggest that the parasite drag is 50.6 % of the total drag and drag due to the lift is 49.37%.

3.4.3 Payload and Lines Drag Calculation

- Height of the payload = 0.46mX 0.015mX0.05m
- Length of the Payload = 0.55mX 0.015mX0.05m
- Width of the Payload = 0.32mX0.015X0.05m
- Therefor total drag area of the payload = 0.05m^2

For which the drag coefficient is 0.057, the drag coefficient for the lines comes out to be 0.01.

Therefore the total drag of the vehicle comes out to be C_d= 0.21.

3.4.4 Lift to Drag Ratio of the Complete System (PAV)

$$E = \frac{C_l}{C_d} = 2.5 \tag{3.13}$$

Where, E is known as the lift to drag ratio.

3.4.5 Gliding Flight Performance of PAV

Velocity of the vehicle during gliding flight is given as

$$V = \sqrt{\frac{2XW}{\rho XSXC_l}} = 10 m/s \tag{3.14}$$

Gamma (glide angle) is given by

$$\gamma = -\frac{1}{E} = -0.4 radians = -22 \deg rees \tag{3.15}$$

During the level flight lift to drag ratio is zero, which make glide angle 0.

3.5 THRUST REQUIREMENT

The motor used for the developed UPPAV if E Flite 60 which generates a power of 1200 Watts which comes out to be 1.6 bhp. The motor used is capable of lifting a payload upto 5 Kgs.

Thrust required by UPPAV can be estimated from the following formula [11]

$$T = \frac{VW}{L/DX(motor(bhp))} = 8N \tag{3.16}$$

3.6 DATA ACQUISITION AND CONTROL SYSTEM

The data acquisition system consist of a micro controller, which monitors airspeed, altitude, location, ground speed, velocity etc.

3.6.1 Inertial Measurement Unit

The IMU used is MPU-600. The device has inbuilt 3-axis accelerometer and a 3-axis gyroscope. The device communicates with the microprocessor in SPI mode. The accelerometer has a range of +16g to -16g and gyroscope has a range of +2000deg/sec to -2000deg/sec.

The three steps should be followed to initialize the IMU

1. Low pass filter frequency must be set to half of the sample rate.
2. The range of the accelerometer and gyro must be set.
3. The sample time must match with the sample time of the microprocessor.

3.6.2 Barometric Pressure Sensor

The MEAS Switzerland MS5611 is a small digital device having an inbuilt 24 bit ADC. The chip provides static pressure value that helps in determining the altitude in inches. The sensor works on 75Hz.

3.6.3 Magnetometer

The Honeywell HMC5843 3-axis digital Magnetometer measures the magnetic field strength in each of the three axes. The device communicates with serial bus. As the earth's field strength is very weak, the device is sensitive and has high resolution. The device is susceptible to the noise due to the noise in the vicinity of the sensor. The engine with induced magnetic field further degrades the quality of the sensor.

3.6.4 GPS

The MediaTek MT3329 10Hz GPS Receiver includes the GPS receiver, processor, and an antenna. The input values are the simulated GPS values.

3.6.5 Pitot Probe

This probe is pitot static probe which is mounted in the forward direction in the triac. The Freescale MPXV7002DP measures the Differential pressure sensor connected to the pitot tube measures the airspeed. Once calibrated, the output is the value of pressure in terms of voltage.

3.6.6 Ultrasonic Sensor

Parallax PING ultrasonic sensor provides an easy method of distance measurement. A single I/O pin is used to trigger an ultrasonic burst (well above human hearing) and then "listen" for the echo return pulse. The sensor measures the time required for the echo return, and returns this value to the microcontroller as a variable-width pulse via the same I/O pin. The following table gives the brief idea about the components used and their specifications.

S.No.	**Component**	**Specification**	**Usage**
1.	BLDC Motor	Eflite 60 • Equivalent to a 60-size glow engine for 6 to 10 lb (2.7 to 4.5 kg) airplanes • 8880 RPM with 22.2V battery	Provides throttle, to maintain altitude, take off and landing

2.	ESC	100 Amps, Turnigy Requires 3-6 cell Li-Po battery	Provides PWM signals to BLDC motor, to control the speed of the motor
3.	Propeller	13X4	Provides thrust of 5.5 Kg
4.	Battery	• Li-Po • 22.2V • 5000 mAh • 6 Cell	Power supply, up to 20 minutes, for continuous flying
5.	Futaba Trans Receiver	22.4 GHz • 6 channel • 1 Km Range	To control the vehicle
6.	Servo Motor	16 Kg	For direction control
7.	Ardu Pilot	• ATMEGA2560 (Arduino Mega) • Supported telemetry 433 MHz • 4 PWM Channels • 4 USART • 10 bit ADC	Controller for auto pilot,
8.	Barometric Pressure Sensor	MEAS Switzerland MS5611 • 8 bit ADC • 75 Hz	Static Pressure and Temperature
9.	Magnetometer	Honeywell HMC5843 3-axis digital Magnetometer • USART Communication	Magnetic field in X, Y and Z direction
10.	GPS	MediaTek MT3329 10Hz GPS Receiver, Includes the	Latitude, Longitude, Altitude, Ground

		GPS receiver, processor, and an antenna	Speed, Time,
11.	Pitot Probe	Freescale MPXV7002DP	Dynamic Pressure
12.	IMU	MPU 600 • 3 axis Accelerometer +2000 deg/s to -2000 deg/s • 3 axis gyroscope +16g to –16g	P,q,r (roll rate, pitch rate and yaw rate)
13.	Ultrasonic Sensor	Parallax PING ultrasonic sensor	Distance in meters

Table 3.3: Component Specification used in UPPAV

Figure 3.4: UPPAV

The methodology followed for achieving the above mentioned target is to develop embedded system (Hardware Model), Autopilot design and the algorithm design. The hardware model is divided into two parts, which are, onboard embedded system design and ground station design the communication between the onboard embedded system and the ground station is done using 433 MHz Transceiever protocol

3.7 HARDWARE DEVELOPMENT

The development of the control system for autopilot is done to provide artificial stability. The autopilots are capable of maintaining pitch roll and heading angles. These control systems are then coded in the microcontroller using "Embedded C" programming. For the powered parachute aerial vehicle two different autopilots have to design which are, altitude hold autopilot and altitude heading autopilot. For programming these autopilot using Embedded C an algorithm have be designed. A detail description of the on board embedded system, ground station embedded system, altitude hold autopilot, altitude heading autopilot and algorithm design is given.

3.7.1 On board Embedded system

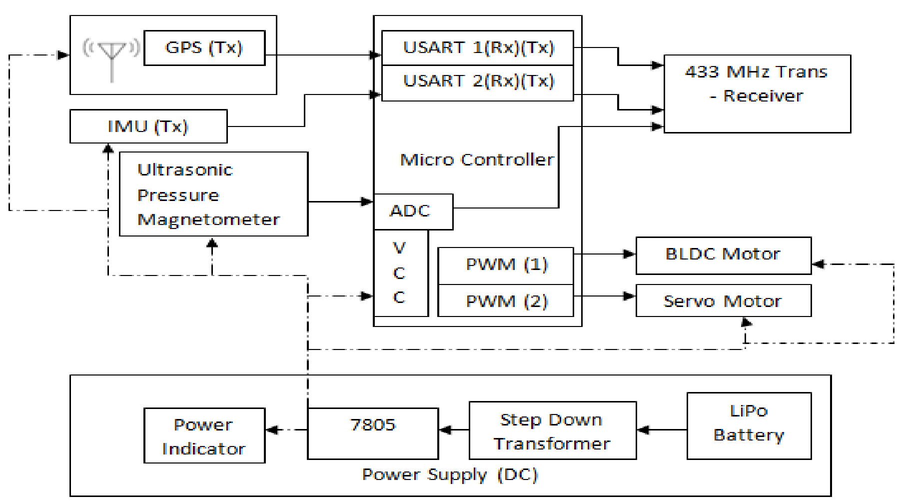

Figure 3.5: Hardware model of Powered Parafoil Aerial Vehicle

The block diagram of transmitting and receiving sections (system with the aerial vehicle and ground station) are given above. The on board Embedded system is basically placed on the aerial vehicle. The system is interfaced with three sensors GPS, IMU and Ultrasonic sensors. GPS measures the vehicle speed, latitude, longitude and altitude whose values are used to control the vehicle direction also, are transmitted to the ground station using 433 MHz Transmitter Receiver for the operator.

3.7.2 Ground Station

The ground station receives the signal from the onboard embedded system and displays all the sensor information to the user.

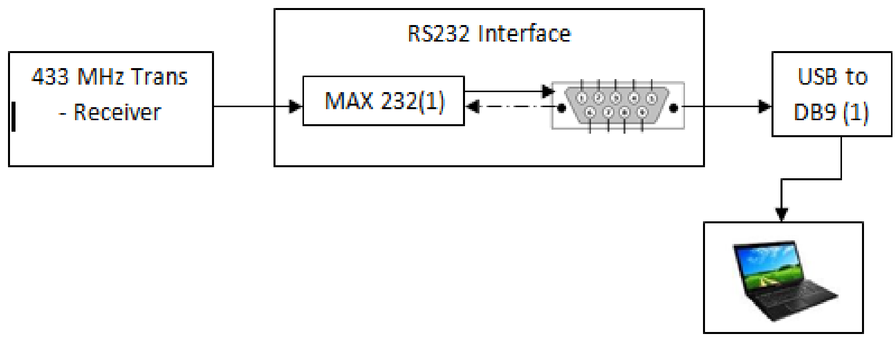

Figure 3.6: Hardware model of Powered Parafoil Aerial Vehicle (Ground Station)

3.8 FLIGHT TEST PLAN

The flight tests are planned in two phases. i.e. open loop flight tests and closed loop flight tests to meet the below objectives.

The project aims at making an Autonomous Flying Para Drone moving on pre-defined path with obstacle avoidance and path restoration technique.

- To develop a Servo motor based direction control System
- To develop a GPS Based navigation system
- To develop a Ultrasonic sensor based obstacle avoidance system
- Interfacing all the above control systems

The following open loop flight tests are planned in the following manner. The UPPAV has inherent static stability; therefore the planned light tests would help in acquiring the precise aerodynamic data.

3.8.1 Open loop flight test plan

- *To demonstrate that the flight can be carried out with a single servo*

Most of the developed vehicles use two servos to control the direction of the vehicle, but in UPPAV a single servo is used which has advantages in terms of power and control algorithm design

- *To check the take off*

This test would help us in determining the power required for takeoff, which is generally in full throttle condition.

- *To analyze the turn performance*

Before the closed loop system is designed, the turn rate, turn radius with respect to the servo tilt must be known. Therefore, the turn performance analysis is done

- *Gliding test*

This test would help us understand the AOA, Glide angle and pitch angle performance. This test would also help us in estimating the landing distance and throttle condition.

3.8.2 Closed loop Tests

- *Attitude Stability*

The UPPAV inherently has pendulum stability, due to the turning the vehicle tends to oscillate, these oscillations has to be reduced for precise controller design. The gains of attitude controller is determined using the attitude stability and incorporated in the controller

- *Longitudinal Altitude hold controller*

The vehicle is taken to a certain height and controller is designed such that the vehicle must maintain the same altitude with the same throttle called level flight. The gains are calculated using the controller and are used in the embedded program to hold the required altitude

- *Lateral Heading control*

The heading controller is designed to maintain a heading angle for way point navigation. The gains are calculated using the controller and are used in the embedded program to execute the way point navigation algorithm.

The chapter gives the detailed description of the experiment designed to execute the given PhD problem. The few initial topics deal with the UPPAV structure, the relationship between the payload and the Parafoil, which helped us in determining the size of the Parafoil for executing the experiment. The basic aerodynamic parameters of the vehicle are also determined using the basic formulae. The later section deals with the DAQ system used and their specifications. The Output devices used are also discussed in detail. Flight tests are planned to meet the objectives of the PhD work which are given in detail.

CHAPTER 4

MATHEMATICAL MODELLING

4.1 PARAFOIL PAYLOAD MODEL

Parafoil is entirely made of fabric and is a non- rigid wing. A Parafoil get inflated just like a parachute when dripped from a height. The wing has a low aspect ratio with an elliptical or a rectangular plan form when inflated. To act as an airfoil, the upper membrane and the lower membrane are sewn together with a gap between both. The leading edge is kept open so as to allow the air inside the cells creating air pressure, which maintains the shape of the Parafoil as a wing. The vents in the ribs allow the air pass from one cell to another which helps in maintaining uniform air pressure in the wing. To avoid the air loss the fabric is made of non-porous material. The suspension lines are used to connect the Parafoil to the payload.

Directional control is achieved by pulling the fly-bar, which changes the direction of the lift making the aircraft turn. The Powered Parafoil has a tendency to fly at constant airspeed. These systems have pendulum stability and oscillations, because of the mass of the airframe suspended significantly below the canopy, which allows the system to have a yaw motion rather than roll motion. Lateral control is obtained by the canopy itself and the propulsion system attached to the payload [30]. The addition of propulsion system makes the Paraglider an unmanned Aerial vehicle.

The modelling of the Parafoil has been studied in detail. One of the first mathematical model was studied by Goodrick [24]. He developed three degrees of freedom model in 1975 to study longitudinal stability of Parafoil.

Later he developed six degrees of freedom model to study the control in Parafoil [25]. A guidance algorithm was developed using his six degrees of freedom model [26]. Lingard [22] used longitudinal three degrees of freedom dynamic model of Parafoil payload system to study dynamic effects of various system parameters. These equations were derived about the center of gravity of the total system showing longitudinal motion of the system and pitching motion. The model represented Parafoil mass as well as the apparent mass center at canopy quarter-chord, which is an approximation as apparent mass centers located at canopy centroid. This model was used to analyze the effect of changes in canopy size, line length and break deflection, on longitudinal dynamics of the system. There is always a relative motion between Parafoil and payload to introduce additional degrees of freedom this relative motion should be considered. Also, the relative motion should be taken into account as it affects the altitude of the payload on which the propulsion system is attached. The six degrees of freedom model is a single rigid model, where the relative motion between Parafoil and payload is neglected. In 2011, Y Ochi and M Watanabe have described the non-linear dynamic model using Newtonian mechanics [27]. Body fixed Co-ordinate system are defined for canopy and payload where, six degrees of freedom for canopy and two degrees of freedom for payload. The relative pitch and yawing motions between the canopy and payload are modeled as spring damper system. The internal forces are analytically eliminated. A Six DOF model has been developed by Slegers, N and Nahon, M in 2005, where relative motion between payload and canopy is neglected [28]. Since, the payload on which propulsion and measurement units are placed the relative motion should be taken into account. In early 90's a nine degrees of freedom model was proposed by Doherr and Schilling [29] considering Paraglider as a 2 body system. By constraining to zero the rotation about one or two axes, a seven degrees of freedom and eight degrees of freedom models could be obtained. Mooij et al. [29] used nine degrees of freedom flight dynamic model to develop hardware-in-loop flight simulation environment for the small Parafoil Autonomous Delivery System (SPADES). The Parafoil-

Payload system was represented by two rigid bodies connected by two rigid bars and a hinge. The hinge was modeled as a damped spring. Slegers and Costello [28], Mooij et al. [29], and Yakimenko [30] applied the concept of coupling of moments between the payload and canopy at the joining. This assumption can be applied as the tension plays a major role at the join. A Powered Parachute as shown in Fig.4 has eight degrees of freedom, where six degrees of freedom of canopy and two degrees of freedom of payload. In eight degrees of freedom model roll approximation is neglected as it is considered to be relatively small [31]. Muller et al. [32] considered a non-linear two body eight degrees of freedom model. He considered six degrees of freedom model for Parafoil and two degrees of freedom model for relative motion of payload. The author defined the tensions at the joint to introduce back turning moment about the yaw axis and modeled the moment as the function of tension of the suspension lines. The internal forces in equation of motion were not defined clearly. A linear model was developed by Aakasaka et al. [33], by removing the third co-ordinate system and assuming the tension for a trimmed flight condition to be constant. A non-linear model was developed by Slegers [34] for the same configuration without eliminating the internal forces. Modeling of powered parachute can also be done by analytical methods. Using Lagrange's equations Wise [35] modeled the dynamics of a small propeller. The UAV and the Parafoil are taken as six degrees of freedom systems and the constraints are coupled with eight degrees of freedom model. A Quasi-Hamiltonaian formulation was developed by Redelinghuys [36] where, eight degrees of freedom equations were derived. Lagrange's derivations were more complex. An accurate model having nine degrees of freedom, modeled as two-body dynamics, consisting of three degrees of freedom for rotational motion of the Parafoil, three degrees of freedom for the rotational motion of the payload and three degrees of freedom for translational motion of the Parafoil [36]. The turning and gliding flight of Parafoil system is analyzed by Prakash et al. [37] subjected to change in left and right brake deflections. This, nine degrees of freedom model incorporates non-linear aerodynamics to predict all kinds of behavior. The non-linear simulation demonstrates the validity of the proposed model through comparison with the Lingard's data.

4.2 COORDINATE SYSTEMS

Figure 3 shows the coordinate system of the Powered Parafoil Aerial Vehicle used in this study. There are three reference frames called Parafoil Canopy-fixed reference frame (X_p, Y_p, Z_p), payload body fixed reference frame (X_b,Y_b,Z_b) and Joint C-fixed reference frame (X_c,Y_c, Z_c). The Parafoil Canopy-fixed reference frame has its origin located at canopy center of mass P. The X_p axis points forward, parallel to the canopy chord in the plane of symmetry. The Z_p axis points downward in the system's plane of symmetry. The Y_p axis is normal to the plane of symmetry to form a right-handed axis system. In this reference frame, the canopy mass center has translational velocity $V_p = \{u_p, v_p, w_p\}$, angular velocity $\Omega p = \{p_p,q_p,r_p\}$, and Euler angles ($\Phi_p,\theta_p,\psi_p$). The payload body fixed reference frame has origin located at payload center of mass b. The X_b axis points forward normal to the link R_b. The Z_b axis points downward, parallel to link R_b. The Y_b axis is normal to the X_b and Z_b axes as per right-hand rule. In this reference frame the payload mass center has translational velocity $V_b = \{u_b, v_b, w_b\}$, angular velocity $\Omega_b = \{p_b, q_b, r_b\}$, and Euler angles ($\Phi_b,\theta_b,\psi_b$). The Joint C-fixed reference frame has its origin located at the joint C. the X_c axis points forward, parallel to each horizontal. The Z_c axis is normal to X_c, axis pointing downward. The Y_c is the axis normal to X_c and Z_c. In this reference frame joint C has translational velocity $V_c = \{ u_c, v_c, w_c \}$. The joint C reaction forces are $Fc = (F_{cx}, F_{cy}, F_{cz})$. The suspension lines of the canopy are connected to the payload at to joints C_L and C_R, where C is the midpoint between C_L and C_R. The derivation of nine degrees of freedom dynamic equations of motion of Parafoil payload system involves separation of system from joint C, and creating the following two sub models such that joint C is exposed to internal forces $F_c = (F_{cx}, F_{cy}, F_{cz})$. In the joint C reference frame.

- Payload sub Model

- Parafoil Sub Model

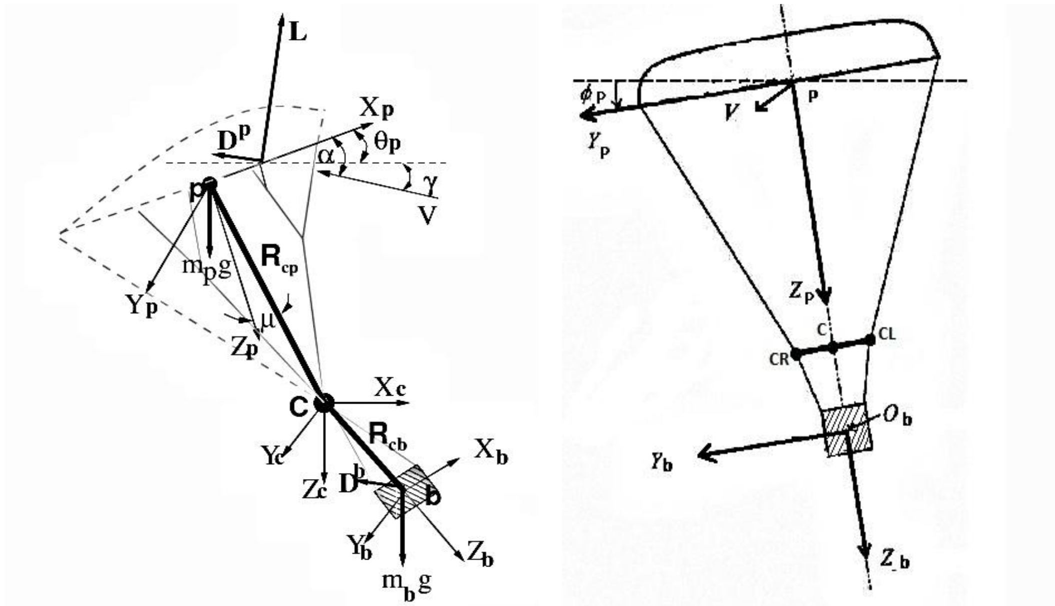

Figure 4.1: Front and Side view of Powered Parafoil Aerial Vehicle

4.3 PAYLOAD SUB MODEL

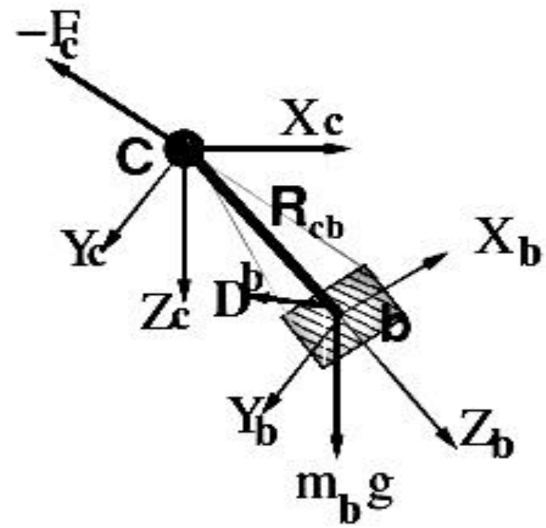

Figure 4.2: Payload Sub Model of Powered Parafoil Aerial Vehicle

The payload sub model consisting of payload center of mass connected to joint C through link R_{cb}. The payload is allowed to freely rotate about joint C with the X_b axis pointing forward normal to the link R_b. The Z_b axis points downward, parallel to link R_b. The Y_b axis is normal to the X_b and Z_b axes as per right-hand rule. In this reference frame the payload mass center has translational velocity V_b = $\{u_b, v_b, w_b\}$, angular velocity $\mathbf{\Omega}_b = \{p_b, q_b, r_b\}$, and Euler angles $(\Phi_b, \theta_b, \psi_b)$. The forces acting on the payload center of mass are aerodynamic force F_b^A, Gravitational force F_b^G, internal Joint force F_b^C and Thrust force F_b^T. The internal joint force F_b^C acting at joint C at a distance of $R_{Cb} = \{X_{cb}, Y_{cb}, Z_{cb}\}$ from payload mass center in joint C reference frame gives rise to moments $R_{Cb} \times F_b^C$ about payload mass center.

Translational equations of motion of payload center of mass in payload body fixed reference frame can be expressed as:

$$M_b \dot{V}_b + \Omega_b \times M_b V_b = F_b^A + F_b^G + F_b^T - F_b^C \tag{4.1}$$

Where,

$V_b, \dot{V}_b$: are inertial reference frame quantities:

$$\begin{aligned} V_b &= T_b V_C + \Omega_b \times R_{Cb} \\ \dot{V}_b &= \dot{T}_b V_C + T_b \dot{V}_C + \dot{\Omega}_b \times R_{Cb} + \Omega_b \times \dot{R}_{Cb} \end{aligned} \tag{4.2}$$

and M_b is the payload mass matrix:

$$M_b = \begin{bmatrix} m_b & 0 & 0 \\ 0 & m_b & 0 \\ 0 & 0 & m_b \end{bmatrix} \tag{4.3}$$

Matrix T_b is the transformation matrix from an inertial reference frame to the payload reference frame:

$$T_b = \begin{bmatrix} C\theta_b C\psi_b & C\theta_b S\psi_b & -S\theta_b \\ S\phi_b S\theta_b C\psi_b - C\phi_b S\psi_b & S\phi_b S\theta_b S\psi_b + C\phi_b C\psi_b & S\phi_b C\theta_b \\ S\phi_b S\theta_b C\psi_b + S\phi_b S\psi_b & C\phi_b S\theta_b S\psi_b - S\phi_b C\psi_b & C\phi_b C\theta_b \end{bmatrix} \quad (4.4)$$

$(\Omega_b \times)$ is a cross-product-equivalent matrix for payload body axis angular velocity:

$$\Omega_b \times = \begin{bmatrix} 0 & -r_b & q_b \\ r_b & 0 & -p_b \\ -q_b & p_b & 0 \end{bmatrix} \quad (4.5)$$

And $(R_{cb} \times)$ is cross product equivalent matrix of components of distance of payload mass center b from joint C in payload body-fixed reference frame:

$$R_{cb} \times = \begin{bmatrix} 0 & -z_{cb} & y_{cb} \\ z_{cb} & 0 & -x_{cb} \\ -y_{cb} & x_{cb} & 0 \end{bmatrix} \quad (4.6)$$

Here $x_{cb} = 0, y_{cb} = 0$ and $z_{cb} = R_{cb}$ due to the choice of the reference frame. The distance between joint C and payload mass center is constant, i.e., $\dot{R}_{cb} = 0$, and $\dot{T}_b = -\Omega_b \times T_b$, hence

$$\dot{V}_b = (-\Omega_b \times T_b)V_c + T_b\dot{V}_c + \dot{\Omega}_b \times R_{cb} \quad (4.7)$$

Substituting, $V_b, \dot{V}_b$ from equations 4. 2 and 4.7 in 4.1, we get

$$M_b T_b \dot{V}_c + M_b \dot{\Omega}_b \times R_{Cb} + M_b \Omega_b \times \Omega_b \times R_{Cb} = F_b^A + F_b^G + F_b^T - F_b^C \quad (4.8)$$

The rotational motion of the payload center of mass in payload-fixed reference frame is described by:

$$I_b \dot{\Omega}_b + \Omega_b \times I_b \Omega_b = R_{Cb} \times F_b^C \quad (4.9)$$

4.4 PAYLOAD FORCES AND MOMENTS

The external forces acting on payload sub model are:

- Aerodynamic Force: The aerodynamic drag (C_D^b) force acting at payload mass center in payload reference frame

$$F_b^A = \bar{q}_b S_b \begin{Bmatrix} C\alpha_b C_D^b \\ 0 \\ S\alpha_b C_D^b \end{Bmatrix} \tag{4.10}$$

Where, $\bar{q}_b = \frac{1}{2}\rho V_b^2$, S_b is payload frontal area and $\alpha_b = \tan^{-1}\left(\frac{w_b}{u_b}\right)$ is the local angle of attack of payload center of mass.

- Gravitational Force: the gravitational force acting at payload mass center in payload reference frame is

$$F_b^G = m_b g \begin{Bmatrix} -S\theta_b \\ S\phi_b C\theta_b \\ C\phi_b C\theta_b \end{Bmatrix} \tag{4.11}$$

Where, g is the acceleration due to gravity

- Joint Force: the internal joint C reaction forces expressed in payload reference are

$$F_b^C = \begin{bmatrix} C\theta_b C\psi_b & C\theta_b S\psi_b & -S\theta_b \\ S\phi_b S\theta_b C\psi_b - C\phi_b S\psi_b & S\phi_b S\theta_b S\psi_b + C\phi_b C\psi_b & S\phi_b C\theta_b \\ S\phi_b S\theta_b C\psi_b + S\phi_b S\psi_b & C\phi_b S\theta_b S\psi_b - S\phi_b C\psi_b & C\phi_b C\theta_b \end{bmatrix} \begin{Bmatrix} F_{Cx} \\ F_{Cy} \\ F_{Cz} \end{Bmatrix} \tag{4.12}$$

- Thrust force: the force due to the attached propulsion system in X_b direction

$$F_b^T = \begin{bmatrix} Th \\ 0 \\ 0 \end{bmatrix} \tag{4.13}$$

4.5 PARAFOIL SUB MODEL

Figure 4.3 shows the Parafoil sub model consisting of Parafoil mass center P connected to joint C through link R_p. The Parafoil is allowed to rotate freely about the joint c having translational velocity $V_p = \{u_p, v_p, w_p\}$, angular velocity $\Omega_p = \{p_p, q_p, r_p\}$, and Euler angles $(\Phi_p, \theta_p, \psi_p)$. The forces acting on the Parafoil center of mass are aerodynamic force F_p^A, Gravitational force F_p^G, and internal Joint force F_p^C acts at joint C.

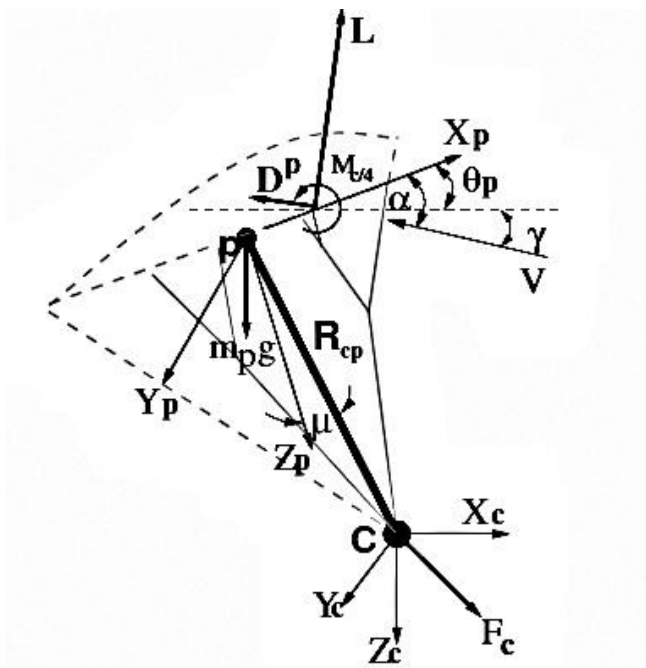

Figure 4.3: Parafoil Sub Model of Powered Parafoil Aerial Vehicle

Translational motion of payload center of mass in Parafoil-fixed reference frame can be expressed as

$$(M_p + M_F)\dot{V}_p + \Omega_p \times (M_p + M_F)V_p = F_p^A + F_p^G - F_p^C \tag{4.14}$$

Where,

$V_p, \dot{V}_p$ are inertial reference frame quantities:

$$\begin{aligned} V_p &= T_p V_C + \Omega_p \times R_{Cp} \\ \dot{V}_p &= \dot{T}_p V_C + T_p \dot{V}_C + \dot{\Omega}_p \times R_{Cp} + \Omega_p \times \dot{R}_{Cp} \end{aligned} \tag{4.15}$$

and M_p is the Parafoil mass matrix and M_F is Parafoil Apparent mass:

$$M_p = \begin{bmatrix} m_p & 0 & 0 \\ 0 & m_p & 0 \\ 0 & 0 & m_p \end{bmatrix} \tag{4.16}$$

$$M_F = \begin{bmatrix} A & 0 & 0 \\ 0 & B & 0 \\ 0 & 0 & C \end{bmatrix} \tag{4.17}$$

Matrix T_p is the transformation matrix from an inertial reference frame to the Parafoil reference frame:

$$T_p = \begin{bmatrix} C\theta_p C\psi_p & C\theta_p S\psi_p & -S\theta_p \\ S\phi_p S\theta_p C\psi_p - C\phi_p S\psi_p & S\phi_p S\theta_p S\psi_p + C\phi_p C\psi_p & S\phi_p C\theta_p \\ S\phi_p S\theta_p C\psi_p + S\phi_p S\psi_p & C\phi_p S\theta_p S\psi_p - S\phi_p C\psi_p & C\phi_p C\theta_p \end{bmatrix} \tag{4.18}$$

$(\Omega_p \times)$ is a cross-product-equivalent matrix for Parafoil body axis angular velocity:

$$\Omega_p \times = \begin{bmatrix} 0 & -r_p & q_p \\ r_p & 0 & -p_p \\ -q_p & p_p & 0 \end{bmatrix} \tag{4.19}$$

And $(R_{cp} \times)$ is cross product equivalent matrix of components of distance of Parafoil mass center b from joint C in Parafoil body-fixed reference frame:

$$R_{cp} \times = \begin{bmatrix} 0 & -z_{cp} & y_{cp} \\ z_{cp} & 0 & -x_{cp} \\ -y_{cp} & x_{cp} & 0 \end{bmatrix} \tag{4.20}$$

The distance between joint C and payload mass center is constant, i.e., $\dot{R}_{cp} = 0$, and $\dot{T}_p = -\Omega_p \times T_p$, hence

$$\dot{V}_p = (-\Omega_p \times T_p)V_C + T_p\dot{V}_C + \dot{\Omega}_p \times R_{Cp} \tag{4.21}$$

Substituting $V_p, \dot{V}_p$ from equations 4.15 and 4.21 in 4.14, we get

$$\begin{aligned}&(M_p + M_F)T_p\dot{V}_c + (M_p + M_F)\dot{\Omega}_p \times R_{Cp} - M_F\Omega_b \times T_pV_C + \Omega_p \times M_FT_pV_C \\ &+ \Omega_p \times (M_p + M_F)\Omega_p \times R_{Cp} = F_p^A + F_p^G - F_p^C\end{aligned} \tag{4.22}$$

The rotational motion of the Parafoil center of mass in Parafoil-fixed reference frame is described by:

$$I_p\dot{\Omega}_p + \Omega_p \times I_p\Omega_p = M_p - R_{Cp} \times F_p^C \tag{4.23}$$

4.6 PARAFOIL FORCES AND MOMENTS

The external forces acting on Parafoil sub model are:

- Aerodynamic Force: The aerodynamic forces acting at Parafoil mass center in payload reference frame

$$F_p^A = \bar{q}_p S_p \begin{Bmatrix} C_X \\ C_Y \\ C_Z \end{Bmatrix} \tag{4.24}$$

Where, $\bar{q}_p = \frac{1}{2}\rho V_p^2$, S_p is Parafoil surface area and $\alpha_p = \tan^{-1}\left(\frac{w_p}{u_p}\right)$ is the local angle of attack of payload center of mass and C_X, C_Y, C_Z are components of aerodynamic force in Parafoil – fixed reference frame.

- Gravitational Force: the gravitational force acting at Parafoil mass center in Parafoil reference frame is

$$F_p^G = m_p g \begin{Bmatrix} -S\theta_p \\ S\phi_p C\theta_p \\ C\phi_p C\theta_p \end{Bmatrix} \tag{4.25}$$

Where, g is the acceleration due to gravity

- Joint Force: the internal joint C reaction forces expressed in payload reference are

$$F_p^C = \begin{bmatrix} C\theta_p C\psi_p & C\theta_p S\psi_p & -S\theta_p \\ S\phi_p S\theta_p C\psi_p - C\phi_p S\psi_p & S\phi_p S\theta_p S\psi_p + C\phi_p C\psi_p & S\phi_p C\theta_p \\ S\phi_p S\theta_p C\psi_p + S\phi_p S\psi_p & C\phi_p S\theta_p S\psi_p - S\phi_p C\psi_p & C\phi_p C\theta_p \end{bmatrix} \begin{Bmatrix} F_{Cx} \\ F_{Cy} \\ F_{Cz} \end{Bmatrix} \tag{4.26}$$

4.7 NINE DEGREES OF FREEDOM MODEL

Collecting Parafoil translational and rotational motion equations, Payload translational and rotational motion equations we get nine degrees of freedom equations of motion of combines Parafoil payload system in concatenated matrix form as:

$$\begin{bmatrix} -M_b R_{cb} & 0 & -M_b T_b & T_b \\ 0 & -(M_p + M_F) R_{cp} & -(M_p + M_F) T_p & -T_b \\ I_b & 0 & 0 & -R_{cb} T_b \\ 0 & I_p + I_M & 0 & R_{cp} T_p \end{bmatrix} \begin{bmatrix} \dot{\omega}_b \\ \dot{\omega}_p \\ V_c \\ F_c \end{bmatrix} = \begin{bmatrix} B_1 \\ B_2 \\ B_3 \\ B_4 \end{bmatrix} \tag{4.27}$$

$$\begin{aligned} B_1 &= F_b^A + F_b^G + F_b^T - \omega_b \times M_b \omega_b \times R_{cb} \\ B_2 &= F_p^A + F_p^G - \omega \times (M_p + M_F) \omega_p \times R_{cp} + M_F \omega_p \times T_p V_c - \omega_p \times M_F T_p V_c \\ B_3 &= -\omega_b \times I_b \omega_b - M_c \\ B_4 &= M_p^A - \omega_p \times (I_p + I_M) \omega_p + M_c \end{aligned} \tag{4.28}$$

Where,

$$M_c = \begin{bmatrix} 0 \\ 0 \\ K_c(\Psi_p - \Psi_b) + C_c(\dot{\Psi}_p - \dot{\Psi}_b) \end{bmatrix} \tag{4.29}$$

$$\Psi_p = \tan^{-1}\left(\frac{Sin\Phi_p Sin\theta_p Cos\Psi_p + Cos\Phi_p Sin\Psi_p}{Cos\theta_p Cos\Psi_p}\right)$$
$$\Psi_b = \tan^{-1}\left(\frac{Sin\Phi_b Sin\theta_b C\Psi_b + Cos\Phi_b Sin\Psi_b}{Cos\theta_b Cos\Psi_b}\right) \tag{4.30}$$

$$\dot{\Psi}_p = -Cos\Psi_p \tan\theta_p p_p + Sin\Psi_p \tan\theta_p q_p + r_p \tag{4.31}$$

$$\dot{\Psi}_b = -Cos\Psi_b \tan\theta_b p_b + Sin\Psi_b \tan\theta_b q_b + r_b \tag{4.32}$$

$$\tan\theta_p = \frac{Cos\Phi_p Sin\theta_p Cos\Psi_p - Sin\Phi_p Sin\Psi_p}{Cos\theta_p Cos\Psi_p} Cos\dot{\Psi}_p \tag{4.33}$$

$$\tan\theta_b = \frac{Cos\Phi_b Sin\theta_b Cos\Psi_b - Sin\Phi_b Sin\Psi_b}{Cos\theta_b Cos\Psi_b} Cos\dot{\Psi}_b \tag{4.34}$$

The rotational stiffness and damping coefficients at joint C is taken as 0.35N.m/rad and 0.25N.m/rad

$$\begin{Bmatrix} \dot{x}_C \\ \dot{y}_C \\ \dot{z}_C \end{Bmatrix} = \begin{Bmatrix} u_C \\ v_C \\ w_C \end{Bmatrix}$$
$$\begin{Bmatrix} \dot{\phi}_b \\ \dot{\theta}_b \\ \dot{\psi}_b \end{Bmatrix} = \begin{bmatrix} 1 & S\phi_b t\theta_b & C\phi_b t\theta_b \\ 0 & C\phi_b & -S\phi_b \\ 0 & \dfrac{S\phi_b}{C\theta_b} & \dfrac{C\phi_b}{C\theta_b} \end{bmatrix} \begin{Bmatrix} p_b \\ q_b \\ r_b \end{Bmatrix}$$
$$\begin{Bmatrix} \dot{\phi}_p \\ \dot{\theta}_p \\ \dot{\psi}_p \end{Bmatrix} = \begin{bmatrix} 1 & S\phi_p t\theta_p & C\phi_p t\theta_p \\ 0 & C\phi_p & -S\phi_p \\ 0 & \dfrac{S\phi_p}{C\theta_p} & \dfrac{C\phi_p}{C\theta_p} \end{bmatrix} \begin{Bmatrix} p_p \\ q_p \\ r_p \end{Bmatrix} \tag{4.35}$$

Equation 4.27 gives 12 equations of 9 equations of motion and 3 joint force equations. Thus, the 9 equations from equation 4.27, together with kinematic equations 4.27, 4.28 and 4.35 give 21 equations of motion for combined Parafoil

– payload system in 18 state variables. The 3 additional equations in equation 4.26 give magnitude of internal forces at joint C.

4.8 RIGGING ANGLE MODELING

As shown in figure 4.4, the rigging angle μ is the angle between the line joining mid-baseline point of the canopy to the joint C and the line parallel to the Z_p axis passing through the mid baseline point. Therefore,

$$\begin{aligned} Z_{cp} &= R_{cp} Cos\mu \\ X_{cp} &= R_{cp} Sin\mu \\ Y_{cp} &= 0 \end{aligned} \qquad (4.36)$$

4.9 DIRECTION CONTROL MODELING

As shown in figure 4.5, the angle δ_S is the angle between the mid-baseline point and the steer bar tilt, this angle is called canopy tilt angle. Therefore,

$$\begin{aligned} Z_{cp}^{2} &= Z_{cp} Cos\delta_s \\ X_{cp}^{2} &= Z_{cp} \\ Y_{cp}^{2} &= -Z_{cp} Sin\delta_s \end{aligned} \qquad (4.37)$$

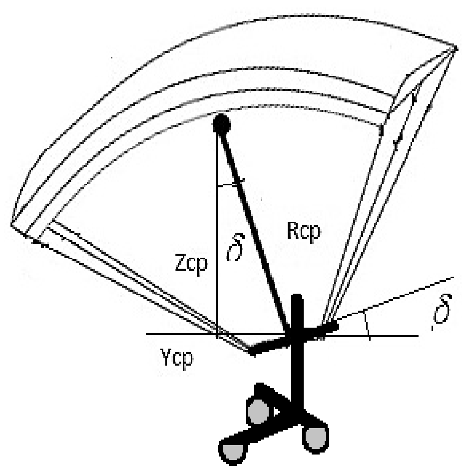

Figure 4.4: Direction Control Model

4.10 APPARENT MASS TERMS

Unlike aircraft, Parafoil-payload is a lightly wing-loaded system. Therefore, apparent mass terms show a strong effect on Parafoil- payload system dynamics. The apparent mass terms show a strong effect on Parafoil-payload system dynamics. The apparent mass (A, B, C) and inertia (Ia, Ib,Ic) terms are estimated from the analytical formulas.

$$\begin{aligned} A &= K_A \frac{\pi}{4} t^2 b \\ B &= K_B \frac{\pi}{4} t^2 c \\ C &= K_C \frac{\pi}{4} c^2 b \\ I_A &= K_A^* \frac{\pi}{48} c^2 b^3 \\ I_B &= K_B^* \frac{\pi}{48} c^4 b \\ I_C &= K_{C\backslash}^* \frac{\pi}{48} t^2 b^3 \end{aligned} \tag{4.38}$$

Where

$$\begin{aligned} K_A &= 0.85(1+\frac{8}{3}h^{*2}) \\ K_B &= 1(Barrows[24]) \\ K_C &= [1+2h^{*2}(1-t^{*2})]^{1/2} \frac{A^*}{1+A^*} \\ K_A^* &= 0.84 \frac{A^*}{1+A^*} \\ K_B^* &= 1.161 \frac{A^*}{1+A^*}[1+\frac{\pi}{6}(1+A^*)A^* h^{*2} t^{*2}] \\ K_C^* &= 0.855(1+8h^{*2}) \end{aligned} \tag{4.39}$$

These apparent mass and inertia terms are to be multiplied by local air density ρ.

The included mass $m_{pI} = \rho bct/2$ and corresponding inertia of the air inside the canopy are added to respective terms of equation 4.39 to get the final apparent mass and inertia of the Parafoil.

4.11 AERODYNAMIC MODEL

The aerodynamic forces and moments acting at Parafoil canopy mass center are modeled in terms of aerodynamic force and moment coefficients as (the values are extracted from Table 4.1):

$$\begin{aligned} C_L &= C_L(\alpha_p, \delta_s) \\ C_D^p &= C_D(\alpha_p, \delta_s) \\ C_Y &= C_{Y\beta} + C_{Y\gamma} r_p \frac{b}{2V_p} \end{aligned} \tag{4.40}$$

In terms of Parafoil canopy-fixed axis coefficients:

$$\begin{aligned} C_X &= (-C_D^p u_p + C_L w_p)/V_p \\ C_Y &= C_Y \\ C_Z &= (-C_D^p w_p + C_L u_p)/V_p \\ C_l &= C_{l\beta}\beta + C_{lp} p_p \frac{b}{2V_p} + C_{lr} r_p \frac{b}{2V_p} \\ C_m &= \{C_{m c/4}(\alpha_p, \delta_s) + x_{pa} C_Z\} + C_{mq} q_p \frac{C}{2V_p} \\ C_n &= C_{n\beta}\beta + C_{np} p_p \frac{b}{2V_p} + C_{nr} r_p \frac{b}{2V_p} \end{aligned} \tag{4.41}$$

Parameter	**Value**
C_{L0}	0.45[34]
C_{D0}	0.15[34]
$C_{Y\beta}$	-0.0095/deg
$C_{Y\gamma}$	-0.0060/deg
$C_{l\beta}$	-0.0014/deg

C_{lp}	-0.1330
C_{lr}	0.0100
$C_{n\beta}$	0.0005/deg
C_{np}	-0.0130
C_{nr}	-0.0350/deg

Table 4.1. Lateral Derivatives

Since a single servo is used to control the direction of the PAV, the servo angle is represented as δ_s. Since both the ends of the canopy is connected to a "fly-bar" δ_s gives positive and negative values representing left and right turn, as there is no asymmetric brake deflection in our model.

4.12 OPEN LOOP SIMULATION RESULTS

The developed PAV model has been validated using the Lingard model. Angle of attack (alpha), pitch angle (theta) and glide angle (gamma) values obtained (shown in the Figure 4.5) are compared with the Lingard values under no thrust conditions

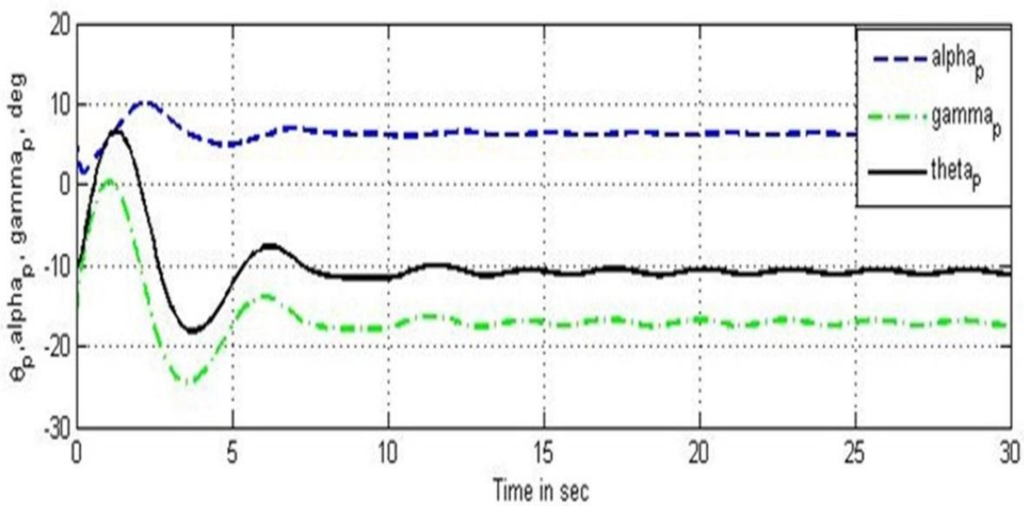

Figure 4.5. Parachute Aerial Vehicle under no Thrust condition

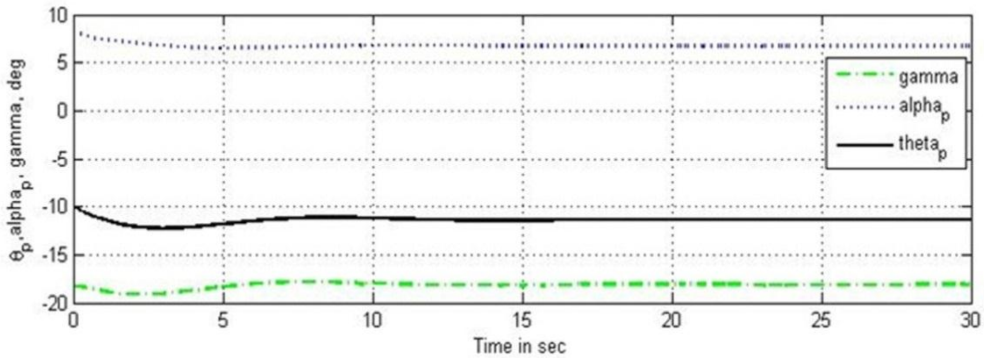

Figure 4.6. Validation of Parachute Aerial Vehicle with Lingard model

The model is validated using the Lingard results (shown in Figure 4.6) by checking the values of angle of attack (alpha), pitch angle (theta) and glide angle (gamma) of the Parafoil with respect to time. From Table 4.2 it can be observed that the developed 9 DOF model is providing accurate data. The developed 9 DOF simulation model has been simulated at various thrust conditions, keeping the thrust as 4.5N, 7.75N and 10N (Shown in Figure 4.6). It is observed that the gamma value is zero at the thrust input of 7.75N. This indicates that at thrust value 7.75N the vehicle is maintaining a level flight. Table 4.3 also indicates the same.

	Lingard	**Parachute Arial vehicle (Thrust = 0N)**
Alpha_p (deg)	3	5
Theta_p (deg)	-9	-10
Gamma(deg)	-18	-18

Table 4.2. Powered Parafoil Model validation with Lingard's Model

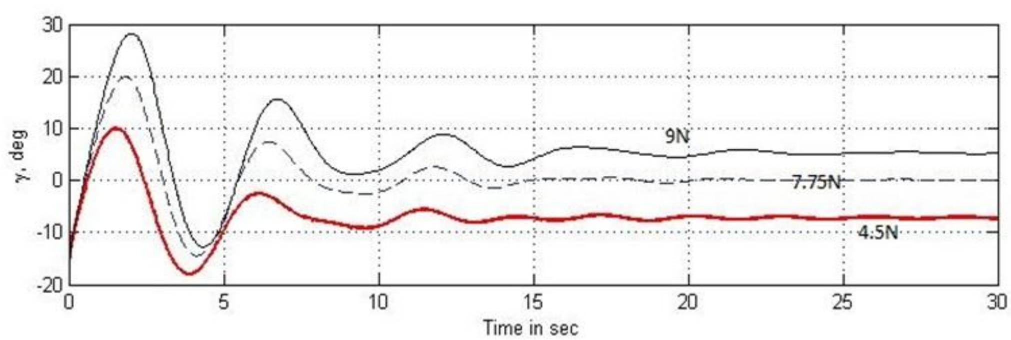

Figure 4.7. Gamma values for various thrust conditions

S.No.	Thrust (N)	Gamma(deg)
1	4.5	-8
2	7.75	0
3	9	7

Table 4.3. Gamma values for various thrust conditions

Keeping the thrust value 7.75N the alpha, theta and gamma values are seen in Figure 4.7.

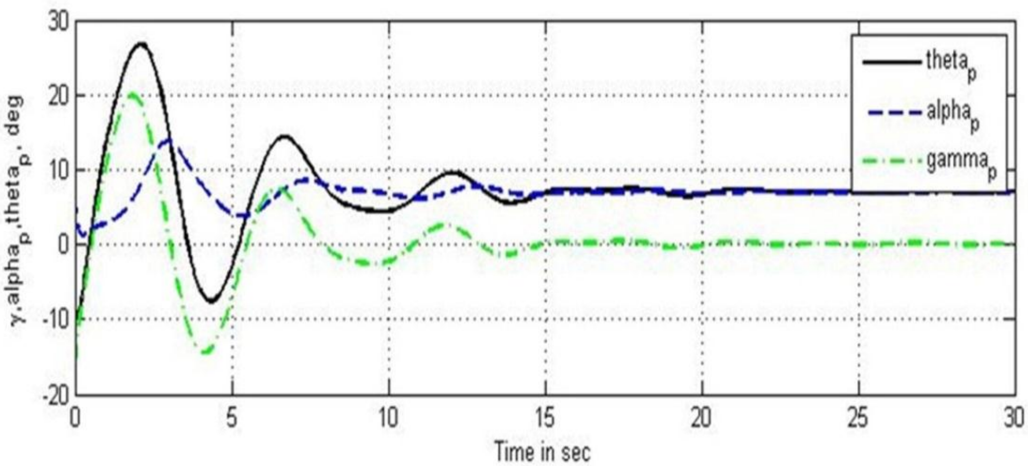

Figure 4.8. Parachute Aerial Vehicle with 7.75N thrust

	Parachute Arial vehicle (Thrust = 4.5N)	**Parachute Arial vehicle (Thrust= 7.75N)**	**Parachute Arial vehicle (Thrust = 9N)**
Alpha_p (deg)	10	8	7
Theta_p (deg)	0	8	10
Gamma(deg)	-8	0	7

Table 4.4. Alpha, beta and gamma values for various thrust conditions

From the figure 4.8, the theta value can be observed, while landing there is glide angle of approximately 8 degrees.

Figure 4.9, shows that, at 0N thrust the vehicle loses 150ft altitude as it move 450ft forward. Theoretically the L/D ratio of a ram air Parafoil is 3. From this Figure 4.9 the ratio of the altitude lost to the distance covered is 3, which can be validated with the Lingard's L/D value. It can be further concluded that, as the thrust increases the amount of altitude lost decreases. Figure 4.9, further describes that under gliding condition the Parafoil vehicle loses 70 m as it travels 240 m.

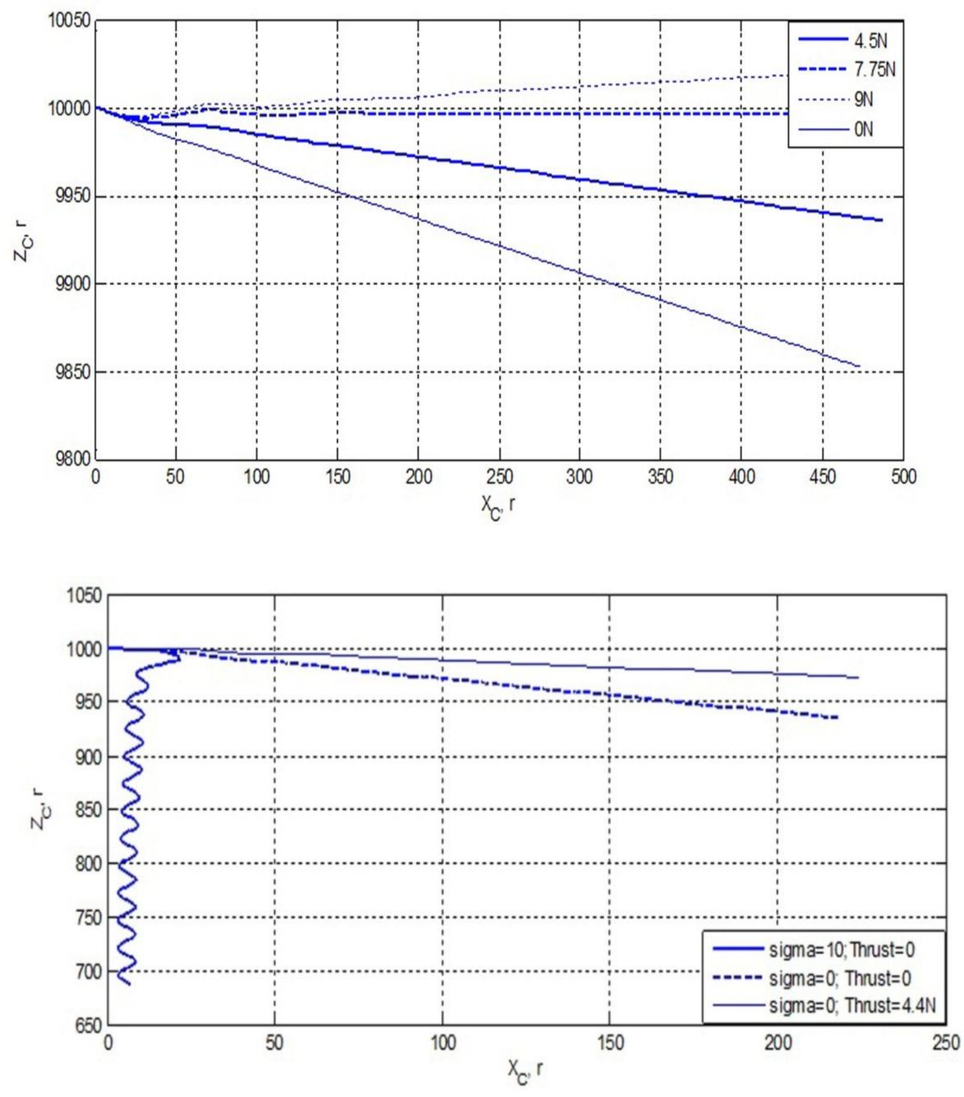

Figure 4.9. Altitude loss at various thrust and sigma inputs.

When the thrust is added to the vehicle the vehicle covers a distance up-to 300ft to lose an altitude of 60ft. To land the vehicle with in the glide range one end of the steer bar should be pulled so that the vehicle turns and make spiral landing. Figure 4.9 shows the front view and the top view of the direction control model keeping the canopy tilt angle to be 10 degrees. Keeping the sigma value to be 10 degrees, the Y_c, X_c, plot is as shown in the figure 4.10.

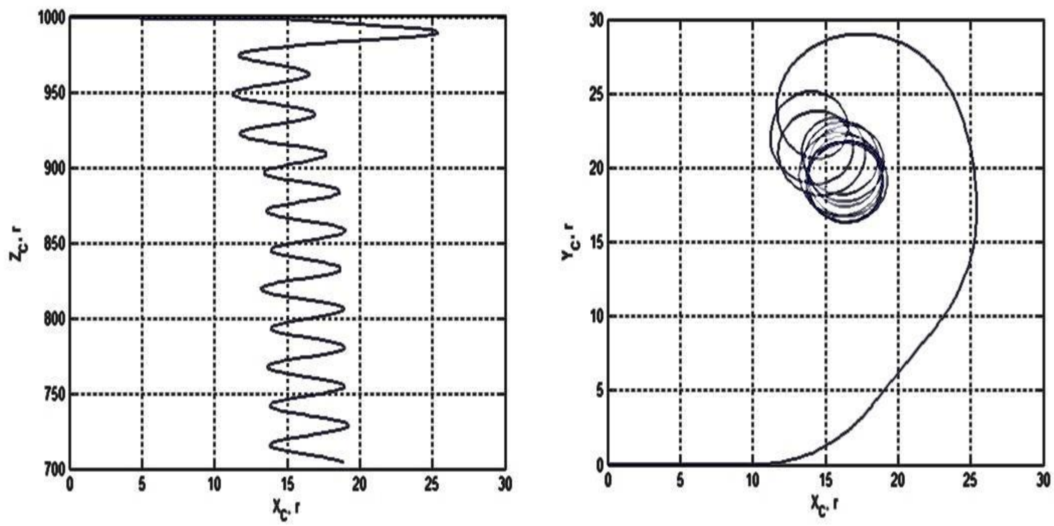

Figure 4.10. X_c Vs Z_c and X_c Vs Y_c Plot with $\delta = 10$ degrees

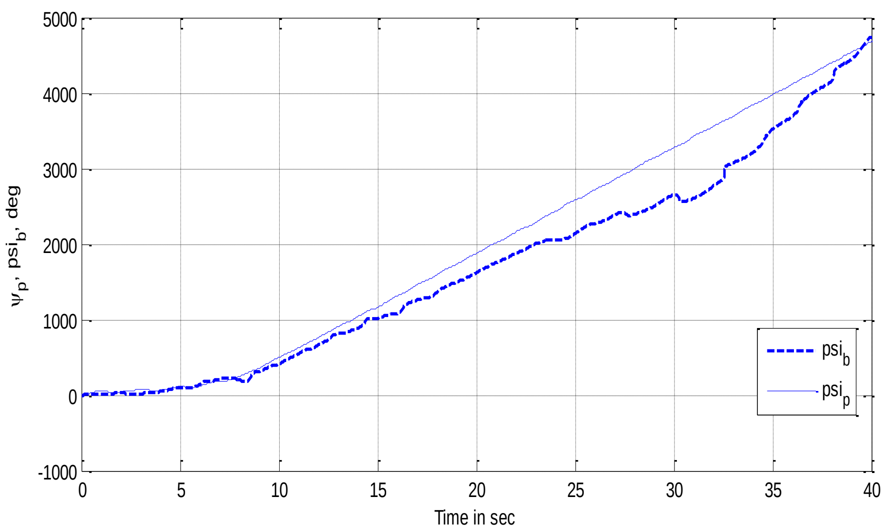

Figure 4.11.psi_b, psi_p Vs Time

The psi_b and psi_p curve with respect to time is plotted for about 5000 degrees with the sigma value 10 degrees as shown if figure 4.11. It is observed that the payload tends to have certain oscillations but after certain time it tries to re-orient itself when Parafoil yaws during a turn.

Cases	**Tilt Angle (Degrees)** δ_s	**Turn Rate (Degrees/Sec)**
A	+20	20
B	+10	10
C	+5	5
D	+2	2
E	-2	-2
F	-5	-5
G	-10	-10
H	-20	-20

Table 4.5. Tilt Angle and Turn Rate values for various cases

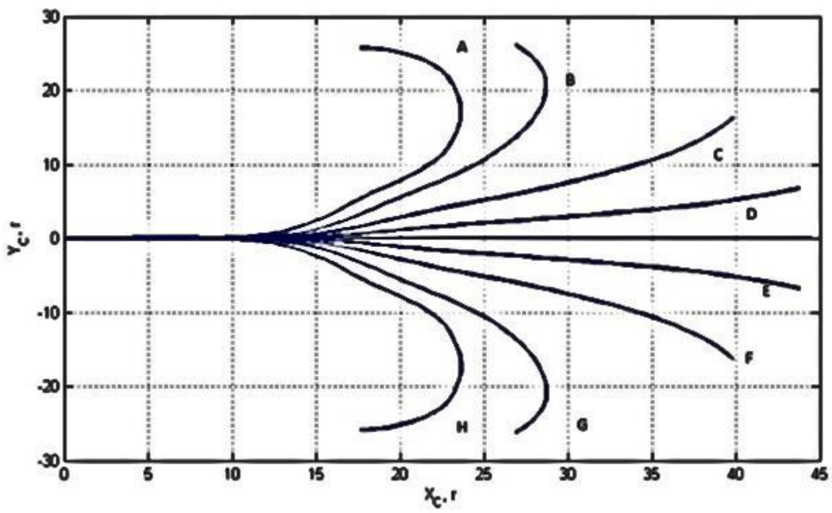

Figure 4.12. Canopy Tilt angle Vs Horizontal Distance Covered (Simulated and Flight Results)

Figure 4.12 shows the response of the powered Parafoil vehicle with different canopy tilt angles. For positive tilt angle the vehicle turns in the positive Y direction and for negative tilt angle the vehicle moves in the negative Y direction. Figure 4.13 shows the turn rates for various tilt angles under various cases, A, B, C, D, E, F, G, H, I. In the practical flight test the vehicle was responding in the similar manner, i.e. when the servo tilts right the vehicle also moves right and when servo tilts left the vehicle also turns left and the same can be observed in figure 4.13.

S.No	Servo	Simulated Radius (m)	Flight Test Radius (m)
1	Minimum Servo Angle	25m	18m
2	Maximum Servo Angle	50m	52m

Table 4.6. Turning Radius Vs Distance Covered (Simulated and Flight Results)

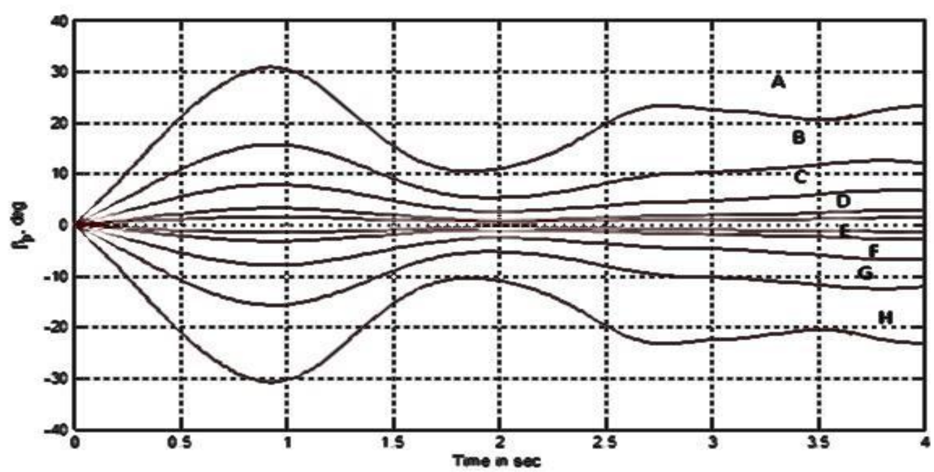

Figure. 4.13. Turn Rate Vs Time

As seen in the figure 4.12, it can be observed that the vehicle took 18m radius to turn with minimum servo turn. Similarly the vehicle took 52 m radius to turn with maximum servo turn.

4.13 OPEN LOOP FLIGHT TEST RESULTS

As discussed in chapter 3, open loop flight tests were done to understand the system behavior. Flight tests were done for take-off, landing and turn performance analysis.

These results would give an insight about the attitude of the Powered Parafoil Aerial Vehicle. Which helped us in interpreting the controller gain values as discussed in chapter 3.

4.13.1 Take-Off Mode

During the take-off mode the pitch angle observed is about 20 degrees. These variations are due to vibration of the motor.

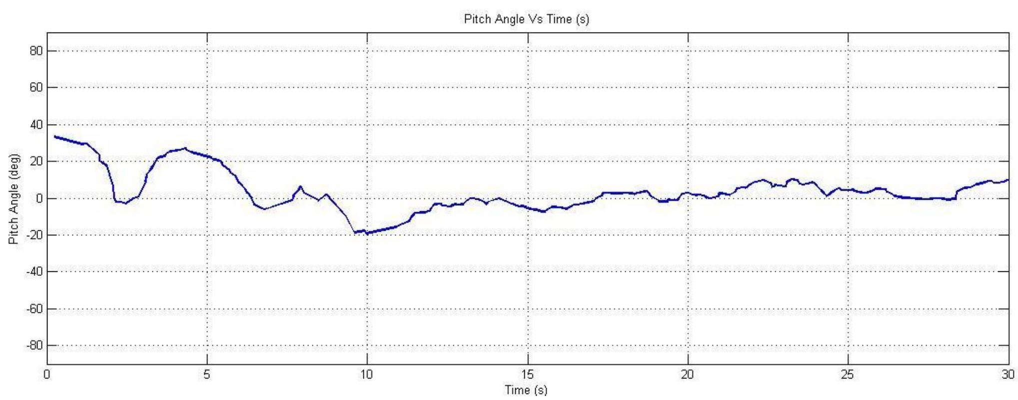

Figure. 4.14. Pitch Variation of PAV during Take off

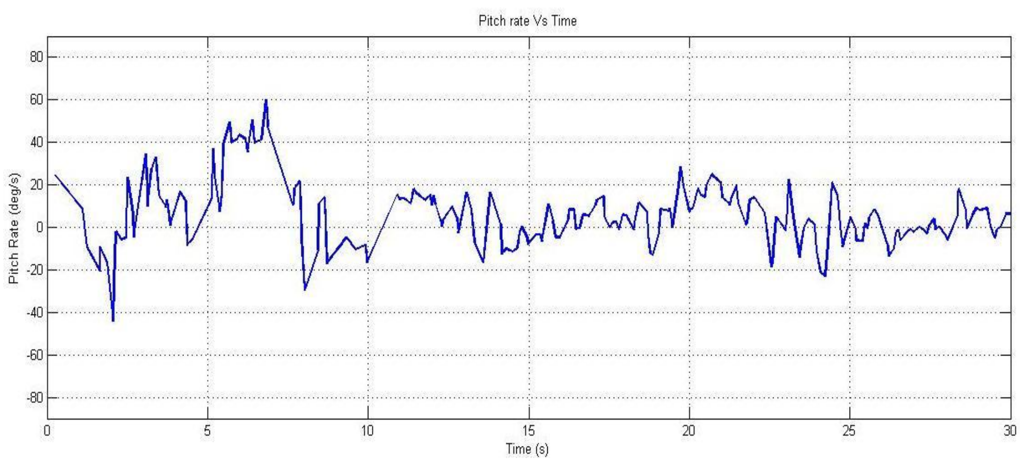

Figure. 4.15. Rate of Pitch Variation of PAV During Take Off

The pitch angle tends to increase indicating that the vehicle tends to climb for 7 seconds. After 7 seconds the PAV tried achieve a level flight decreasing the pitch angle. The rate of pitch also is also maintained about zero. This can be observed in figures 4.14 and 4.15.

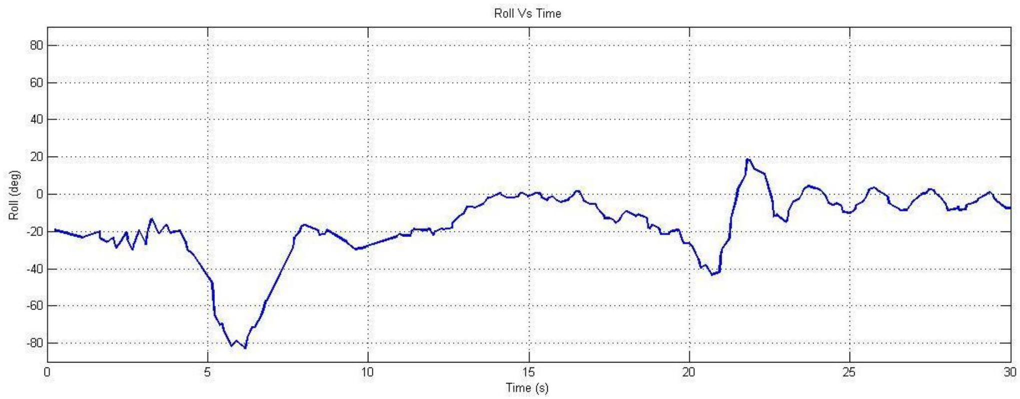

Figure 4.16. Roll Variation of PAV During Take Off

The roll variation is about -20 degrees initially. This initial angle is due to the turn as seen in the latitude lomgitude graph. The variations are due to the vibrations due to the motor attached on the payload. Figure 4.16 and 4.17 replictes the same. The roll rate is also about zero degrees due to the static stability of the vehicle. The oscillation are about +/- 20 degrees.

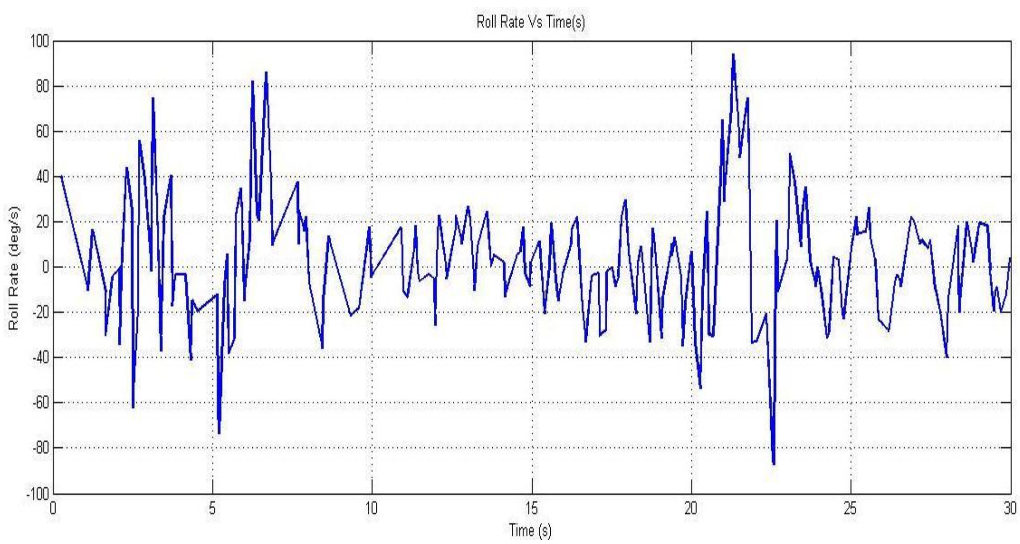

Figure 4.17. Roll Rate Variation of PAV During Take Off

The vibrations are observed due to the large motor propeller. It can be highlighted that due to the vibrations a variation in the values are observed. The range of the variations tends to be very small. In figure 4.18 it can be observed that the PAV take off and the takes a left turn

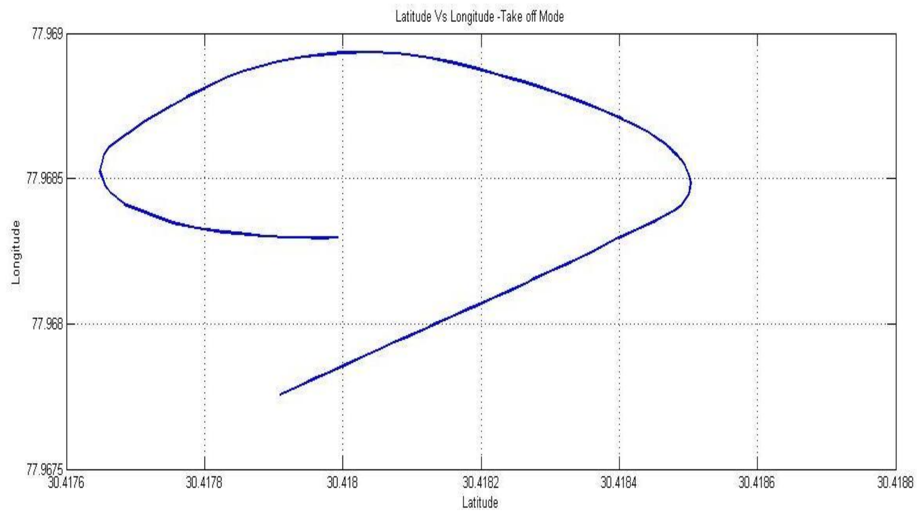

Figure 4.18. PAV Latitude and longitude Positions During Take-Off.

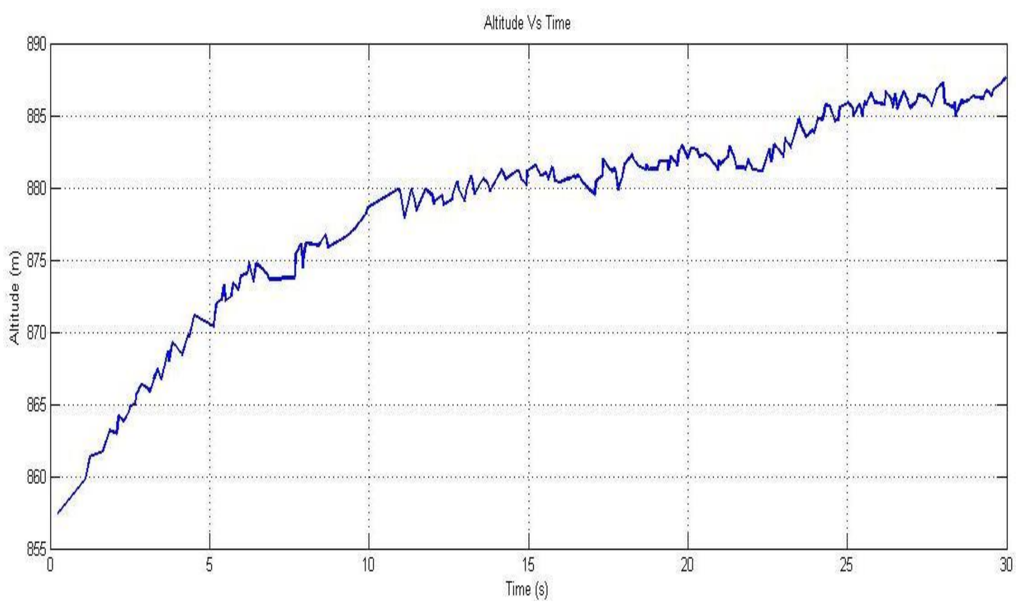

Figure 4.19. PAV Altitude variation during the takeoff

Figure 4.18 and 4.19 shows the PAV position with respect to latitude, longitude and altitude. The PAV tends to gain an altitude of 30m in 250ms.

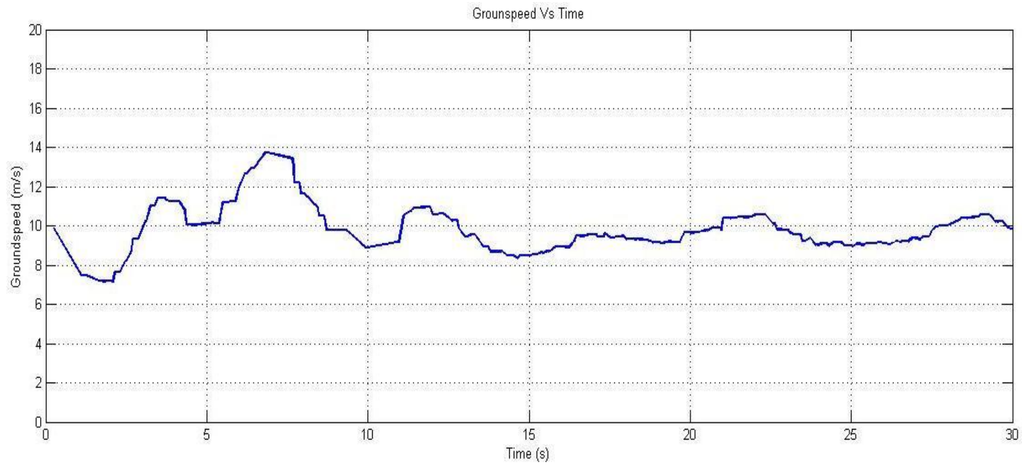

Figure 4.20. PAV Ground Speed during Take-Off

The ground speed remains to be approximately 10m/s during take-off which can be seen in figure 4.20. It can be further observed from figure 4.18 and 4.19 that during the take-off flight, while the vehicle is turning it there are less number of oscillations, while the vehicle is climbing up oscillations is more.

4.13.2 Landing

During the landing mode the pitch angle observed is about -2.5 degrees. These variations are due to vibration of the motors. The pitch angle tends to decrease indicating that the vehicle is tending to climb down. The rate of pitch also is also maintained about zero. The same can be seen figure 4.21 and 4.22.

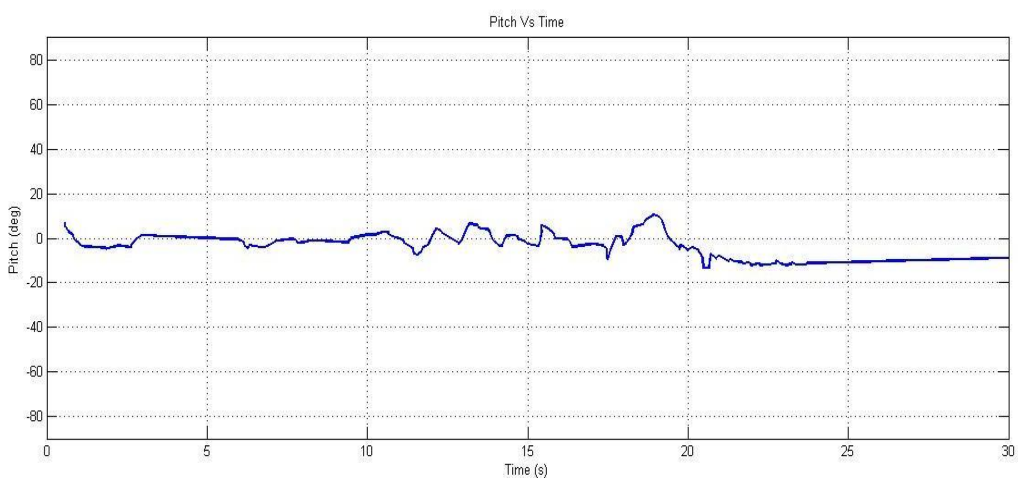

Figure 4.21. Pitch Variation of during Landing

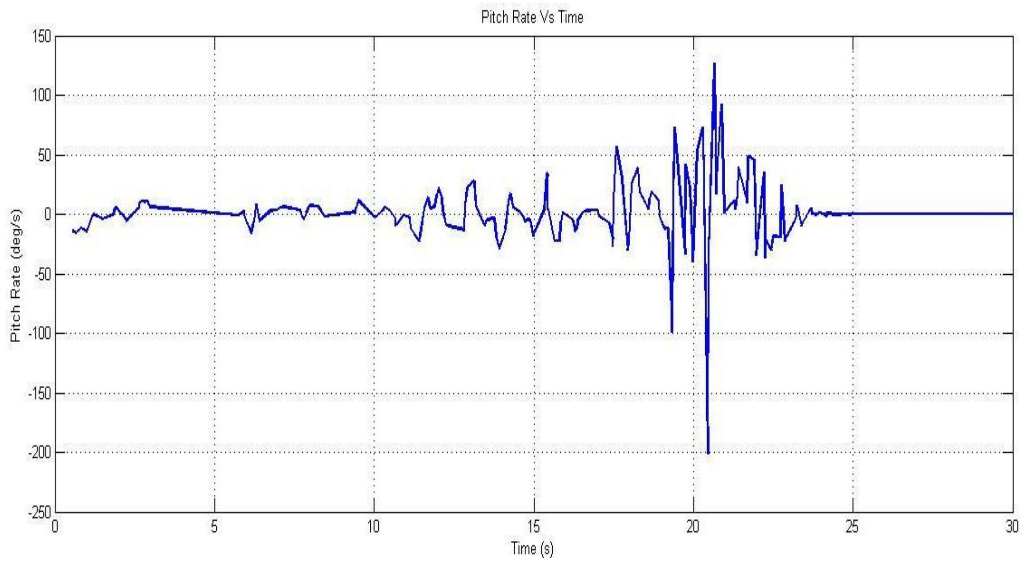

Figure 4.22. Pitch Rate Variation of during Landing

The roll variation is about 11 degrees. The variations are due to the vibrations due to the motor attached on the payload. Figure 4.23 and 4.24replictes the same.

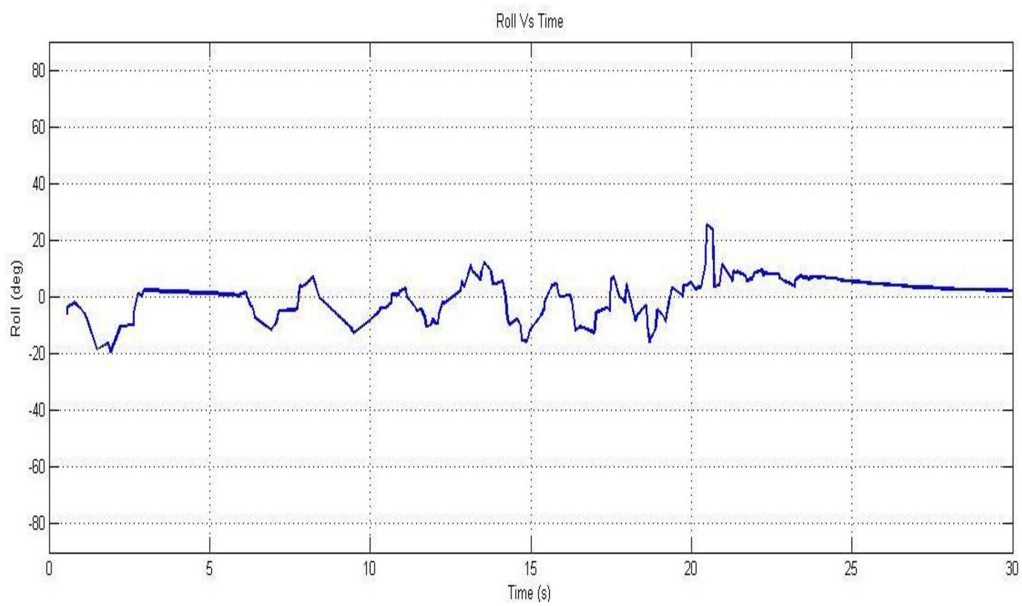

Figure 4.23. Roll Variation of PAV during Landing

The roll rate is also about zero degrees due to the static stability of the vehicle. The oscillation are about +/- 5.7 degrees.

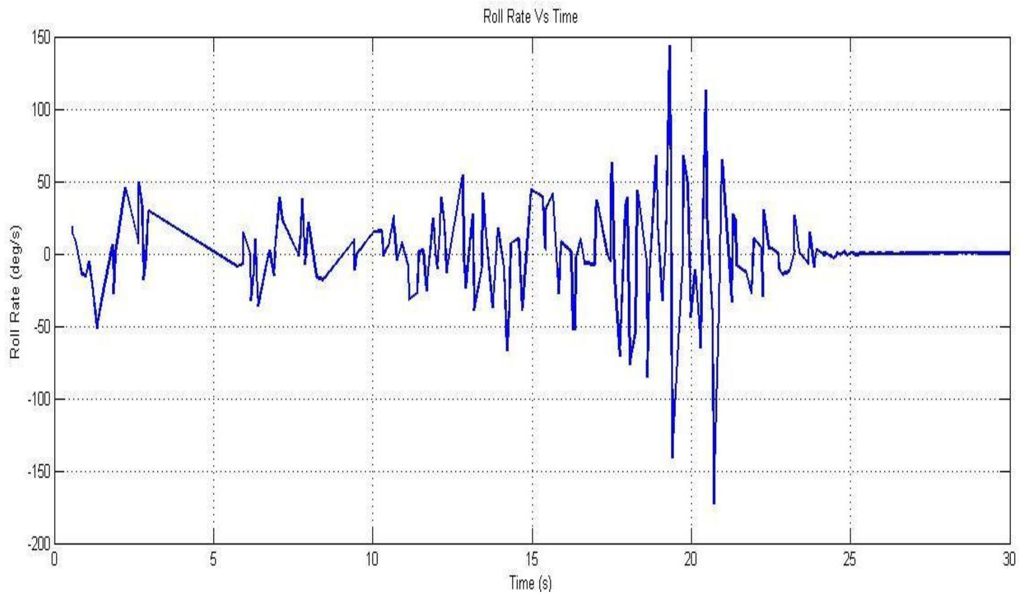

Figure 4.24.Roll Rate Variation of PAV during Landing

The Yaw Pitch and Roll values are plotted while take off the. The vibrations are observed due to the large motor propeller. A lot of oscillations are found in pitch rate, roll rate and yaw rate during touch down. These oscillations are due to the flare maneuver. Figure 4.25 shows the PAV position with respect to latitude, longitude and altitude.

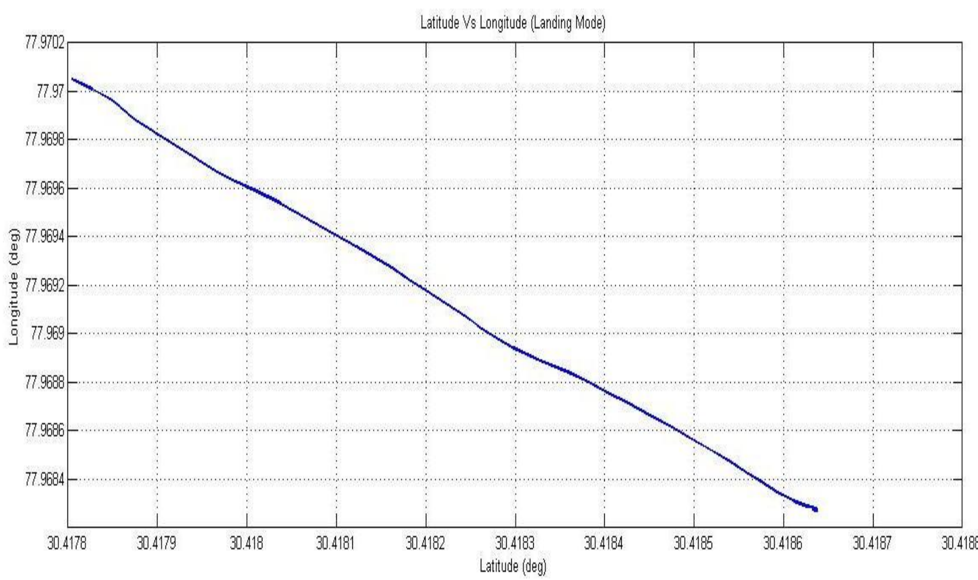

Figure 4.25. Latitude and Longitude variation of PAV during Landing

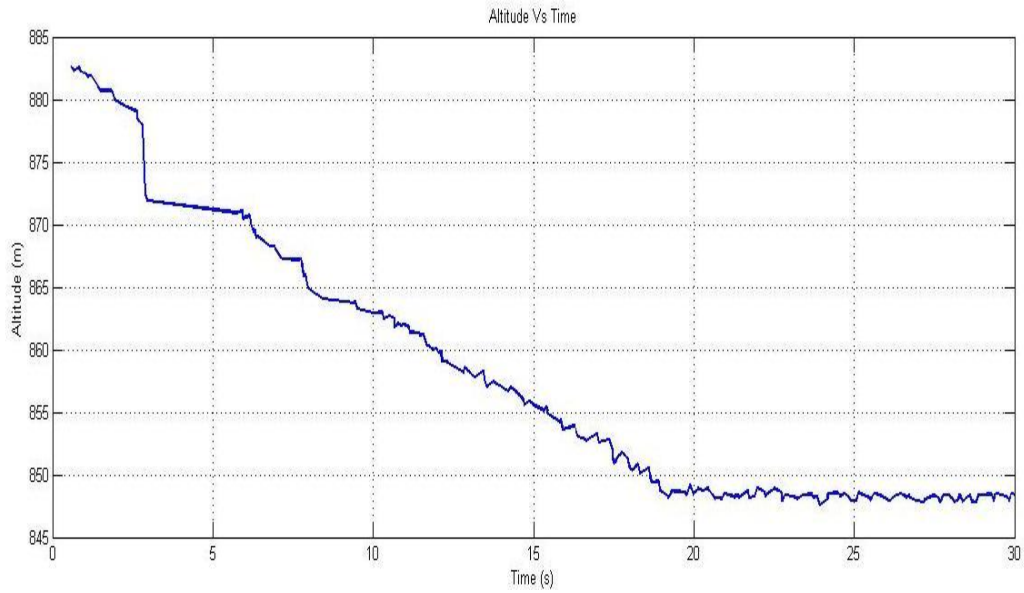

Figure 4.26. Altitude Variation during Landing

PAV loses an altitude of 40 meters in 20 seconds with a minimum thrust provided as seen in figure 4.26.

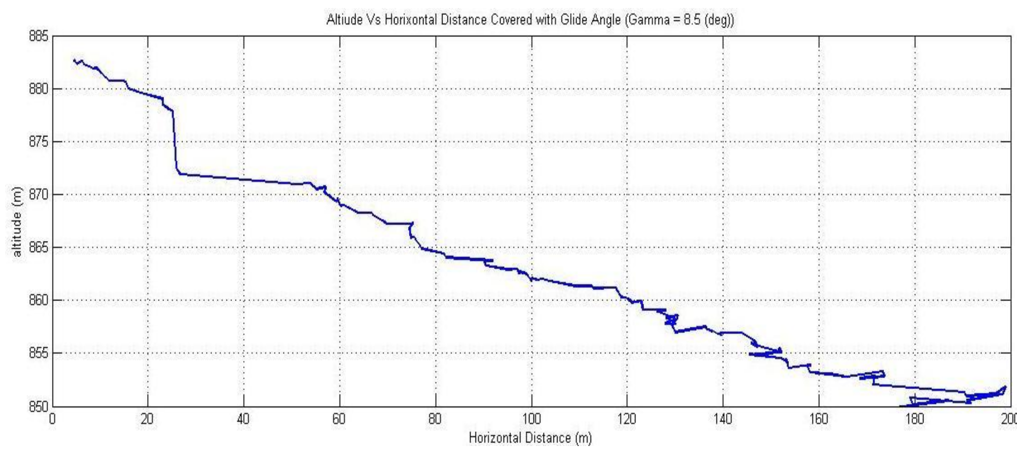

Figure 4.27. Altitude lost to the horizontal distance covered

In figure 4.27 the gamma angle tends to be 8.5 degrees which can be seen by horizontal distance covered to the altitude lost graph

The ground speed value of the vehicle remains to be 10 m/s, as discussed in chapter 3; theoretically the velocity of the vehicle tends to be in 10m/s, as seen figure 4.28.

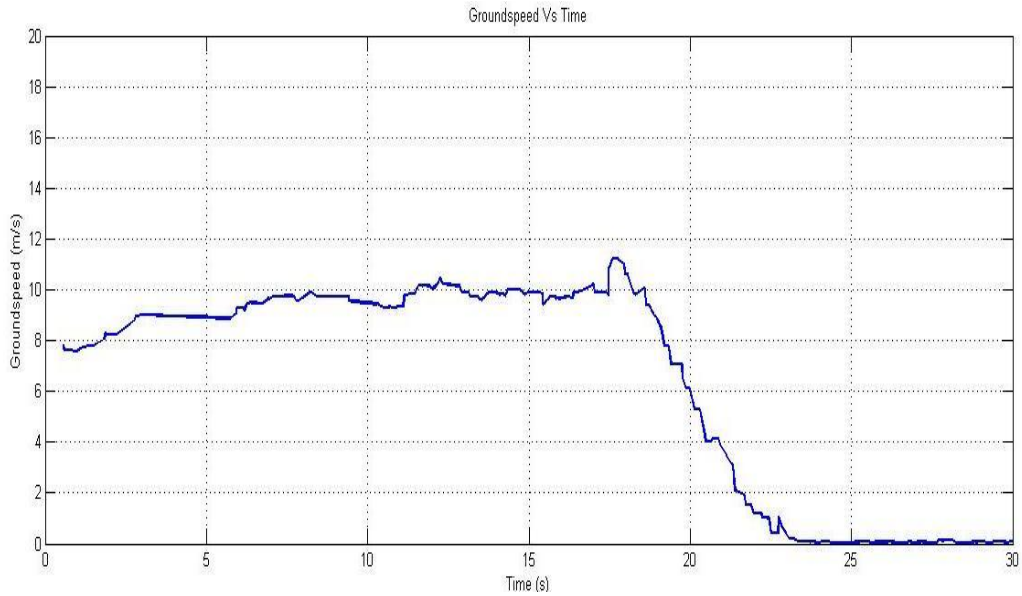

Figure 4.28. PAV Groundspeed during Landing

4.13.2 Turn Flight

During the take-off mode the pitch angle observed is about zero degrees. The variation in roll is about zero degrees which is very less.

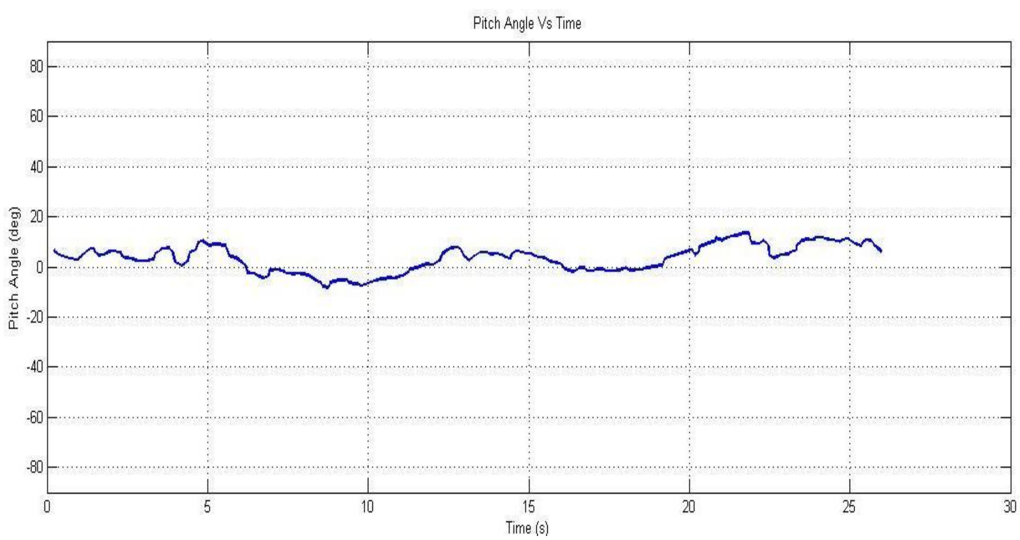

Figure 4.29. Pitch Variation During PAV Turning Flight

These variations are due to vibration of the motors. The pitch angle tends to be around zero indicating that the vehicle tends to maintain level flight. The rate of pitch also is also maintained about zero. The same can be seen figure 4.29 and 4.30.

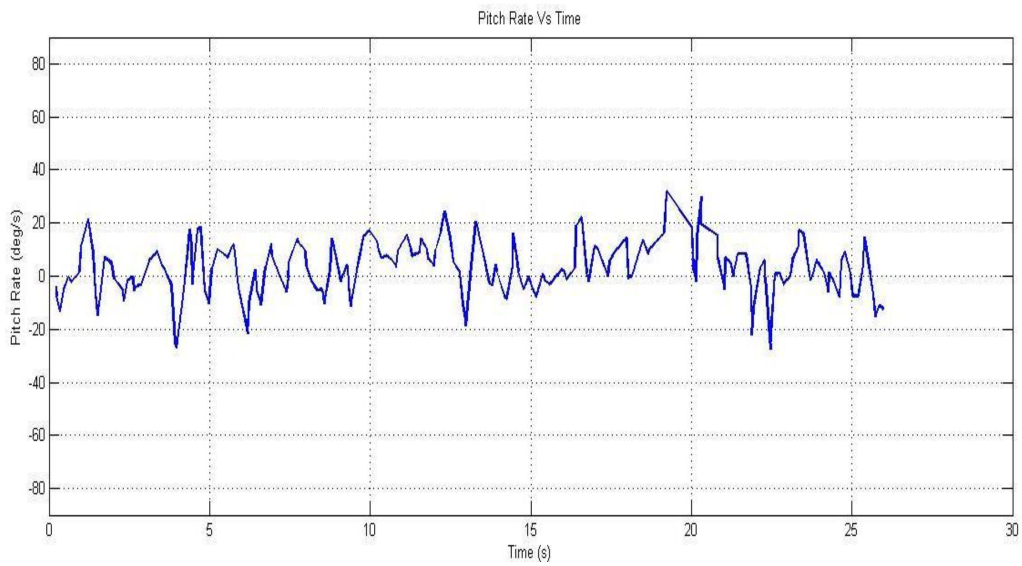

Figure 4.30. Pitch RateVariation During PAV Turning Flight

The roll variation is about zero degrees which is again negligible. The variations are due to the vibrations due to the motor attached on the payload. Figure 4.31 and 4.32 replictes the same.

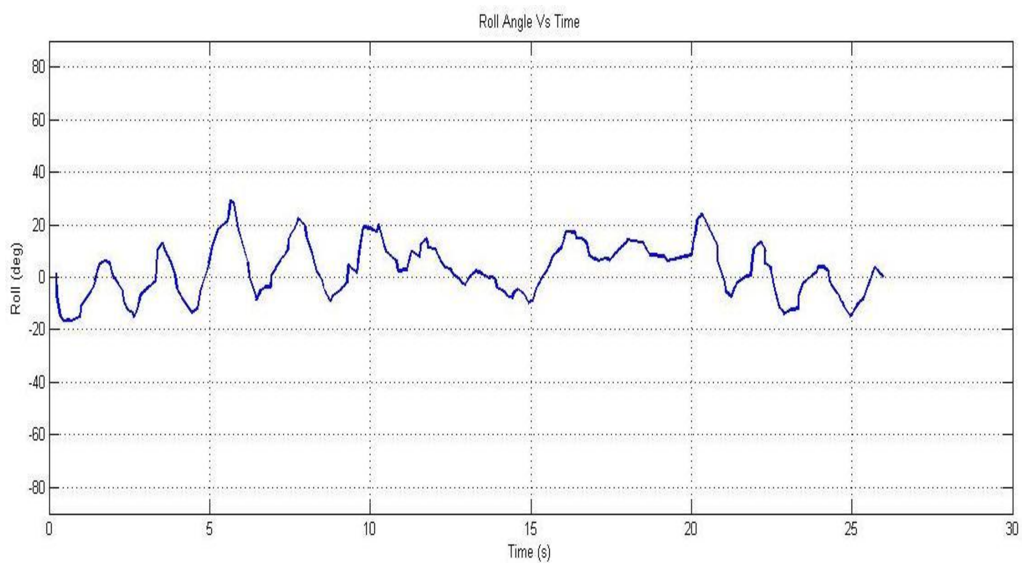

Figure 4.31. Roll Variation During PAV Turning Flight

The roll rate is also about zero degrees due to the static stability of the vehicle. The oscillation are about zero degrees which again very low. It can be observed from figure 4.31 that during the turn (from 14 seconds to 19 seconds) there was a cnage in roll angle of about 10 degrees due to the turn.

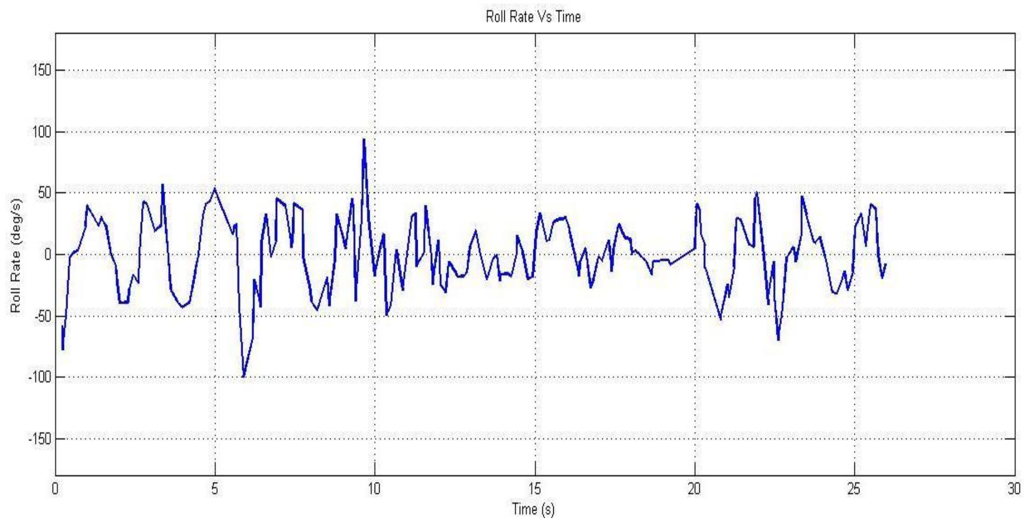

Figure 4.32. Roll Rate Variation During PAV Turning Flight

Figure 4.33 shows the PAV position with respect to latitude, longitude and altitude. There is no altitude change and the vehicle is maintaining a turn rate of 18 deg/s.

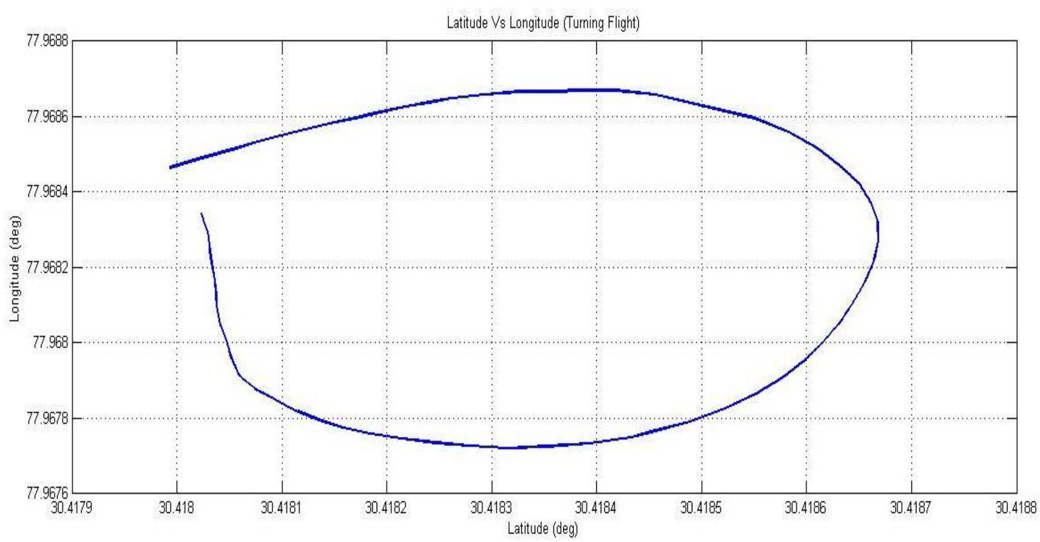

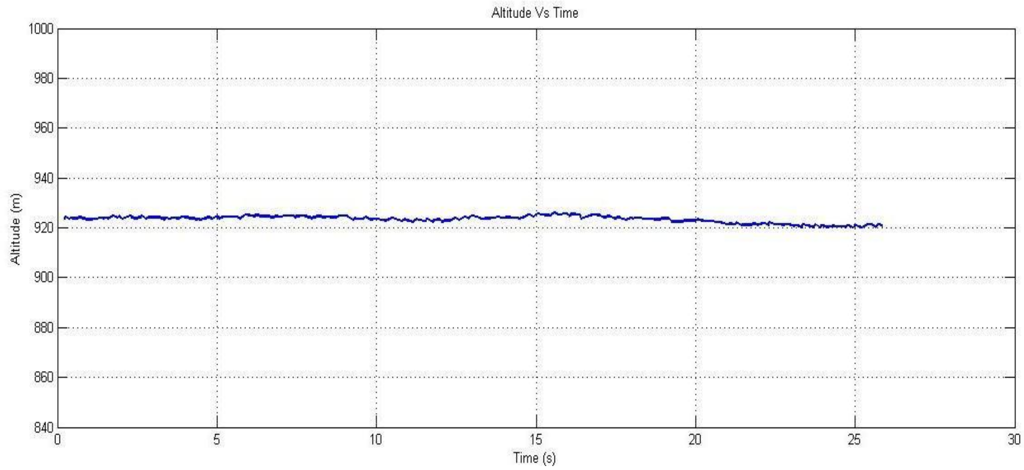

Figure 4.33. Latitude, Longitude and Altitude Variation During PAV Turning Flight

Figure 4.34 shows that the glide angle for the level flight is 0. When seen from altitude lost with respect to the horizontal distance covered. Since the PAV is in level flight as discussed in the open loop simulation result the glide angle is zero.

Analytically, as discussed in chapter 3, the velocity is 10 m/sec using the empirical formula, It can also be seen from figure 4.35 that the PAV maintains a velocity of 10 m/s for level flight and during the turn the velocity goes up to 12 m/s. and the vehicle tends to loose the altitude which is then covered up by increasing the speed to 12 m/s.

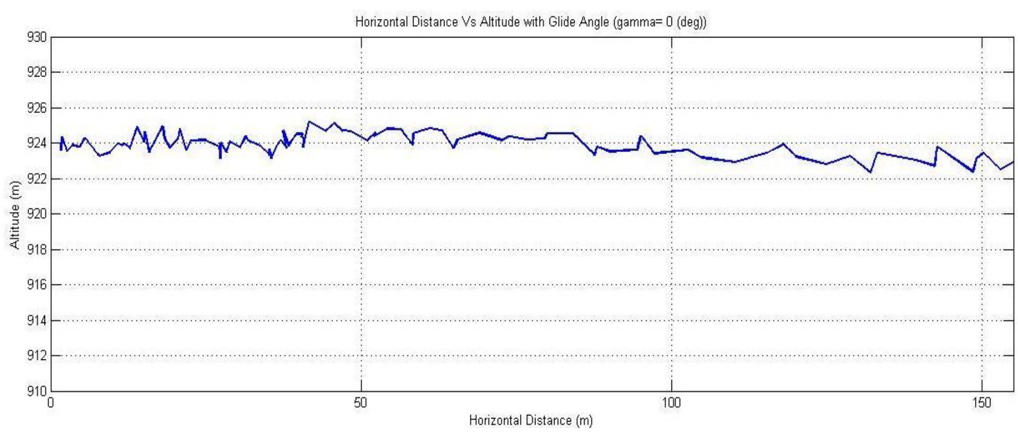

Figure 4.34. Altitude lost to the horizontal distance covered During PAV Turning Flight

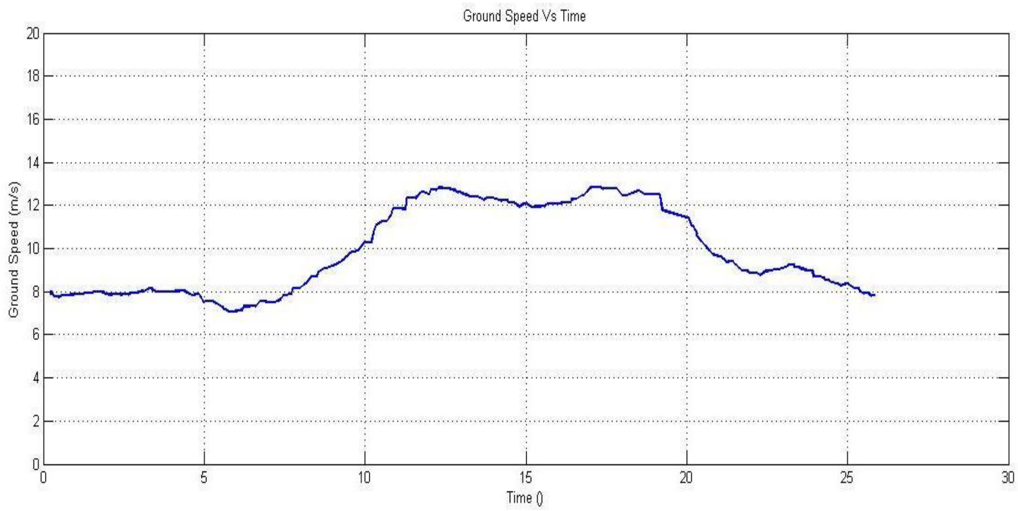

Figure 4.35. Velocity During PAV Turning Flight

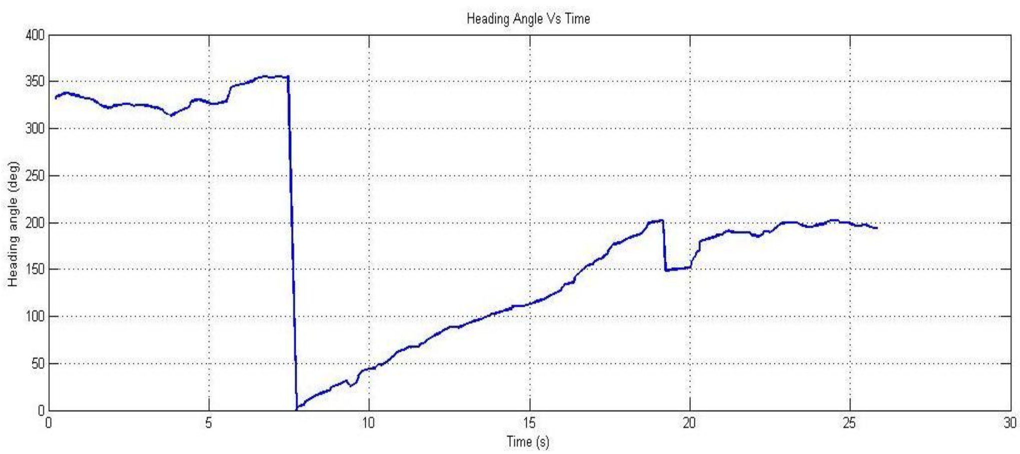

Figure 4.36. Heading Angle During PAV Turning Flight

From the figure 4.36, in the heading angle graph, it can be observed that the PAV is taking turn from 14 seconds to 19 seconds, at the turn rate of 18 deg/s with a bank angle of 10 degrees. It can also be observed that the vehicle took a smooth turn in figure 4.36. All the observations in this section are done on Payload. A lot of oscillations/ vibrations are seen in the graphs as the sensors are placed on the Payload. The vibrations on the Parafoil would be comparatively lesser. Pitch angle, Glide Angle, heading angle, latitude, longitude, altitude and ground speed give the performance analysis of the complete system. The above mentioned graphs would help us in understanding the Parafoil performance.

4.14 COMPARISON OF SIMULATED VS FLIGHT RESULTS

The results are classified in two categories. The first part of the results shows the validation of the developed simulation results with Lingard and Flight test results during the unpowered glide condition and the second part shows the direction control using a single servo, which will help us in understanding the servo tilt and turn condition of the Parafoil.

4.14.2 Pitch angle, Glide angle and Angle of Attack Results during Unpowered Glide Condition

The developed Powered Parafoil Aerial vehicle model has been validated using the Lingard model. Angle of attack (alpha), pitch angle (theta) and glide angle (gamma) values obtained are compared with the Lingard values under no thrust conditions. The model is validated using the Lingard results by checking the values of angle of attack (alpha), pitch angle (theta) and glide angle (gamma) of the Parafoil with respect to time.

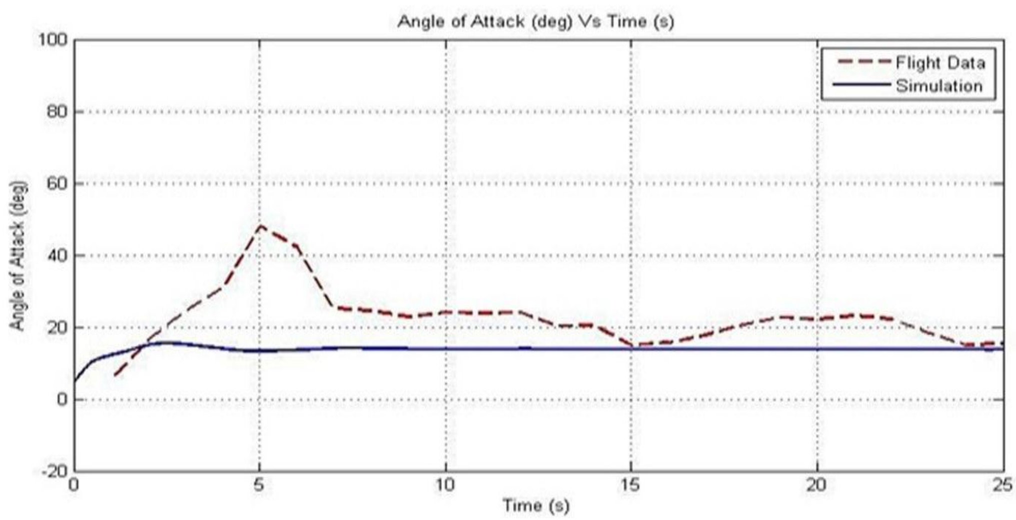

Figur.4.37. Angle of Attack Simulated Vs Flight Test

	Lingard	Simulated Parafoil Arial vehicle no thrust condition
Alpha_p (deg)	3	5
Theta_p (deg)	-9	-10
Gamma(deg)	-18	-18

Table 4.7. Powered Parafoil Model validation with Lingard's Model

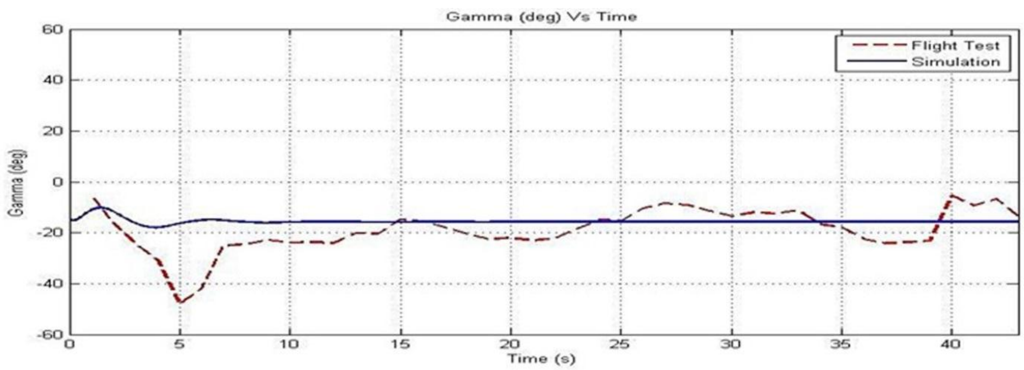

Figure.4.38. Glide Angle Simulated Vs Flight Test

Keeping the zero thrust value under unpowered condition, the simulated and flight test values of angle of attack (alpha), pitch angle (theta) and glide angle (gamma) of the Parafoil are plotted with respect to time. The same can be observed in figures 4.37 through 4.39. It can be observed from figure 4.38 that the glide angle gamma replicates the Parafoil condition. The actual and flight test data approximately match the same.

	Simulated Results of Parafoil Arial vehicle with zero thrust condition	Flight Test results of Parafoil aerial vehicle under zero thrust
Alpha_p (deg)	12	13
Theta_p (deg)	-5	-5
Gamma(deg)	-18	-17

Table 4.8. Simulated Powered Parafoil Model Comparison with Flight Test data

In the figure 4.39, during the simulation, there tends to be oscillations for a time period of 5 seconds as the system is the dynamic system. The same pattern is observed in flight test but there are internal oscillations due to the pendulum effect of the payload. The same can be treated as phugoid dynamics as in aircraft.

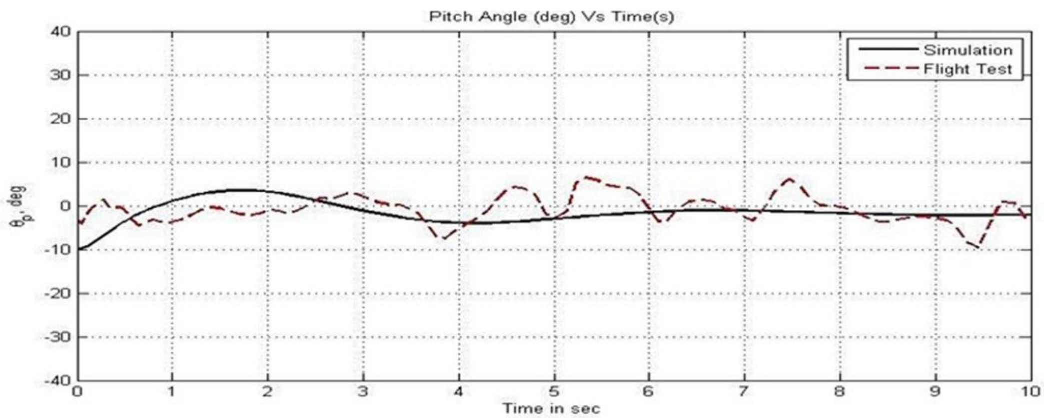

Figure.4.39. Pitch Angle Simulated Vs Flight Test

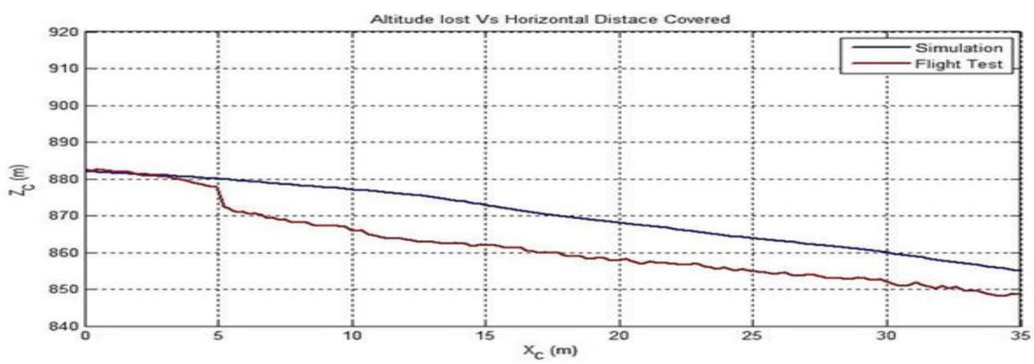

Figure.4.40. Comparison of Altitude lost and Horizontal Distance Covered, Simulated Vs Flight Test

Theoretically the L/D ratio of a ram air Parafoil is 2.5 as discussed in chapter 3. From this Figure 4.38 the ratio of the altitude lost to the distance covered almost remains to be the same in case of the practical and simulation results. As seen in the figure 4.40 there is a sudden drop of height in the flight test result initially after five seconds but it maintains the same glide ratio as that of the simulation in the later stage. The glide rate (gamma) as in the above figure tends to be following the same manner. The estimated glide rates are used to estimate the lift and drag coefficients needed for the dynamic model. The estimated glide angle is 15 degrees. The PAV covered 12mts distance for a loss of altitude of 10mts.

4.14.3 Direction Control Using a Single Servo

Parafoils are made up of flexible membranes. Therefore, pulling down one side would deflect the Parafoil resulting in a turn. In this model the two ends of the Parafoil is attached to a single control called "Fly-Bar" unlike the conventional systems. Deflection of the fly-bar helps the Parafoil to tilt to one side. The two rotations that can be observed in these kinds of vehicles are yaw and pitch.

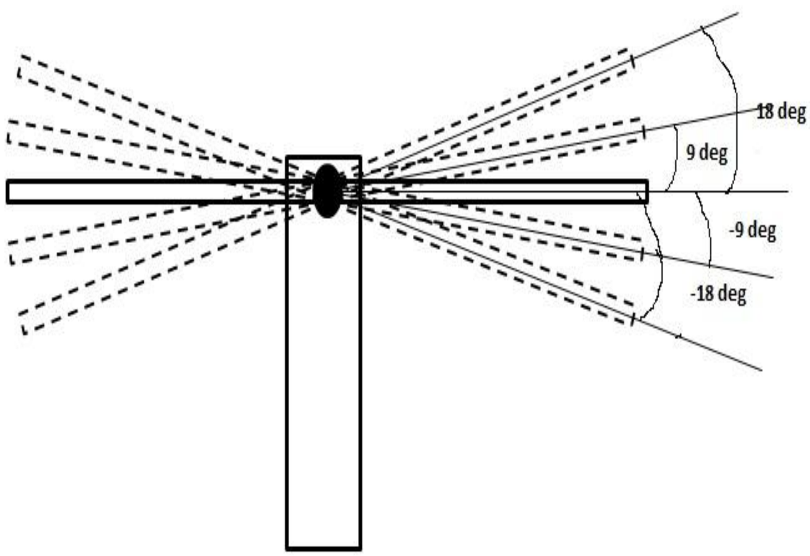

Figure 4.41. Control Deflection of Fly-Bar

The figure above (4.41) indicates how the fly-bar works and helps in tilting. It is observed that there was a maximum turn with a tilt of 18 degrees to the right for right turn and 18 degrees to the left. Here the flight test is performed at an altitude 890 m providing a constant thrust of 7.75N indicating the level flight. This test is performed to analyze the turn performance due to the servo tilt.

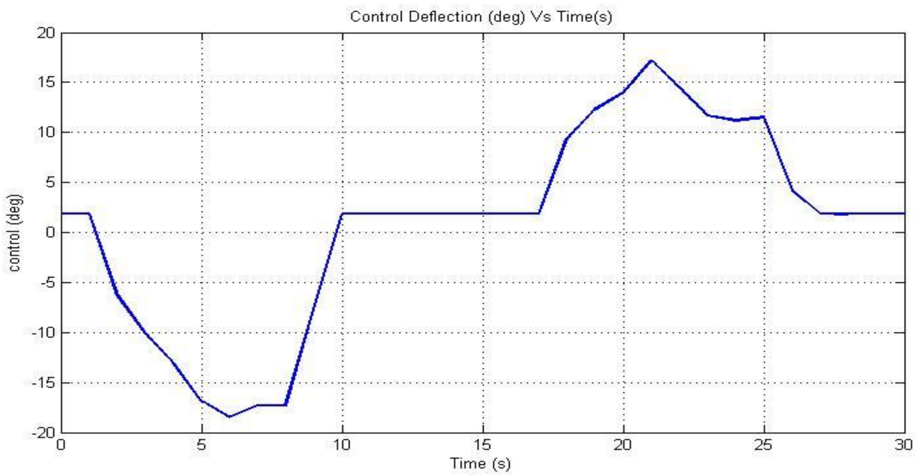

Figure.4.42. Fly- Bar Deflection

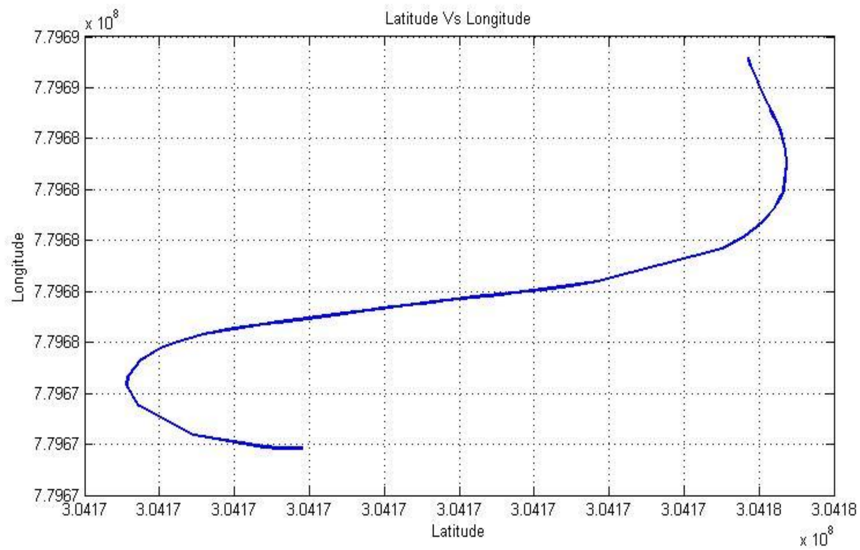

Figure.4.43. Flight Path with the Given Fly-Bar Deflection

Figure 4.42 shows the servo tilt in positive and negative side going maximum upto +/- 18 degrees. Figure 4.43 shows the change in direction indicating an ‘S’ turn. The yaw change is also seen in figure 4.44 oscillating between +/- 15 degrees. The experiment was performed for 30 seconds.

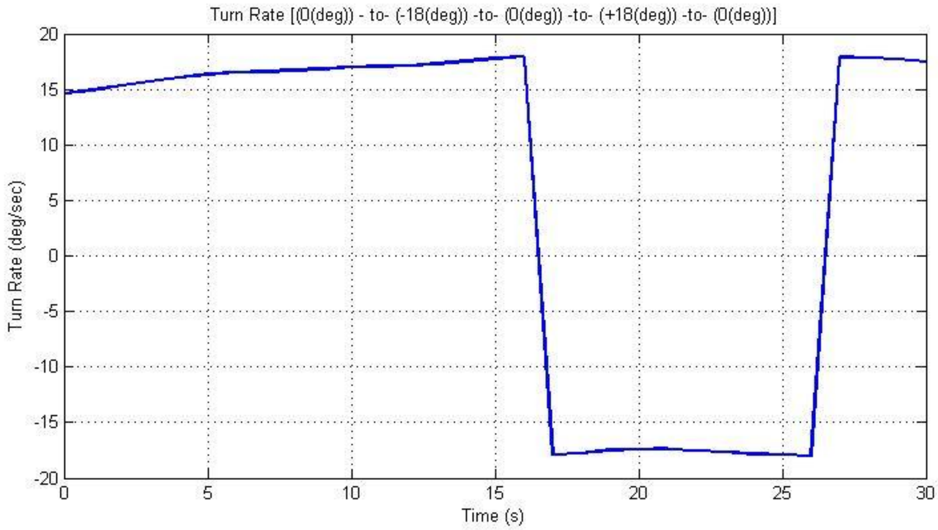

Figure.4.44. Turn Rate with the Given Fly-Bar Deflection

CHAPTER 5

CONTROL SYSTEM DESIGN AND ALGORITHM

5.1.GUIDANCE LOGIC

The task of guidance logic is to generate heading and altitude signals that will enable the PAV to follow desired path specified by the sequence of points. For the autonomous flight conducted, the only concern was to maintain the altitude; hence, the guidance logic is only concerned with the heading angle of the vehicle in the horizontal plane. A simple scheme was implemented as depicted in the figure 5, which shows the guidance logic, specified distance to generate heading angle that will direct PAV back to the path between the waypoints.

5.1.1. Lateral Heading controller

The controller has a heading tracking algorithm, which receives the target heading angle from the higher level guidance logic and outputs a control signal to minimize the error between the measured and the target heading [42].

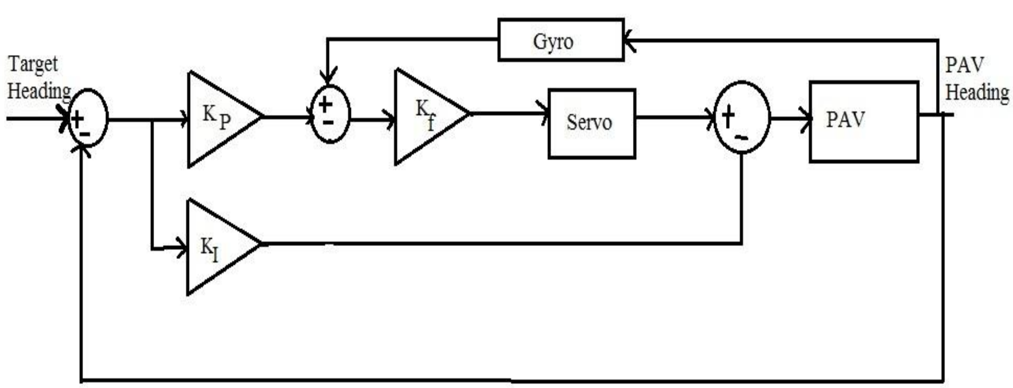

Figure 5.1 Lateral Heading Controller Powered Parafoil Aerial Vehicle

Classical feedback compensation controller was adopted such that the gyroscope output can be used directly. The servo is modeled by simple first order transfer. The servo transfer function is simply

5.1.2. Longitudinal Altitude Controller

The controller has an altitude tracking algorithm, which receives the target altitude from the guidance scheme and outputs throttle signal to minimize the error between measured and the target altitude [42]. A classical proportional, integral and derivative (PID) controller was implemented.

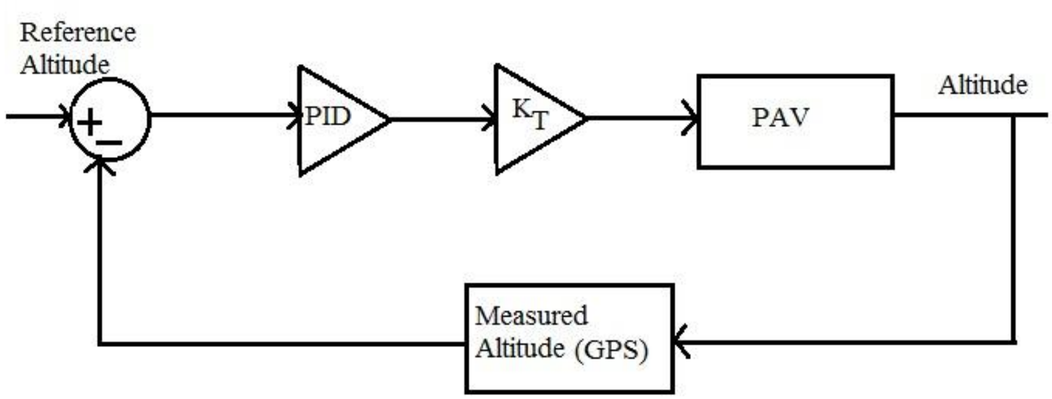

Figure 5.2 Altitude Hold Controller Powered Parafoil Aerial Vehicle

A throttle control regime has been developed. A PID controller has been and is implemented in the cascade configuration scheme. The PID is used to supply the exact signal to be supplied to the motor to eliminate the steady state altitude error. A simple feedback loop has been used to stabilize the PAV. A relationship between thrust and altitude is developed so altitude gained is linearly proportional to the throttle provided. The throttle is allowed to vary from 0 to unity.

5.1.3. Attitude

The attitude of the PAV is controlled by a nested PI->PID loop. Tuning the inner PID loop is essential to good stable flight. The outer PI loop is less sensitive and effects mostly the style of flying desired (fast or slow). The inner PID loop looks at the desired rate of angular rotation and compares that to the raw gyro output. The difference is feed back into the PID controller and sent to the motor to correct the rotation. This is the heart of both Rate mode, Stabilize mode, and all other modes. It is also the most critical gain to adjust for PAV. The outer PI loop generates the desired rate of angular rotation. The input for this loop can either be user with stick movement, or the stabilizer, which tries to achieve a specific angle.

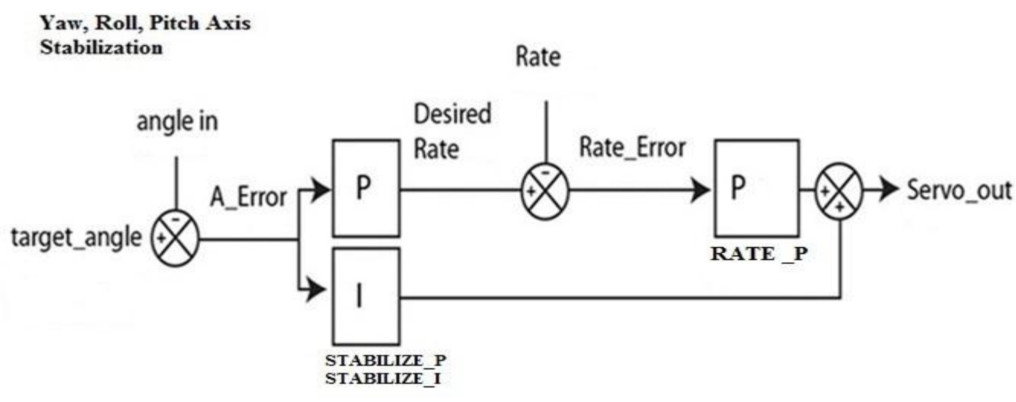

Figure. 5.3. Roll, Pitch and Yaw Axis Stabilizer for Powered Parafoil Aerial Vehicle

- STABILITY_ P is 1.3 or 1.3° per second rotation for every 1° of error. If you want more or less speed of rotation based on user input, adjust this value.
- STABILITY_I is 0.1, used to overcome imbalance in the PAV. If the PAV is not symmetrical this term will bring the PAV to level. The higher the number the faster the PAV will compensate. Low numbers can have adverse effects by causing a very slow oscillation measured in seconds.
- RATE_ P is the proportional response and the default is 0.2. The PAV will vary quite a bit depending on the weight and thrust of the motor.

5.1.4. PI control for Loiter and Navigation

Loiter and navigation uses the same PID rate controllers. The location error is calculated in centimeters for X (Longitude) and Y (Latitude) which is fed to the controller. The first stage of the controller takes the XY position error and decides how fast the PAV should go to reach the correct location.

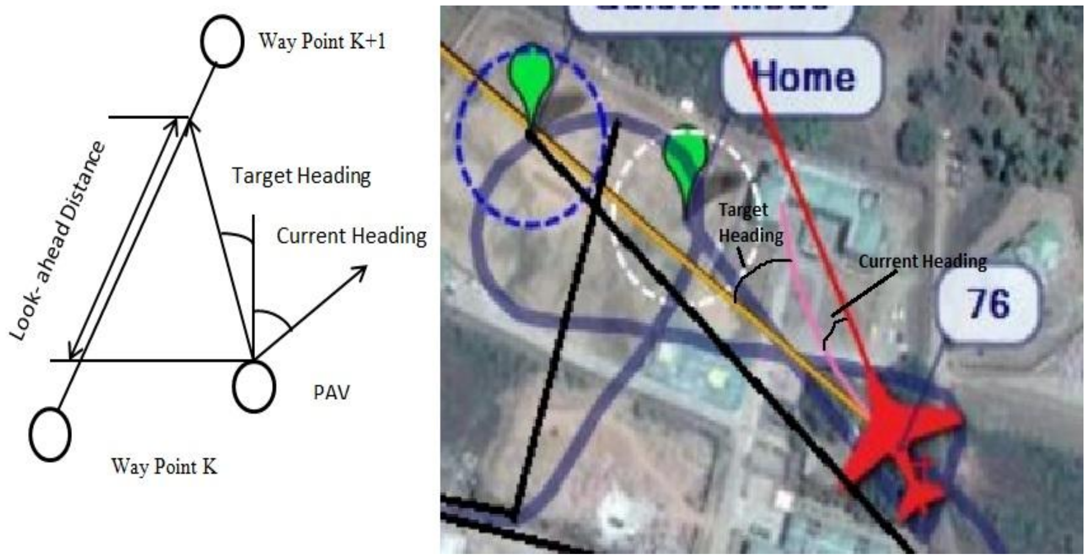

Figure.5.4. Loiter and Navigation Control for Powered Parafoil Aerial Vehicle

Now that we have a desired rate, we need to change the copter pitch and roll to give us that rate of travel.

- Parameter: LOITER_LAT_P and LOITER_LON_P are the proportional response and the default is 2.2. PAV will vary quite a bit depending on the weight and thrust of the engines.

5.1.5. PI Control for altitude hold

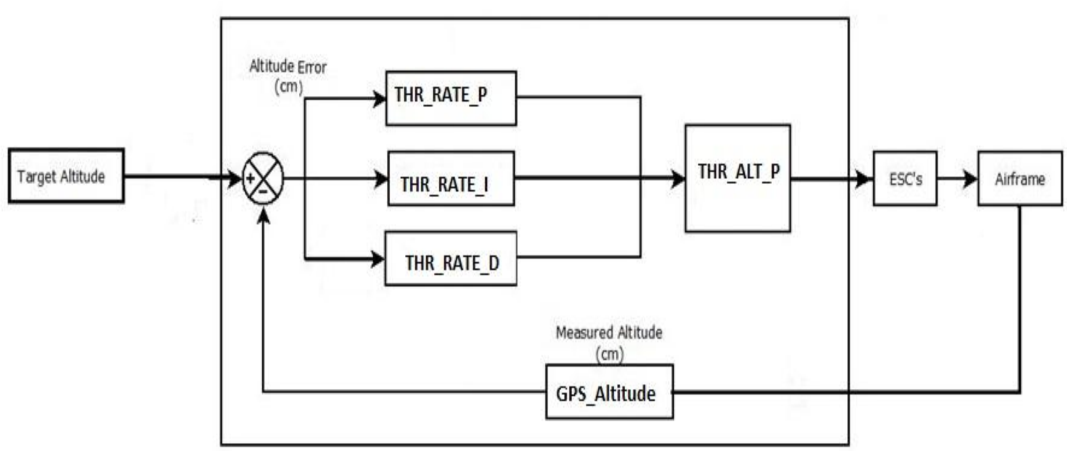

Figure.5.5. Altitude Hold Control for Powered Parafoil Aerial Vehicle

The altitude error is calculated in centimeters and fed to the controller. The first stage of the controller takes the altitude error and decides how fast the PAV should go to reach the correct altitude.

- Parameter: THR_ALT_P is 4 or 4 m/s for a 1m error. The desired rate maxes out at 1m/s.
- Parameter: THR_ALT_I is used to close the gap between the actual hover throttle and current assumed hover throttle.

PID Rate Control for altitude hold

Now that we have a desired rate, we need to change the thrust to give us that rate.

- Parameter: THR_RATE_P is the proportional response and the default is .35. PAV will vary quite a bit depending on the weight and thrust of the motors. The value should be loweredin order to minimize the oscillations
- Parameter: THR_RATE_I is set to 0 by default.
- Parameter: THR_RATE_D is 0.02 by default, but the noise of the Baro sensor can cause issues. If the value is too high bad oscillations are seen.

There was similar study done for simila Parafoil Vehicle by Jack Umenberger et al. [42], the gain values for various two different controls have been compared. Table 5.1. shows the theoretical and flight test gain of the PAV

#	**Theoretical [42]**			**Practical Flight Test**		
Gain	**K_P**	**K_I**	**K_D**	**K_P**	**K_I**	**K_D**
Attitude	-	-	-	1.3	0	0.0025
Later Heading Control	1.8	0	0	2.2	0	0
Altitude hold	0.17	0.02	0.01	0.35	0	0.02
	4.5 (Throttle)	-	-	4 (Throttle)	-	-

Table 5.1. Gain Values for Theoretical and Practical

5.2.ALGORITHM DESIGN FOR GUIDANCE LAW

The algorithm general takes in the sensors value and a defined path is followed using the sensors data. The algorithm starts with starting data logging of all the sensor information. The received sensor information a path is defined for the aerial vehicle. For achieving the defined path the servo motors are controlled automatically to change the direction and BLDC motor is controlled for holding the vehicle at desired altitude. The guidance logic is developed using way point navigation technique, where the controller gets the latitude, longitude and the altitude values from the GPS. The controller then calculates the heading angle and distance to the next waypoint. If the calculated distance and the angle, determines that the vehicle is within the path, then the controller executes steer to target algorithm. If the vehicle is deviated from the path due to wind or any other problem then the controller executes path deviation algorithm.

5.2.1. Main Control Loop

The guidance logic is developed using way point navigation technique, where the controller gets the latitude, longitude and the altitude values from the GPS. The controller then calculates the heading angle and distance to the next waypoint. If the calculated distance and the angle, determines that the vehicle is within the path, then the controller executes steer to target algorithm. If the vehicle is deviated from the path due to wind or any other problem then the controller executes path deviation algorithm.

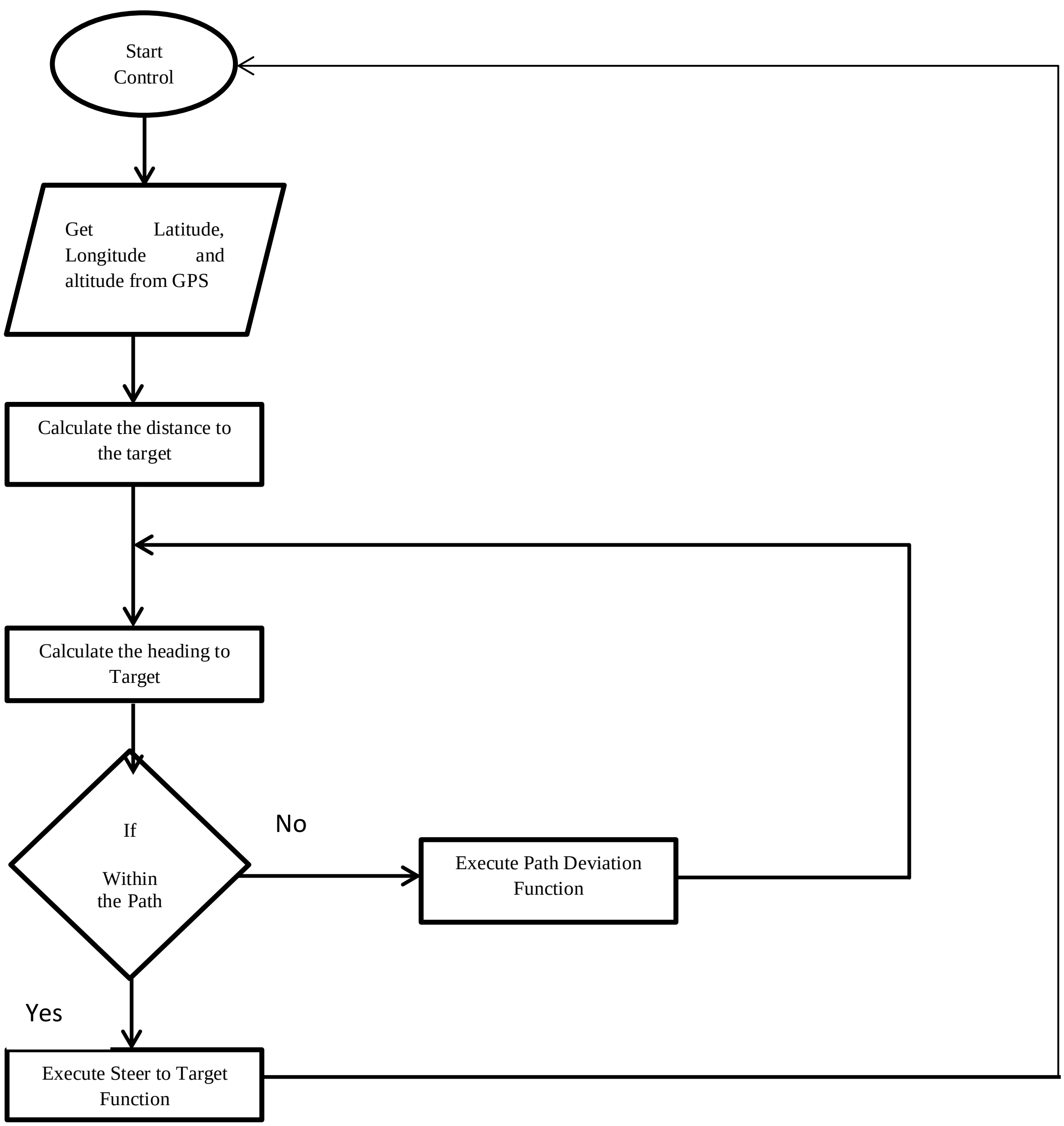

5.2.2. Steer to Target Algorithm

During this algorithm the vehicle gets the actual heading from the control loop and the current heading from the GPS and then calculates the deviation error. The deviation error along with the gain is given to the servo with the calculated yaw rate

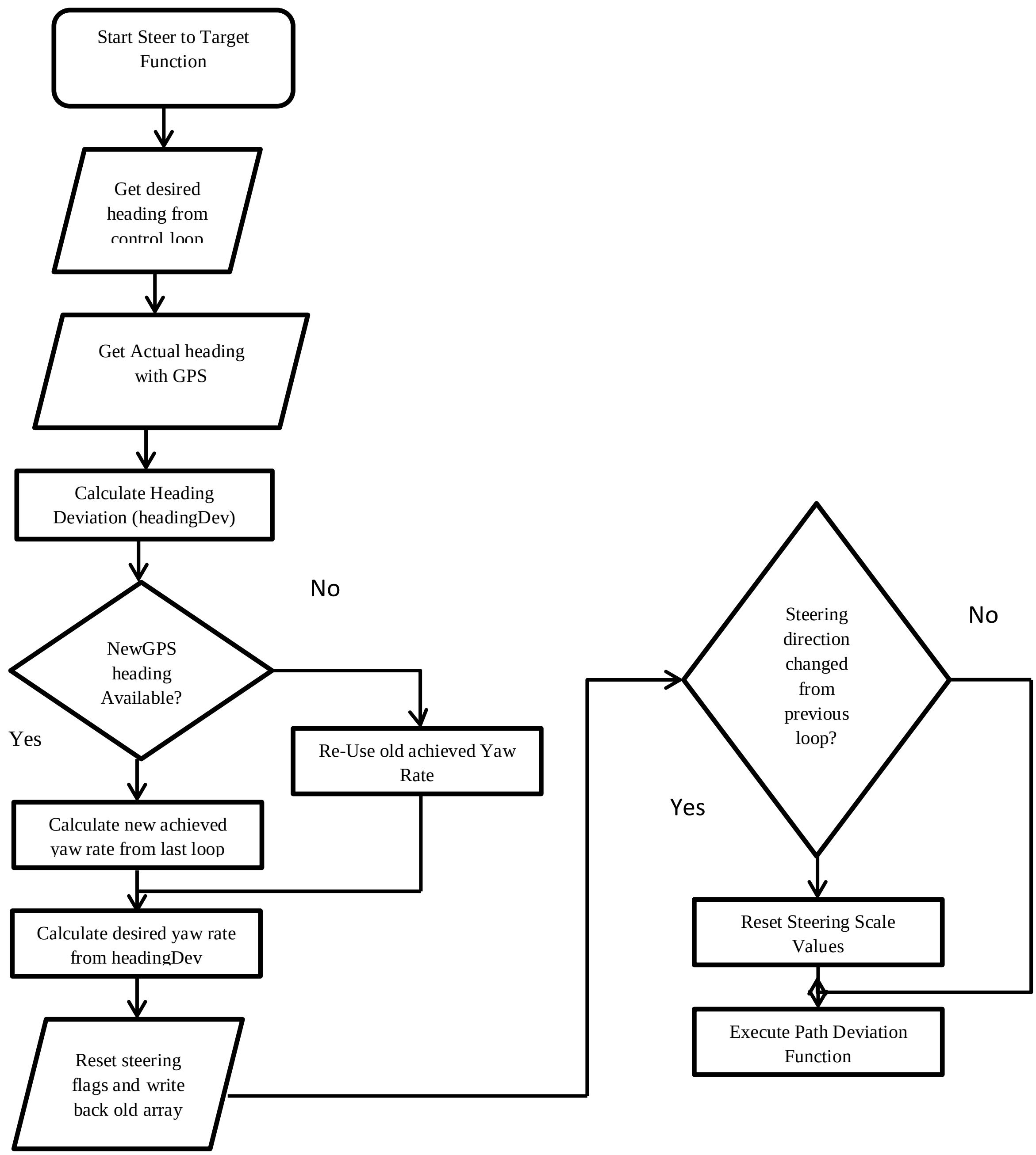

5.2.3. Path Restoration Algorithm

In this algorithm the controller compares the heading deviation angle with the desired deviation angle, two conditions occur in the case:

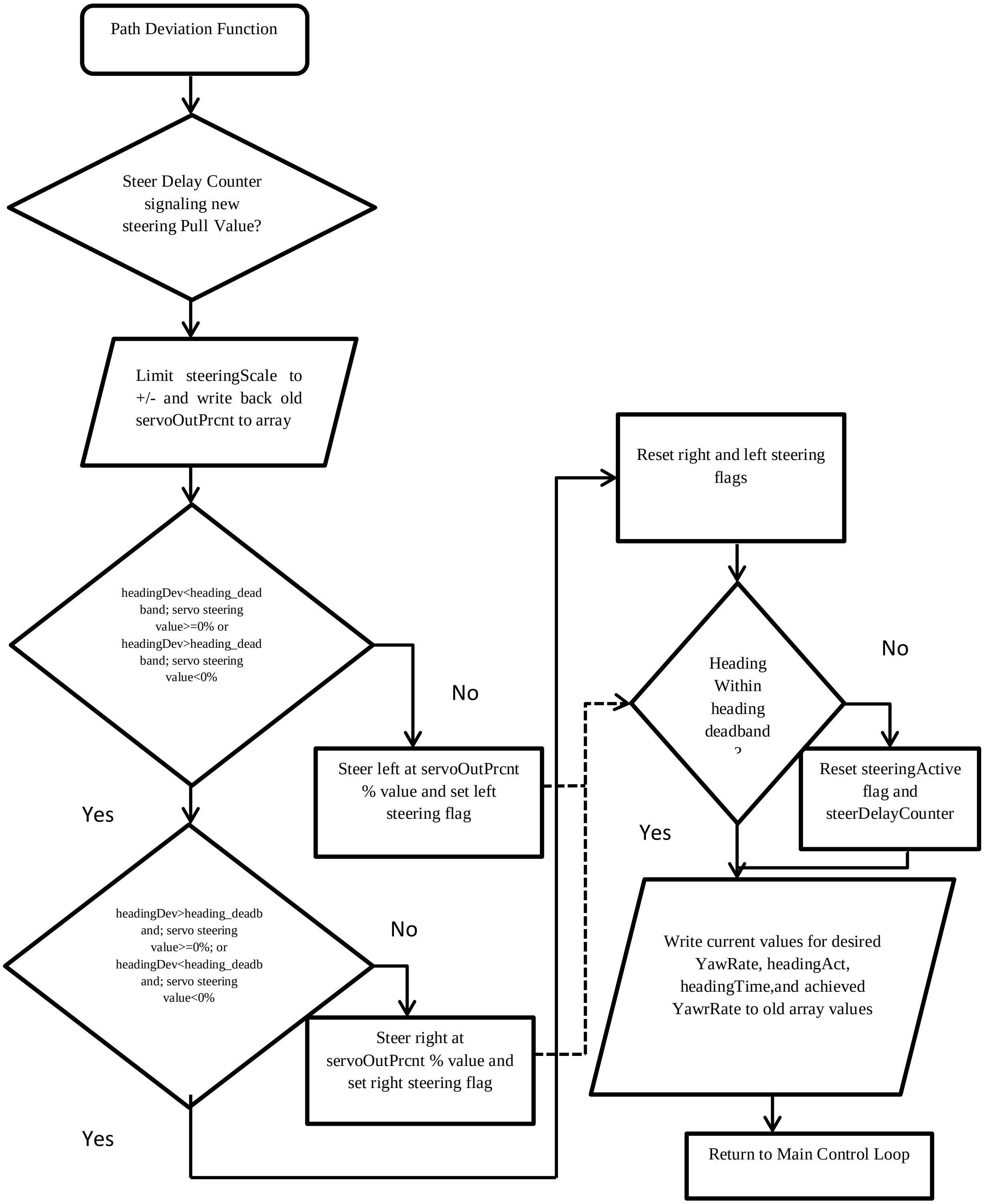

5.2.4. Obstacle Avoidance Algorithm

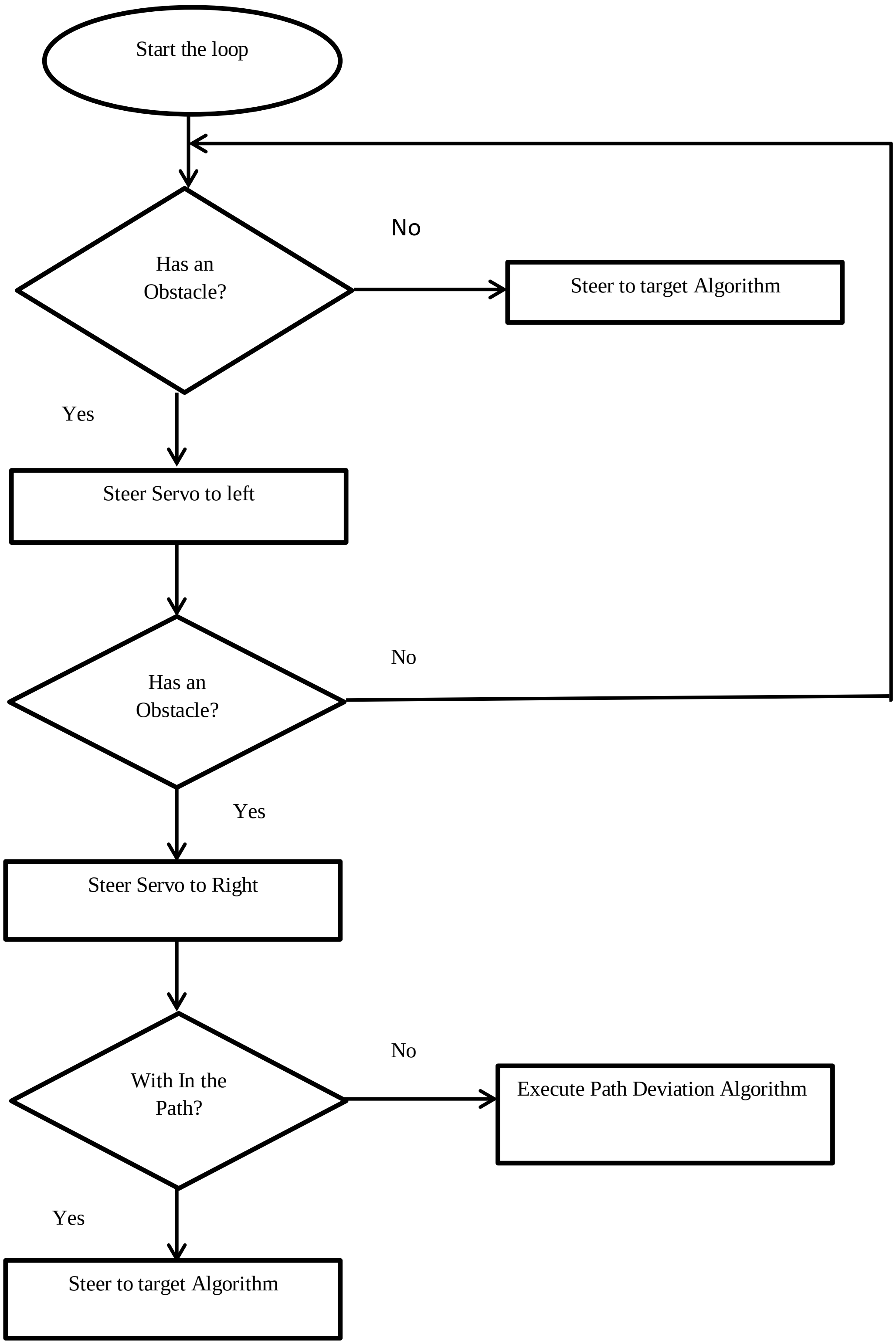

5.3. CLOSED LOOP RESULTS

The control system described in chapter 5 was implemented in the PAV. The PAV was launched under manual control and after reaching an altitude of 100 meters the control was made autonomous and attitude stability was performed.

5.3.1. PID Tuning for Attitude Stability

In figures 5.6 through 5.9 it is observed that initial gain value was considered to be 2.4, and was reduced in steps to 2 and then 1.3. The gain value was set to 1.3 using visual inspection. By visual inspection we could conclude that the roll oscillations were damped down to almost zero. But certainly, there were internal oscillations due to the motor vibrations. Altogether the major oscillations were damped down keeping the proportional gain value to be 1.3.

The Proportional gain effect on roll rate can be clearly observed in figure 5.6. It can be seen that with proportional gain 2.4, the oscillations were there for 5 seconds. With the implementation of gain value to 1.3 the oscillation were reduced down to 3 seconds. Since the Parafoil Aerial Vehicle has a pendulum effect, the attitude is much effected due to the roll moment, whereas, yaw moment and pitch moment has less oscillations. Similar damping of oscillations can be seen in figure 5.7 in Roll angle.

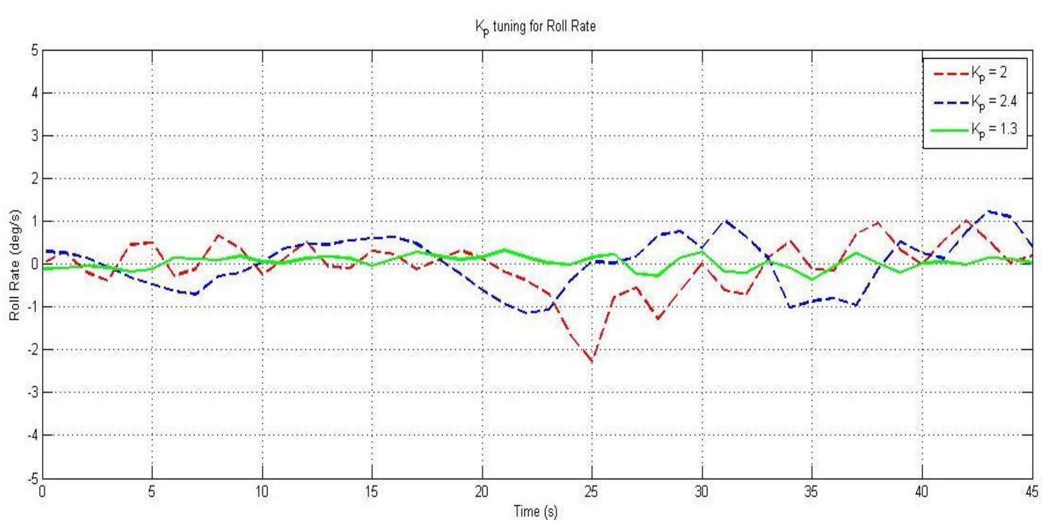

Figure. 5.6. P Tuning Roll Rate

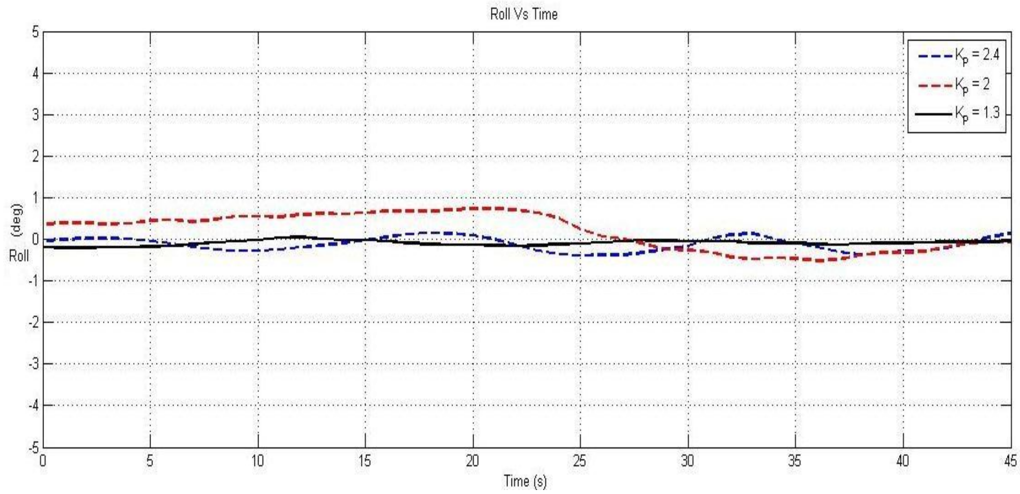

Figure. 5.7. P Tuning Roll Angle

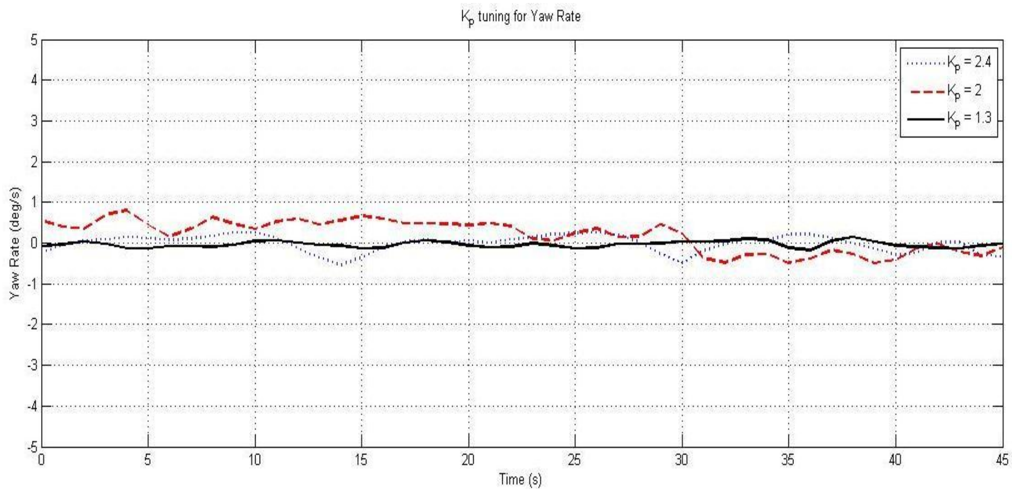

Figure. 5.8. P Tuning Yaw Rate

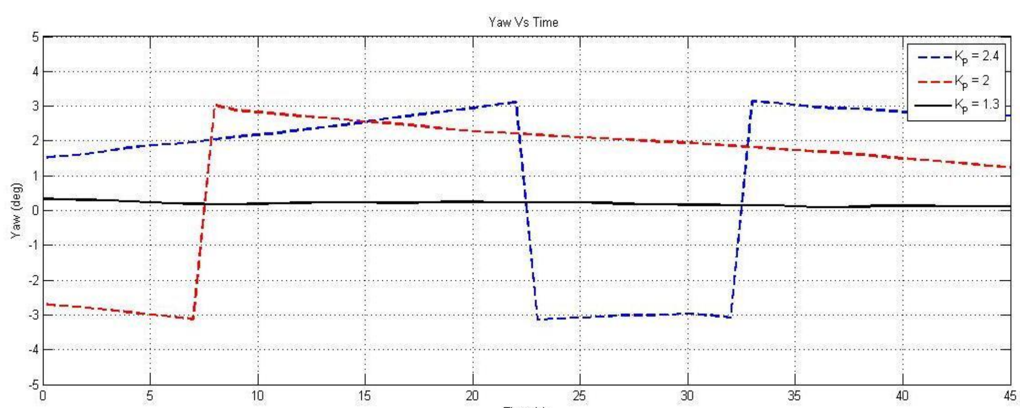

Figure. 5.9. P Tuning Yaw Angle

Proportional gain effect on yaw rate can be seen in figure 5.8. With gain value of 1.3 the oscillations were completely damped down. As stated earlier Yaw moment has very less effect on attitude stability due to pendulum stability, which was discussed in detail in chapter 1. Similar damping effect can be seen in Yaw angle in figure 5.9.

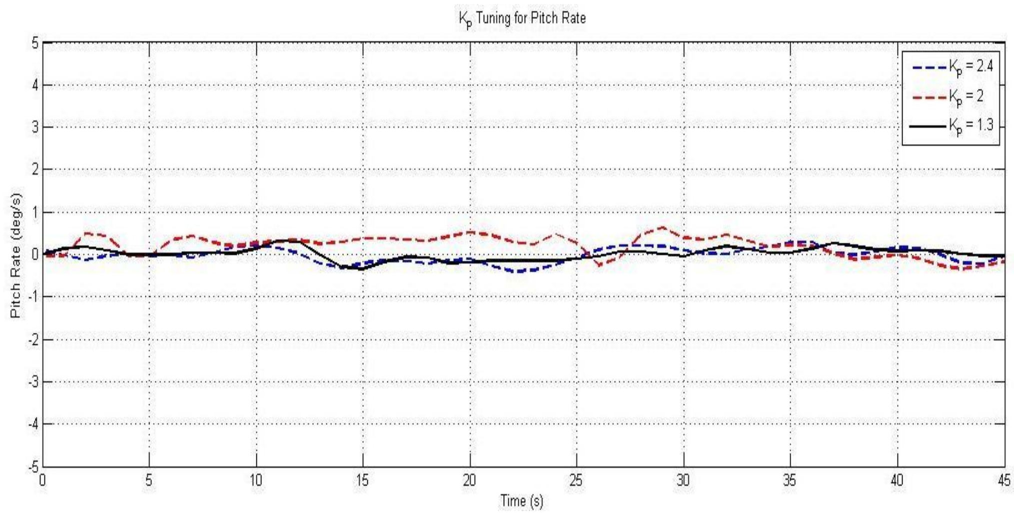

Figure. 5.10. P Tuning Pitch Rate

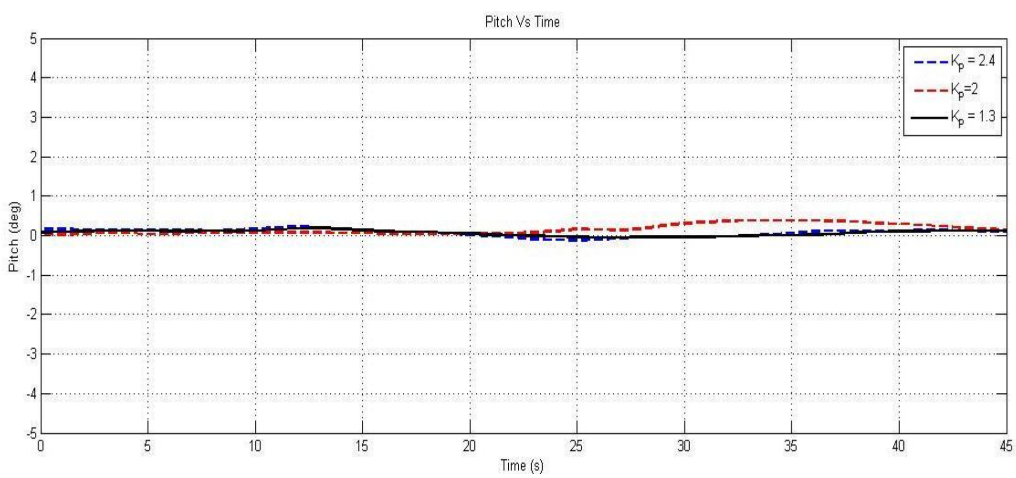

Figure. 5.11. P Tuning Pitch Angle

The effect of proportional tuning on pitch rate can be observed in figure 5.10. The oscillations were damped down to zero having a frequency of less than 1 second. Pitch angle also show similar changed due to the tuning can be seen in figure

5.11. In figure 5.12 it can be observed the effect of proportional gain 1.3 on roll pitch and yaw rates. As discussed due to the pendulum stability the oscillations can be much seen in roll moment. Total effect of tuning gain of 1.3 can be seen in figure 5.13 in angles.

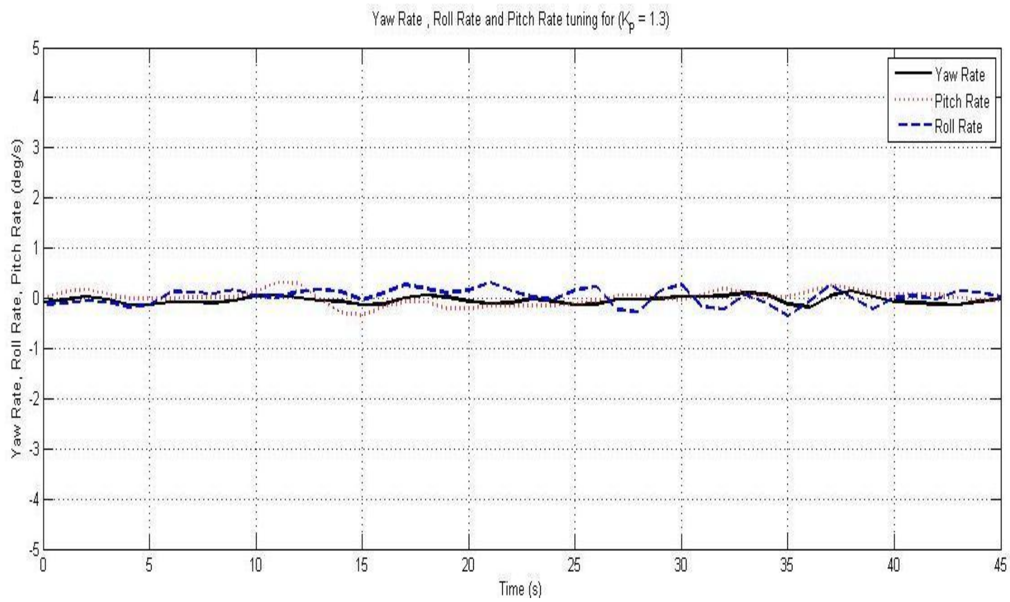

Figure. 5.12. P Tuning Roll Rate, Pitch Rate, Yaw Rate

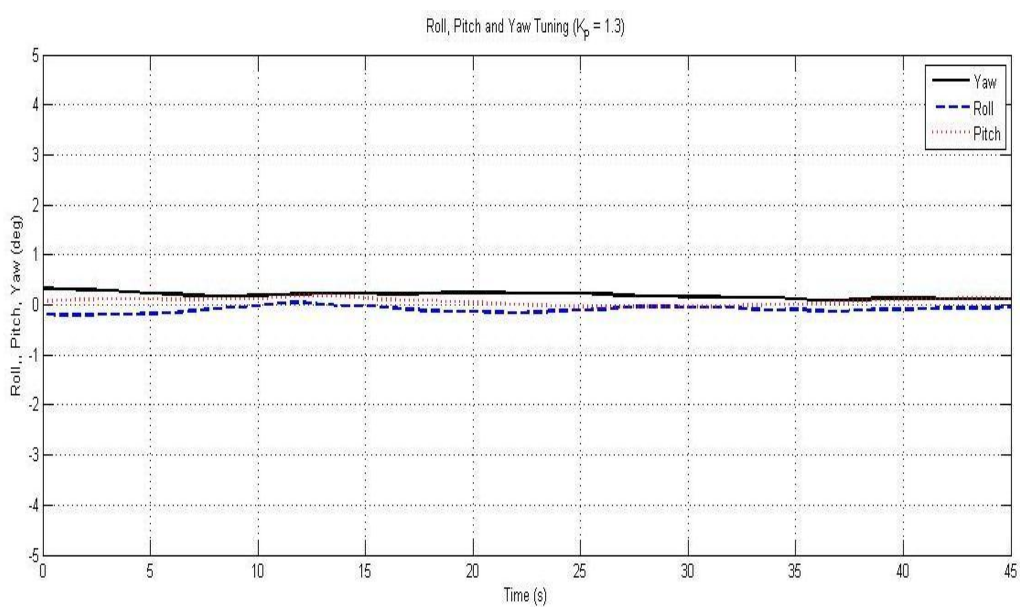

Figure. 5.13. P Tuning Roll, Pitch, Yaw

5.3.2. Closed loop Lateral Heading Controller with P = 2.2

In the above section we have achieved attitude stability and the oscillations were damped down. After the attitude stability, later heading controller was designed for way point navigation and loiter operations according to the steer to target algorithm. According to the algorithm the heading difference angle was supposed to get down to zero degrees, when travelling from one way point to another, keeping the servo value positive or negation according to the way point, indicating a turn. It was observed in the open loop flight test and simulation results that there were not many oscillations in the turning situation. Therefore only a proportional controller was used keeping the gain value to 2.2 to achieve a smooth turn. The same effect can be seen in figure 5.14 to 5.15.

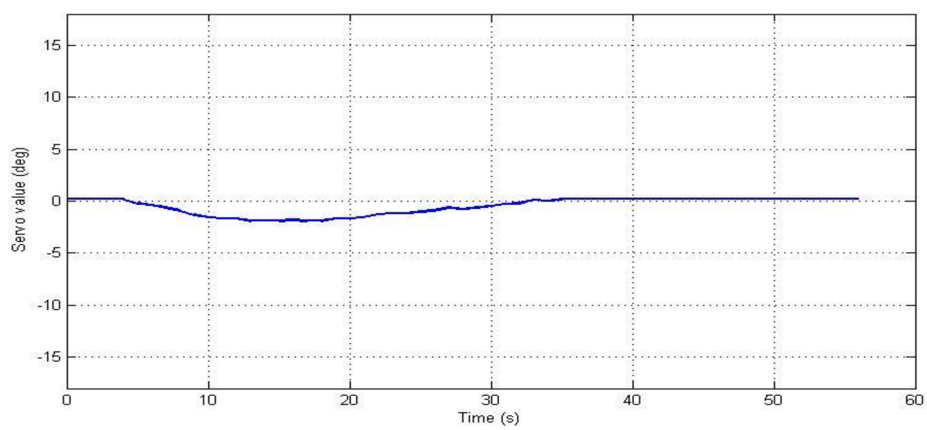

Figure.5.14. Servo Tilt for Heading Control

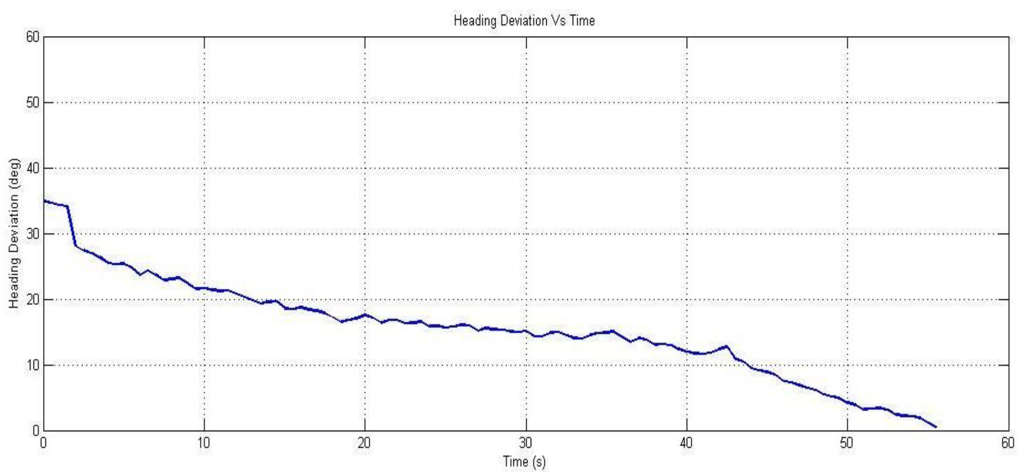

Figure.5.15. Heading Control angle tending to zero

5.3.3. Closed loop Longitudinal Altitude Hold Controller With P (Throttle) = 4 and P = 0.35

Once the heading control was achieved, an altitude hold controller was designed to maintain a certain altitude to complete the waypoint navigation task. The P (Throttle) is used to provide the exact signal to be supplied to the motor to eliminate the steady state altitude error which is kept as 4 to achieve throttle control regime. It can be seen from figure 5.16 that the trottle was maintained at 7.5 N to achieve the altitude of 920 m in order to ececute proper way point navigation.

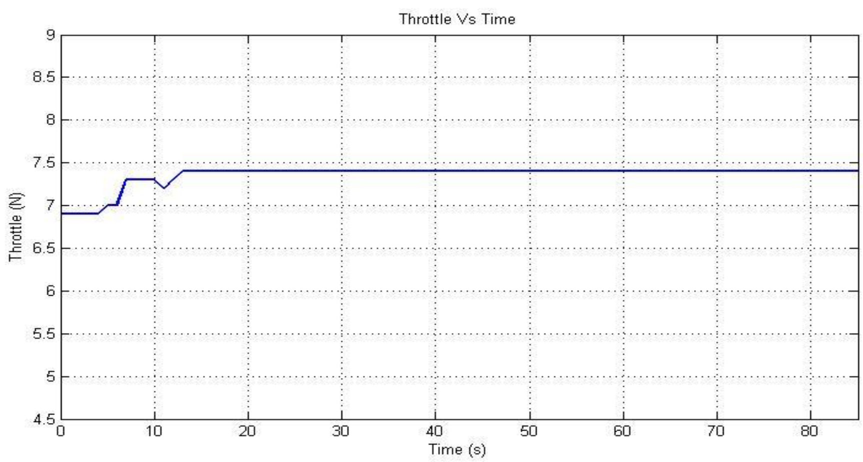

Figure.5.16. Altitude hold with throttle control at 7.5 N

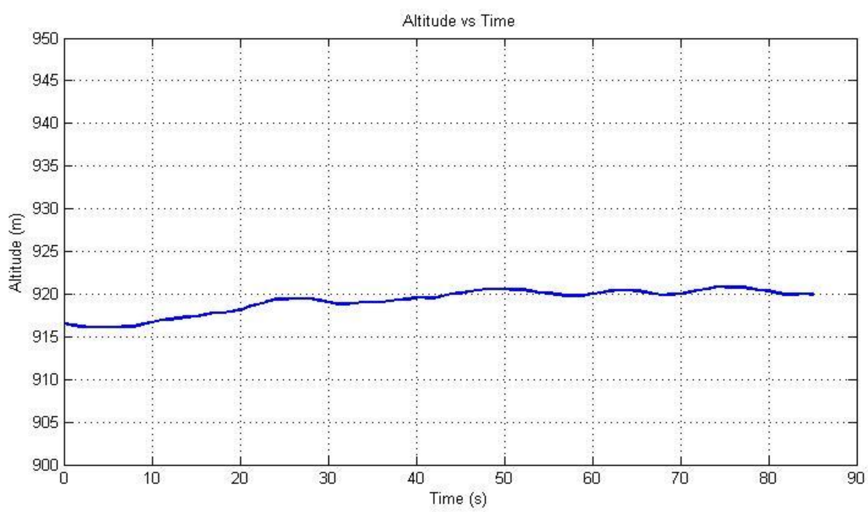

Figure 5.17. Altitude hold at 920 meters

In figure 5.13 it can be seen that due to the throttle hold at 7.5 N, an altitude of approximately 920 m was maintained so that the vehicle can travel to the other way point easily. As discussed in attitude stability a lot of oscillations were observed in take-off mode than in turning flight test. Therefore a PID was implemented keeping the proportional, Integral and derivative coefficients to be 0.35, 0 and 0.02.

A path comprised of four way points was selected to demonstrate the performance of the guidance logic. Each way point have effective radius of 5m. These way points along with the path have been shown in the figure 5.14 and 5.15. Finally, the path shows that the heading angle tracker along with guidance logic provides a reliable means of way point navigation.

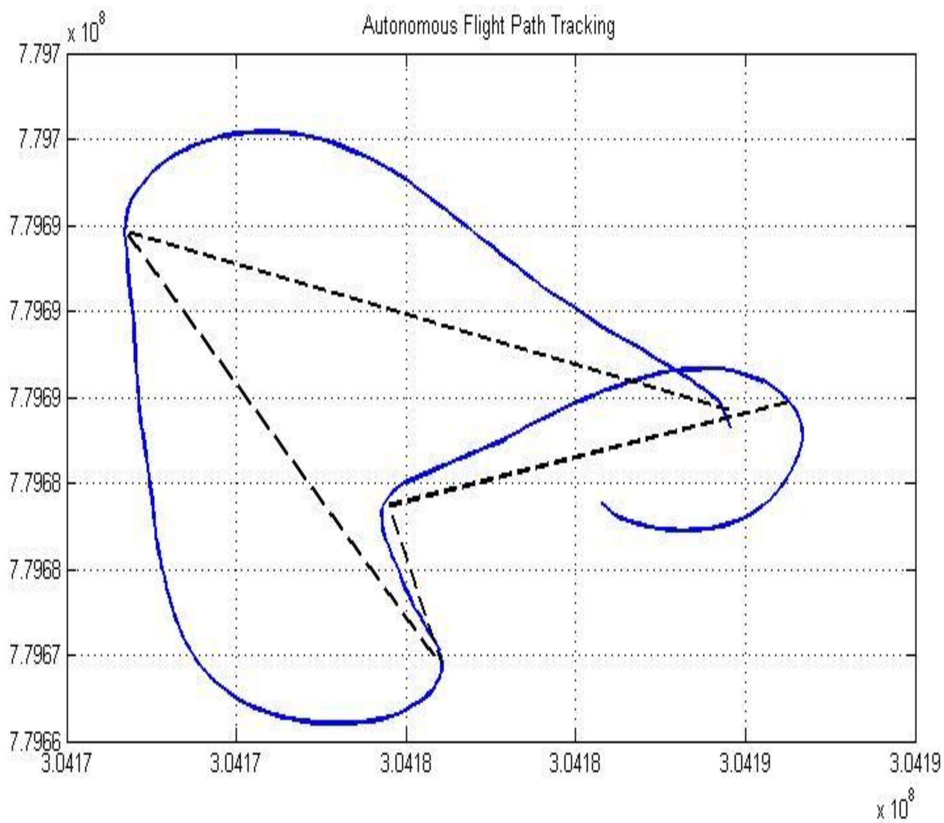

Figure. 5.18. Autonomous Path Covered 2D

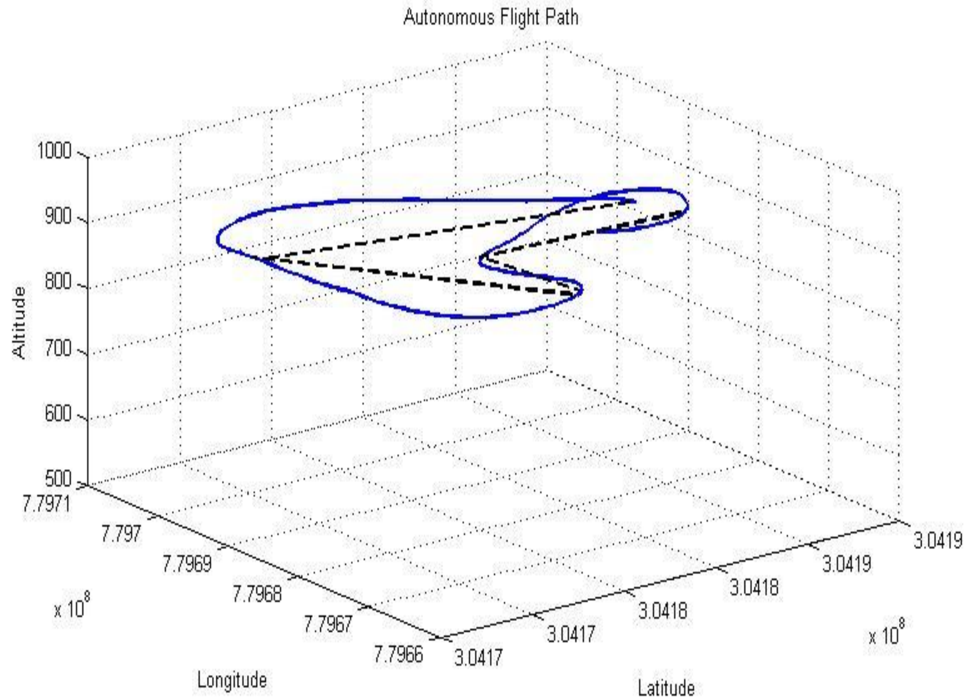

Figure. 5.19. Autonomous Path Covered 3D

5.3.4. Aerial Distance covered by the Vehicle

The complete flight test was observed in mission planner software. The vehicle was successfully tested at University of Petroleum and Energy Studies, Dehradun, Bidholi Campus. The vehicle covered the above way points in the complete mission

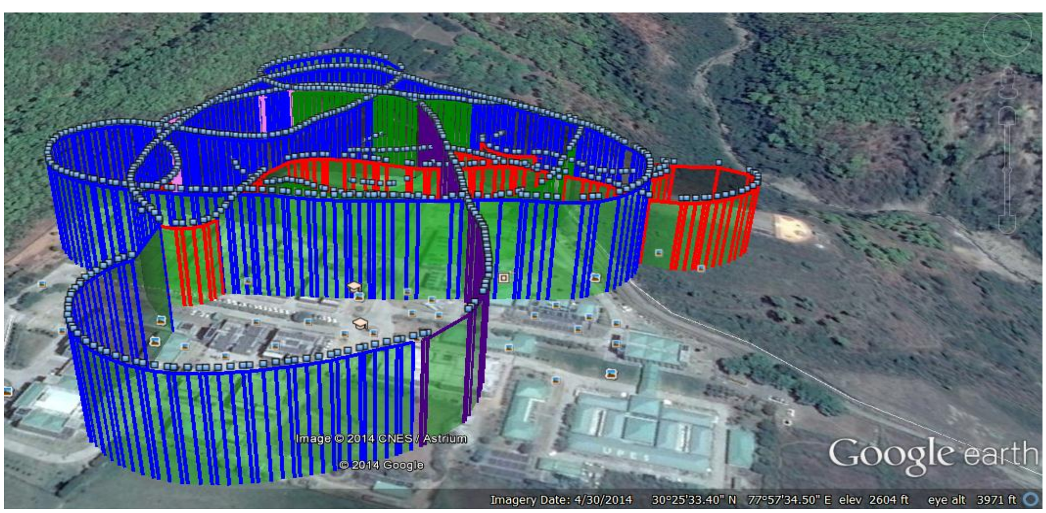

Figure. 5.20. Autonomous, Semi- Autonomous, Take off, Landing Path Covered

The above figure indicates the autonomous mode of the vehicle.

- Red: Semi-Autonomous Mode and take off
- Blue: Autonomous (the vehicle auto stabilizing itself)
- Violet: Guided Mode (covered the given Way Points with altitude hold)
- Green: Total Path (overall path covered)
- Pink: Semi – Autonomous and Landing Mode

CHAPTER 6

CONCLUSION AND FUTURE SCOPE

6.1.CONCLUSION

The initial section of the work discussed in detail about the Powered Parafoil Aerial Vehicles, the terms involved and the aerodynamic parameters that should be considered. The section also explains about different types of Unmanned Aerial Vehicles, their features, advantages and disadvantages. Keeping all the factors in view a Parafoil aerial vehicle is considered to be the most stable Aerial vehicle. Applications that require accurate vertical positioning like crop dusting, proximity sensing of targets and detection of substances and organisms that are altitude specific, high resolution and close range imaging can be performed easily using PAV platform. A benefit of the powered Parafoil for unmanned aircraft use is their unique ability to glide to the ground in a relatively safe manner, even if all control systems are disabled. This is particularly desirable in urban environments where a failure of any large UAV would likely result in collateral damage to structure on the ground. Powered Parafoils, on the other hand, would be unlikely to land with a vertical speed above 10m/s, making severe damage to any ground edifice or even the airframe itself is unlikely. As we can observe clearly from the comparison table discussed in chapter 2, PAV emerges as the most appropriate system for deployment in various fields such as oil and gas pipeline monitoring, regional surveying, etc. These systems can be easily automated as they do not need any high end equipment. A low end GPS and IMU can be used which reduces the complexity in programming and hardware development.

The experimental design section of this work shows that the flight test results and the analytical results of the Unmanned Powered Parafoil Aerial Vehicle match within the range. The section also discussed about the construction of the vehicle. The vehicle shape is in the triac from having a nose fitted with the electronics and control unit. A single servo is used for controlling the direction of the UPPAV. And BLDC motor used is used to take off, land and to maintain a level flight. The total weight of the payload is 3.8 kg. The next section gives the relation between size of the Parafoil and the payload weight. For a 4 kg payload the size of the Parafoil is taken as 2X0.65 m Parafoil. The system performance is also calculated where the lift and drag of the system is calculated. The Parafoil flight velocity is determined and turn performance is also determined. Three types of flight tests were performed and the flight test were compared with the analytical results and concluded the vehicle was performing as desired. It can be observed that during the level flight, while the vehicle is turning there are less number of oscillations, while the vehicle is climbing up the oscillations are more.

All the observations in this section are done on Payload. A lot of oscillations/ vibrations are seen in the graphs as the sensors are placed on the Payload. The vibrations on the Parafoil would be comparatively lesser. Pitch angle, Glide Angle, heading angle, latitude, longitude, altitude and ground speed give the performance analysis of the complete system. The above mentioned graphs helped us in understanding the Parafoil performance.

The mathematical modeling section describes the 9 DOF model. A thrust vector is added on the payload to understand the powered Parafoil performance under various thrust conditions. The direction control simulation was done by a single servo connected to the “fly-bar”. The control effects are observed by tilting the “fly-bar” left and right indirectly controlling the Parafoil. The angle of attack, glide angle and pitch angle results were compared with the 9 DOF simulated results. The resulting glide angles can be used in the dynamic model for closed loop simulations and controlled flight. The estimated glide rates are used to estimate the lift and drag coefficients needed for the dynamic model. The Control System and algorithm design section provides a comparison of lateral and longitudinal control theoretical results with practical results. The results indicate a small difference as in practical flight tests environmental conditions comes into picture especially wind conditions. Altitude hold using throttle control was successfully tested.

The following conclusions can be further made

- The successful completion of Autonomous Powered Parafoil Aerial Vehicle has produced a prototype capable of autonomous flight. Total flight duration was approximately 10 minutes for a 22.2V, 6000mah battery
- The developed vehicle was successful in carrying a payload of 3 kg with a 2 meter span Parafoil. For a larger payload the Parafoil span must be increased
- The ratio of horizontal base to the vertical base should be maintained 3:2 in order to avoid stall conditions
- The vehicle needs an air strip on 7 meters for a successful take off under zero wing conditions.
- The 9 DOF dynamic model has shown that the Parafoil uses two modes of direction control, skid steering and roll steering. It is observed that the Parafoil changes the direction due to the roll moment.
- The speed of the vehicle is approximately 10 meters/second. The low speed feature would help the vehicle to survey an area more efficiently compared to other conventional models.
- A turn rate of 18 degrees/second was observed when the vehicle takes a turn. It is observed that the PAV maintains a velocity of 10 meters/second for level flight and during the turn the velocity goes up to 12 meters/second, and the vehicle tends to lose the altitude which is then covered up by increasing the speed to 12 meters/second.

- The bank angle is observed to be 10 degrees while the vehicle is taking the turn and the turn indicated to be smooth without any oscillations. The effect of Parafoil deflection due to the canopy tilt is modeled using direction control modeling, which successfully replicates the turn performance.
- The incorporated collision avoidance sensors, GPS, Pressure and remote sensing device with telemetry transmitted the data successfully to the ground station.
- This project has shown that way point navigation has provided means for autonomous navigation.
- The guidance logic developed was able to generate heading and altitude signals, which enabled the PAV to follow desired path specified by the sequence of points.
- During the flight, if the GPS link is lost in the autonomous mode, PAV was rotating around the waypoint maintaining a radius of 2 meters.
- The Parafoil and electronics package was extremely rugged. Flight test landings occurred in muddy fields and hard road tops without sustaining any damage to the Parafoil and the electronics. Similar landings for the conventional fixed wing or rotor craft would have damaged the structure.

6.2. RECOMMENDATIONS FOR FUTURE WORK

- There are number of applications where the PAV would provide a unique capability that is not adequately satisfied by other devices currently available. The PAV is superior in terms of cost, ruggedness/durability, ease of use, portability, time to activate and reusability when compared with the competing technologies in variety of mission scenarios.
- There are number of military uses for developed PAV which include airdrop guidance, battle damage assessment, and communication in the rugged terrain. Civilian application include; an aid in search and rescue efforts, evaluating plant health by farmers and land management workers, and as a communications and observation device for forestry firefighting crews.

6.3.ADVANTAGES

- *Aerial Surveillance*

  The developed prototype was successfully deployed to survey the given area.

Figure 6.1. Aerial Surveillance UPES Dump Area

- *Disaster Management*

  The developed vehicle can be used in the case of a disaster such as floods, earthquakes, and draughts. These vehicles can drop packages safely from a low altitude in the affected areas.

- *Coastal Area Surveillance*

  The vehicle can be used effectively for surveillance in coastal areas as parachute as a wing is much appropriate in wind conditions to hover around

- *Oil and gas pipeline monitoring*

  The vehicle has the ability to hover slowly and in a straight line. This feature can be used in tracking a pipeline by giving the coordinates of the pipeline. This can be used to detect the leaks and thefts near and around the pipelines

6.4.IMPACT OF THE DEVELOPED PROJECT

The biggest problem oil and gas industry facing today is the safety and security of the pipelines. The development of the major sectors such as transportation, aviation, tourism is directly related to oil and gas in developing countries. Therefore proper and steady flow should be maintained in pipelines for the wealth and wellbeing of these economic sectors. Pipelines all over are facing various threats like natural hazards such as corrosion, earthquakes, and landslides, criminal actions such as oil theft and terrorist activities. Pipeline is an easy target to the terrorist organizations which can be a direct aim to damage western economics. A pipeline distribution system extends hundreds of miles having sensors, valves, pumps and controllers. With advancement in sensor technology, communication and signal processing in combination with automation, robotics and unmanned aerial vehicles offer powerful tool for detection of defects in pipelines and monitoring the complex pipeline system. According to the U.S. Department of Transportation's Office of Pipeline Safety (OPS), the majority of pipeline incidents are caused by "damage by outside force." Property damages alone for more than 300,000 miles of transmission pipe can cost operators millions of dollars annually.

PUBLICATIONS

Parachute Aerial Vehicle (Current Work)

Journals

- ✓ *Vindhya Devalla, Om Prakash, "Longitudinal and Directional Control Modeling for a Small Powered Parafoil Aerial Vehicle", Aeronautical Journal, (Accepted).*

Abstract- The biggest problem oil and gas industry facing today is the safety and security of the pipelines which contributes to the increase in the maintenance cost of pipeline directly affecting the cost of fuel. An unmanned powered parachute aerial vehicle was developed for monitoring the oil and gas pipeline. It is envisioned that the vehicle would follow a planned trajectory to the target, and FLIR based system would be employed for extracting details about pipeline leakages, thefts, internal corrosion, internal waxing, etc. In this paper, a 9DOF parafoil simulation was created in the Matlab/Simulink environment to study the parafoil dynamics and assess the feasibility of the system. Longitudinal dynamics and direction control has been modeled and studied in detail. Thrust, pitch angle, glide angle and angle of attack was studied for the developed model and is validated with Lingards's model.

- ✓ *Vindhya Devalla, Om Prakash, "Developments in Powered Parachute Aerial Vehicle: A Review", IEEE Transactions of Aerospace and Electronics System, Volume 29 Issue 11, November 2014.*

Abstract- This paper discusses the recent developments made on powered parachute aerial vehicles over a decade. It reviews various modeling techniques and different parachute aerial vehicles developed for various applications focusing on the instrumentation involved. 9 DOF equations for a powered parachute vehicle are discussed in detail. The paper presents the comparison between various UAVs.

- ✓ *Vindhya Devalla, Om Prakash, "Modelling and Simulation of a Small Powered Parafoil Aerial Vehicle", IEEE Transactions of Aerospace and Electronics System Society, (Under Review)*

***Abstract* -** This Article describes the detailed derivation of the modelling of a small powered Parafoil aerial vehicle. In this model the Parafoil is connected to a payload which has a propulsion system attached. The Parafoil is connected to the payload at two joints. It is assumed to have nine degrees of freedom, modeled as two-body dynamics, consisting of three degrees of freedom for rotational motion of the Parafoil, three degrees of freedom for the rotational motion of the payload and three degrees of freedom for translational motion of the Parafoil. The nine degrees of freedom model incorporates nonlinear aerodynamics to predict all kinds of behavior. The nonlinear simulation demonstrates the validity of the proposed model through comparison with the Lingard's data and Flight Tests.

Conferences

- ✓ *Vindhya Devalla, Om Prakash "Angle of Attack, Pitch Angle and Glide Angle Modeling at Various Thrust Inputs for a Powered Parachute Aerial Vehicle" in AEDSS, A Doctoral fellows Symposium, held at IIT Kanpur, 2014.*
- ✓ *Vindhya Devalla, Om Prakash "Development of Position Tracking and Guidance System for Unmanned Powered Parafoil Aerial Vehicle" 4th International Conference on Reliability, Infocom Technologies and Optimization (ICRITO 2015), 2-4 September 2015 (Accepted)*

Awards

- RnD C3 Award for Paper Publication in SCI listed Journals,UPES, RnD, March 2015, Received the award by Prof. C. N. R. Rao, Bharat Ratna, FRS
- Excellent Performance Award in UPES, Communication Meet, 2014, UPES November 2014
- 4th prize in Innovate India 2014, NRDC, DST, UCOST, March 2014, 4th prize in science model competition

Projects

- Received a grant of 6 lakhs from DST- SERB for “Development of Parachute Aerial Vehicle for Oil and Gas Pipeline Monitoring” for a period of 1 year to do the feasibility study

REFERENCES

[1] Dept. of Defense, Unmanned Systems Road map 2007- 2032, office of Secretary of Defense, Washington D. C., 10 Dec. 2007

[2] Jay Gundlach, “Design of Unmanned Aircraft Systems, A comprehensive approach” AIAA Education Series

[3] Hans-peter Thamm , Thomas Ludwig and Christian Reuter, “Design of a Process Model for Unmanned Aerial Systems in Emergencies”, Proceeding of the of the International ISCRAM Conference, May 2012

[4] Inkyu Sa and Peter Corke, “System Identification, Estimation and Control for a Cost Effective Open-Source Quadcopter”, IEEE International Conference on Robotics and Automation, 2012

[5] Mueller, T.J., “Fixed and Flapping Wing Aerodynamics for Micro Air Vehicle Applications”, AIAA, Reston, VA, 2001

[6] Damian Toohey, “Development of Small Parafoil Vehicle for Precision Delivery” Massachusetts Institute of Technology, 2005

[7] Phil Dietro, “History of Paraplane”, Adirondack Chapter Newsletter, EAA Sprit of Aviation, August 2012

[8] John R. Chambers, “Longitudinal Dynamic Modeling and Control of Powered Parachute”, Thesis Report, Department of Mechanical Engineering, Rochester Institute of Technology, New York

[9] US Department of Transportation, Federal Aviation Administration, Flights Standard Service “Powered Parachute Flying Handbook”, Aircraft Technical Book Company, http://www.actechbooks.com, 2007.

[10] Y Ochi and m Watanabe, “Modeling and Simulation of the Dynamics of a Powered Paraglider”, proceedings in IMechE, Vol.225, Part G

[11] Doherr, K.F. and Schilling, H., “Nine-degree-of- freedom simulation of rotating parachute systems”, J. Aircr., 1992.

[12] Mooij, E., Wijnands, Q. G. J., and Schat, B., “9 dof Parafoil/payload simulator development and validation”, Proceedings of AIAA Modeling and Simulation Technologies Conference, Austin, Texas, August 2003.

[13] Yakimmenko, O. A., “On the Development of a scalable 8- DOF model for a generic parafoil – payload delivery system”, proceedings of the AIAA Aerodynamic Decelerator Systems Conference, Munich, Germany, May 2005.

[14] Aviation, U.S. Department of Transportation Federal. Powered Parachute Flying Handbook. Oklahoma, 2007.

[15] Mirasky Aviation, “Para-Ceres”, California Polytechnic State University, 2008

[16] H.P Thamm, “SUSI 62 A Roboust and Safe Parachute UAV With Long Flight Time and Good Payload” International Archives of the photogrammetry, Remote Sensing and Spatial Information Sciences, Vol.XXXVIII-1/C22 UAV-g 2011, Conference on Unmanned Aerial Vehicles in Geomatics, Zurich, Switzerland.

[17] Sema E. Alptekin, Dianne De Turris, Daniel J.Macy, Jon E. Ervin, “Development of a flying Eye: A project-Based learning Experience”, Journal of Manufacturing Systems, Vol. 24, issue.no.3, 2005

[18] Tommy Ike Haily, “The Powered Parachute As An Archeological Aerial Reconnaissance Vehicle”, Archeological Prospectation, John wiley & Sons, Ltd., 2005

[19] Michael A. Kolodny, “Initial Experiment in Using a Powered Parafoil for Employment of Intelligence, Surveillance, and reconnaissance (ISR) Unattended Ground Sensors (UGS)”, Army research laboratory, October 2004.

[20] Yamauchi, B.PackBot: A versatile platform for military robotics. 2004. Orlando, FL, United States: International Society For Optical Engineering, Bellingham, WA 98227-0010, United States.

[21] Yamauchi, B and P. Rudakevych, Griffon: A man-portable hybrid UGV/UAV. Industrial Robot, 2004. 31(5):p.443-450.

[22] J.S. Lingards., "Precision Aerial Delivery Seminar, Ram-air Parachute Design", 13th AIAA Aerodynamic Decelerator System Technology Conference, Clearwater Beach, May 1995.

[23] Y Ochi and M watanabe, "Modelling and Simulation of the Dynamics of a Powered Paraglider", proceedings in IMechE, Vol. 225, Part G: Journal of Aerospace Engineering 2011.

[24] T.F. Goodrick., Theoretical study of longitudinal stability of high performance gliding air drop systems, AIAA 75-1394 1975.

[25] Goodrick, T.F., Simulation studies of the flight dynamics of gliding parachute systems, AIAA Paper 1979-0417, 1979.

[26] Goodrick, T.F., Comparison of Simulation and Experimental data for gliding parachute in dynamic flight, AIAA Paper 1981-1924, 1981.

[27] Slegers, N. and Costello, M. "Model Predictive Control of a Parafoil and Payload System", J.Guid.Control Dyn., 2005.

[28] Slegers, N. and Costello, M. "Aspects of control for a Parafoil and Payload System", J.Guid.Control Dyn., 2003.

[29] Mooij, E., Wijnands, Q. G. J., and Schat, B., "nine degrees of freedom Parafoil/payload simulator development and validation", Proceedings of AIAA Modeling and Simulation Technologies Conference, Austin, Texas, August 2003.

[30] Yakimmenko, O. A., "On the Development of a scalable 8- DOF model for a generic parafoil – payload delivery system", proceedings of the AIAA Aerodynamic Decelerator Systems Conference, Munich, Germany, May 2005.

[31] Hur, G.-B. and Valasek, J., “System Identification of a Powered Parafoil – Vehicle from flight data”, Proceedings of the AIAA Atmospheric Flight Mechanics Conference, Austin, Texas, August 2003.

[32] Muller, S., Wagner, O., and Sachs, G., “A high – fidelity non – linear multi-body simulation model for parafoil systems”, Proceedings of the AIAA Aerodynamic Decelerator Systems Conference, Monterey, California, May 2003.

[33] Akasaka, T., Beppu, G., and Azuma, A., “An investigation of the Paraglider’s turn mechanism”, J. Jpn.Soc.Aeronaut. Space Sci., 1999.

[34] Slegers, N., “Effects of canopy-payload relative motion on control of autonomous parafoil”, J. Guid. Control Dyn., 2010.

[35] Wise, K., “Dynamics of UAV with parafoil under powered flight”, Proceedings of the AIAA Guidance, Navigation and control Conference, Keystone, Colorado,2006.

[36] Redelinghuys, C. “A Flight Simulation Algorithm for a parafoil suspending an Air Vehicle”, J. Guid. Control Dyn, 2007.

[37] Prakash, O., Ananthkrishnan, N., Modeling and Simulation of nine degrees of freedom Parafoil- Payload system Flight Dynamics, AIAA Atmospheric Flight Mechanics Conference and Exhibit 21-24 August 2006, Keystone, Colorado.

[38] Slegers.N.Costello.M and Eric. Beyer., Use of variable incidence angle for glide slope control of autonomous Parafoils, Journal of Guidance, control and Dynamics, Vol. 31, No.3, May- June 2008, pp. 585-596

[39] Oleg A, Yakimenko and Nathan J. Slegers, “Using Direct Methods for Terminal Guidance of Autonomous Aerial Delivery Systems”, Proceedings of the European Control Conference, 2009

[40] Oleg A, Yakimenko, Eugene A. Bourakov, Charles W. Hewgley, Nathan J. Slegers, Red P. Jensen, Andrew B. Robinson, Josh R. Malone, Phil E. Heidt, “Autonomous Aerial Payload Delivery System “Blizzard”, 21st AIAA

Aerodynamic Decelerator Systems Technology Conference Seminar 23-26 May 2011, Dublin, Ireland.

[41] Yakimenko, O. Slegers, N., and Tiaden, R., "Development and testing of the miniature aerial delivery system snowflake," Proceedings of the 20th AIAA Aerodynamic decelerator Systems Technology Conference, seattle, WA, May 4-7, 2009.

[42] Jack Umenberger, "Guidance Navigation and Control of a Small-Scale Paramotor", Proceedings of Australasian Conference on Robotics and Automation, 3-5 Dec 2012, Victoria University of Wellington, New Zealand.

APPENDIX A: OPEN LOOP FLIGHT TEST VALUES

A.1 TAKE-OFF FLIGHT

Roll (rad)	**Pitch(rad)**	**Yaw (rad)**	**Rol' Rate (rad/s)**	**Pitch Rate(rad/sec)**	**Yaw Rate (rad/s)**	**Time(s)**	**Groundspeed (m/s)**	**horizontal (m)**	**alt (m)**	**Heading (deg)**
-0.3358	0.579742	-2.79052	0.69857	0.428751	-0.1159	0.252	9.87	2.48724	857.46	198
-0.40574	0.509943	-2.92591	-0.18393	0.151788	0.063419	1.095	7.49	8.20155	859.81	192
-0.38815	0.517679	-2.90887	0.286983	-0.16429	0.137382	1.245	7.49	9.32505	861.35	192
-0.34433	0.40734	-2.91592	-0.18633	-0.36117	-0.55516	1.655	7.2	11.916	861.76	194
-0.41173	0.349503	-2.96857	-0.52236	-0.15976	-0.48891	1.655	7.2	11.916	861.76	191
-0.45304	0.304857	-2.98989	-0.07485	-0.28667	-0.23403	1.86	7.17	13.3362	863.15	189
-0.40498	0.115397	-3.02023	-0.01393	-0.76637	-0.74246	2.06	7.17	14.7702	863	188
-0.45411	0.006039	-3.07115	-0.60031	-0.44364	-0.64588	2.092	7.14	14.93688	862.98	188
-0.50258	-0.03636	-3.08222	-0.04904	-0.03418	0.011272	2.152	7.63	16.41976	864.18	185
-0.44475	-0.03758	-3.05153	0.768542	-0.0991	0.271474	2.307	7.63	17.60241	863.8	183
-0.35682	-0.05604	-3.04394	0.437836	-0.0842	-0.24334	2.477	8.17	20.23709	864.45	184
-0.42351	-0.03941	-3.10196	-1.08799	0.411724	-0.49423	2.502	8.17	20.44134	864.89	185
-0.52627	-0.01276	3.128624	-0.32202	0.115605	-0.22844	2.672	8.73	23.32656	864.99	184
-0.47609	-0.00168	3.11297	0.971808	-0.08021	-0.15129	2.707	9.34	25.28338	865.67	180
-0.33979	0.020741	3.07734	0.672496	0.229742	-0.48492	2.877	9.34	26.87118	866.36	178
-0.47404	0.159652	2.959844	-0.03042	0.605412	0.197777	3.082	10.25	31.5905	866.06	177
-0.3607	0.224836	2.987146	1.30145	0.171476	0.353685	3.13	10.25	32.0825	865.85	174

5										
-0.22977	0.27305	2.990301	0.463643	0.479834	-0.23483	3.255	11.03	35.90265	866.72	170
-0.30567	0.338202	2.916661	-0.64793	0.577476	-0.50753	3.387	11.03	37.35861	867.5	171
-0.37212	0.380667	2.847188	0.373184	0.260072	-0.24334	3.482	11.43	39.79926	866.67	169
-0.29377	0.400258	2.814946	0.710542	0.163228	-0.24254	3.7	11.43	42.291	868.68	164
-0.29443	0.424428	2.777268	-0.29408	0.231871	-0.34444	3.732	11.32	42.24624	868.02	162
-0.3596	0.441022	2.736303	-0.05862	0.013972	-0.29682	3.837	11.26	43.20462	869.29	160
-0.34136	0.45397	2.656497	-0.05516	0.290669	-0.47268	4.145	11.26	46.6727	868.43	157
-0.444	0.471072	2.585573	-0.71338	0.217237	-0.43171	4.32	10.8	46.656	869.76	153
-0.52281	0.454657	2.551651	-0.25471	-0.14806	-0.31651	4.36	10.05	43.818	869.69	146
-0.55877	0.432708	2.536303	-0.34782	-0.10496	-0.26143	4.522	10.05	45.4461	871.13	145
-0.8321	0.380679	2.544939	-0.21373	0.236393	-0.45911	5.14	10.13	52.0682	870.41	144
-0.94854	0.371183	2.456577	-1.14439	0.650641	-0.51951	5.172	10.18	52.65096	871.14	143
-1.13832	0.366533	2.377257	-1.28274	0.416513	-0.27553	5.21	10.11	52.6731	871.95	138
-1.22481	0.356728	2.346642	-0.14349	0.132366	-0.15076	5.38	10.11	54.3918	872.25	135
-1.21287	0.34406	2.31764	0.098616	0.27843	-0.3612	5.457	10.72	58.49904	873.26	133
-1.27591	0.309047	2.237592	-0.66576	0.680439	-0.60677	5.495	11.2	61.544	872.19	130
-1.39437	0.268805	2.1198	-0.54497	0.870402	-0.50062	5.688	11.2	63.7056	872.5	124
-1.42509	0.239066	2.013958	0.39846	0.696668	-0.35748	5.73	11.25	64.4625	873.43	118
-1.37786	0.204044	1.91962	0.611038	0.720081	-0.52509	5.895	11.25	66.31875	872.9	112

-1.40227	0.146165	1.805126	-0.25524	0.759457	-0.66717	5.995	11.92	71.4604	873.89	106
-1.44666	0.087219	1.696093	0.232175	0.723806	-0.449	6.173	12.65	78.08845	874.04	100
-1.34411	0.047823	1.608116	1.432881	0.618182	-0.47986	6.25	12.65	79.0625	874.82	94
-1.24607	0.000617	1.484523	0.400322	0.886632	-0.76641	6.39	12.95	82.7505	873.46	88
-1.24674	-0.06	1.364244	0.354295	0.69321	-0.71426	6.463	12.95	83.69585	874.73	81
-1.12658	-0.09898	1.260703	1.497	0.72221	-0.57298	6.68	13.39	89.4452	874.26	75
-0.9963	-0.10781	1.121411	0.641634	1.050255	-0.60757	6.823	13.73	93.67979	873.92	68
-0.9912	-0.09948	0.990854	0.172845	0.829962	-0.34923	6.863	13.73	94.22899	873.63	60
-0.49703	-0.01701	0.730746	0.651478	0.184779	-0.17284	7.66	13.41	102.7206	873.76	54
-0.44891	-0.00239	0.706267	0.181093	0.191696	-0.06136	7.69	12.94	99.5086	873.95	42
-0.40461	0.033488	0.691421	0.430386	0.320733	0.079382	7.71	12.19	93.9849	875.48	41
-0.34995	0.08592	0.692574	0.275276	0.378999	0.208419	7.875	12.19	95.99625	876.12	39
-0.30324	0.110244	0.68481	0.386221	-0.07462	-0.14038	7.925	11.65	92.32625	874.48	39
-0.28648	0.053246	0.642328	-0.12354	-0.51628	-0.63976	8.018	11.65	93.4097	876.15	39
-0.3364	-0.01322	0.560523	-0.62559	-0.18743	-0.80126	8.44	10.93	92.2492	876.02	38
-0.38292	-0.02512	0.496659	-0.25604	0.196485	-0.22153	8.473	10.5	88.9665	876.19	34
-0.37361	0.016648	0.488339	0.235634	0.248366	0.376566	8.645	10.5	90.7725	876.74	30
-0.3352	0.035022	0.534383	0.165662	-0.29359	0.456382	8.713	9.77	85.12601	875.88	27
-0.44782	-0.17016	0.48729	-0.37789	-0.08713	-0.21408	9.32	9.77	91.0564	876.67	29
-0.5173	-0.3242	0.428978	-0.3182	-0.1834	-0.1760	9.598	9.389999	90.12521	877.23	31

3	1		9	4	3					
-0.50015	-0.30815	0.451308	0.313056	-0.14407	0.186337	9.923	8.9	88.3147	878.2	24
-0.48677	-0.33431	0.45952	-0.08204	-0.29306	-0.2625	9.963	8.9	88.6707	878.65	24
-0.39594	-0.27471	0.031616	0.301084	0.270981	-0.32635	10.903	9.17	99.98051	879.92	25
-0.3698	-0.2584	-0.01834	-0.1826	0.234265	-0.34098	10.971	9.17	100.6041	879.74	26
-0.38693	-0.24081	-0.06613	-0.23236	0.24065	-0.21354	11.113	10.53	117.0199	877.85	6
-0.38585	-0.2171	-0.09422	0.13879	0.197283	-0.04753	11.318	10.75	121.6685	879.81	0
-0.34778	-0.19267	-0.11825	0.323166	0.217237	-0.10579	11.351	10.78	122.3638	879.86	357
-0.32754	-0.16473	-0.15608	-0.03308	0.31887	-0.30986	11.421	10.92	124.7173	879.25	355
-0.33111	-0.14157	-0.21421	-0.10944	0.286412	-0.4772	11.481	10.92	125.3725	878.4	353
-0.33613	-0.13505	-0.28249	-0.05756	0.220696	-0.52164	11.771	10.95	128.8925	879.87	352
-0.32747	-0.12346	-0.34879	-0.08975	0.268054	-0.39925	11.936	10.95	130.6992	879.53	349
-0.35985	-0.10584	-0.39278	-0.45238	0.187705	-0.17337	11.978	10.78	129.1228	879.59	345
-0.38494	-0.08344	-0.41396	0.047001	0.262201	0.062621	12.033	10.57	127.1888	878.88	341
-0.34554	-0.05643	-0.42429	0.396597	0.189036	-0.00389	12.093	10.57	127.823	879.13	338
-0.32341	-0.05345	-0.45957	0.015075	0.012375	-0.33726	12.293	10.62	130.5517	879.47	336
-0.33134	-0.06977	-0.5203	-0.09427	0.062127	-0.56261	12.333	10.62	130.9765	878.82	335
-0.31635	-0.07829	-0.58865	0.297093	0.17121	-0.47055	12.623	10.25	129.3858	879.24	334
-0.2706	-0.06778	-0.64506	0.393937	0.168283	-0.3056	12.623	10.28	129.7644	879.55	332
-0.22893	-0.05936	-0.6869	0.246808	0.079953	-0.30294	12.768	10.28	131.255	880.42	328

-0.21411	-0.06457	-0.72347	0.176038	-0.0411	-0.246	12.813	9.88	126.5924	879.82	324
-0.17457	-0.06013	-0.7593	0.464441	0.193559	-0.23323	12.998	9.46	122.9611	879.04	321
-0.11568	-0.03316	-0.7908	0.370258	0.290669	-0.17949	13.071	9.46	123.6517	880.02	319
-0.11815	-0.00296	-0.81107	-0.17702	0.145137	-0.07546	13.208	9.53	125.8722	880.83	317
-0.12694	-0.00208	-0.82363	0.156616	-0.1132	-0.1034	13.311	9.53	126.8538	879.54	315
-0.08748	-0.02955	-0.83683	0.425065	-0.28587	-0.13293	13.583	8.929999	121.2962	880.62	313
-0.03603	-0.05731	-0.91205	0.013478	0.063458	-0.28751	13.718	8.929999	122.5017	880.29	312
-0.03409	-0.03024	-0.93353	0.0909	0.287742	-0.05364	13.796	8.679999	119.7493	879.71	306
0.015068	0.003149	-0.92374	0.033432	0.023017	0.01074	14.123	8.7	122.8701	881.04	306
-0.0059	-0.00889	-0.93483	-0.22704	-0.2151	-0.13745	14.153	8.7	123.1311	881.3	306
-0.03097	-0.02904	-0.95582	-0.10625	-0.17706	-0.18907	14.298	8.48	121.247	880.58	306
-0.03229	-0.05039	-0.9799	0.078662	-0.19674	-0.19971	14.508	8.48	123.0278	880.98	305
-0.02462	-0.0723	-0.9997	0.121763	-0.16748	-0.14091	14.658	8.34	122.2477	881.18	304
0.005718	-0.0813	-1.01952	0.308267	-0.03285	-0.12787	14.718	8.5	125.103	881.1	303
0.012395	-0.07761	-1.03444	-0.05437	0.003861	-0.16406	14.778	8.5	125.613	880.56	302
-0.01206	-0.08251	-1.04172	-0.14669	-0.08607	-0.08876	14.948	8.49	126.9085	880.14	301
-0.01745	-0.09801	-1.03886	0.039552	-0.13954	-0.00788	14.971	8.49	127.1038	881.18	300
0.009163	-0.11072	-1.04047	0.197322	-0.05999	-0.11324	15.228	8.54	130.0471	881.52	300
0.00755	-0.11729	-1.0559	-0.24007	-0.05919	-0.19864	15.361	8.62	132.4118	880.92	300
-0.0330	-0.1260	-1.0737	-0.3552	-0.1108	-0.1020	15.401	8.62	132.7566	880.87	300

8	4	9	7	1	7					
-0.05664	-0.12606	-1.07257	0.007625	0.101504	0.055704	15.556	8.69	135.1816	881.02	298
-0.03234	-0.10458	-1.05269	0.335937	0.195687	0.185006	15.618	8.69	135.7204	880.55	298
-0.02478	-0.08397	-1.0449	-0.10172	0.054146	-0.0148	15.751	8.83	139.0813	881.45	299
-0.04776	-0.0831	-1.06454	-0.25577	-0.08154	-0.20503	15.83	8.929999	141.3619	880.46	300
-0.07404	-0.09019	-1.0881	-0.05596	-0.08074	-0.1457	15.968	8.929999	142.5942	880.35	299
-0.05251	-0.10168	-1.09652	0.192893	0.070839	0.003839	16.238	8.92	144.843	880.62	298
-0.04231	-0.0958	-1.09327	0.288939	0.147463	0.090573	16.248	8.92	144.9322	880.59	297
-0.00418	-0.07065	-1.06571	0.382856	0.146399	0.216683	16.415	9.23	151.5105	880.82	297
0.029784	-0.06199	-1.05169	0.212315	-0.01084	-0.07571	16.448	9.469999	155.7625	880.73	298
0.021614	-0.06456	-1.07923	-0.31554	-0.00499	-0.35454	16.583	9.469999	157.041	880.8	299
-0.05492	-0.05498	-1.11399	-0.57388	0.105426	-0.18506	16.69	9.49	158.3881	880.39	298
-0.091	-0.04271	-1.11077	-0.06651	0.09505	0.070087	16.883	9.559999	161.4015	879.94	296
-0.09216	-0.02583	-1.09834	-0.04762	0.17939	0.046674	17.085	9.559999	163.3326	879.52	296
-0.12849	-9.76E-05	-1.10075	-0.52998	0.227013	-0.06693	17.123	9.45	161.8124	880.41	296
-0.19705	0.027998	-1.11025	-0.48555	0.255747	-0.01718	17.333	9.45	163.7969	880.84	297
-0.22456	0.048017	-1.11438	-0.03831	0.084674	0.033903	17.35	9.62	166.907	881.98	296
-0.22516	0.050043	-1.13017	-0.00718	-0.00233	-0.19783	17.523	9.4	164.7162	881.33	296
-0.23862	0.046656	-1.16944	-0.14979	0.039977	-0.3258	17.615	9.4	165.581	881.1	295
-0.26789	0.045458	-1.20758	-0.0713	0.044766	-0.22922	17.718	9.44	167.2579	881.31	293

-0.24471	0.043298	-1.23082	0.388709	-0.01749	-0.16138	17.813	9.44	168.1547	879.89	291
-0.1885	0.043854	-1.25583	0.521204	0.104628	-0.25716	17.925	9.49	170.1083	880.57	289
-0.1553	0.050636	-1.30028	0.121856	0.097711	-0.41573	18.028	9.3	167.6604	881.67	288
-0.1891	0.043484	-1.35096	-0.35704	-0.02095	-0.46575	18.268	9.3	169.8924	882.29	286
-0.20872	0.035484	-1.39379	0.03326	0.078821	-0.32234	18.318	9.309999	170.5406	881.87	283
-0.18891	0.047644	-1.4222	0.159902	0.204665	-0.19357	18.42	9.309999	171.4902	881.58	280
-0.22171	0.06432	-1.44111	-0.56137	0.125114	-0.09247	18.675	9.29	173.4908	881.26	279
-0.31292	0.065178	-1.44325	-0.58026	-0.05155	0.020867	18.705	9.21	172.2731	881.61	277
-0.31981	0.049745	-1.43347	0.29692	-0.20905	0.002509	18.775	9.21	172.9178	881.26	277
-0.28557	0.013492	-1.44959	0.162296	-0.23087	-0.387	18.845	9.139999	172.2433	881.28	277
-0.32169	-0.02158	-1.50835	-0.54435	-0.04383	-0.66662	19.058	9.139999	174.1901	881.3	277
-0.37531	-0.03309	-1.57509	-0.24317	0.150656	-0.47506	19.098	9.099999	173.7918	881.83	274
-0.37412	-0.03222	-1.61779	0.174269	0.131234	-0.22231	19.395	9.19	178.2401	881.85	270
-0.36017	-0.01714	-1.64233	0.09259	0.153582	-0.08023	19.395	9.19	178.2401	881.21	267
-0.34337	-0.01977	-1.66565	0.233599	-0.0002	-0.28137	19.478	9.17	178.6133	882.17	266
-0.33613	-0.01833	-1.7302	-0.07502	0.339023	-0.55408	19.673	9.17	180.4014	881.52	265
-0.3904	0.009215	-1.80989	-0.60713	0.494665	-0.45165	19.733	9.42	185.8849	882.56	262
-0.4596	0.039188	-1.86622	-0.28335	0.333435	-0.21805	19.815	9.639999	191.0166	882.92	257
-0.45909	0.04876	-1.90911	0.123452	0.13283	-0.30292	19.998	9.639999	192.7807	882.04	253
-0.4955	0.032183	-1.9663	-0.5720	0.158105	-0.5676	20.11	9.66	194.2626	882.73	251

2		5	2		5					
-0.60731	0.027748	-2.04064	-0.9389	0.324922	-0.42664	20.285	9.66	195.9531	882.6	248
-0.68935	0.030871	-2.09497	-0.20752	0.263197	-0.2702	20.355	9.719999	197.8506	882.2	244
-0.66726	0.025511	-2.14585	0.429149	0.252289	-0.43888	20.493	9.76	200.0117	882.24	240
-0.67433	0.00902	-2.22647	-0.52146	0.349931	-0.71052	20.535	9.76	200.4216	882.32	238
-0.75498	-0.00359	-2.3105	-0.52732	0.436399	-0.46389	20.688	9.91	205.0181	882.05	234
-0.73124	0.013849	-2.35699	0.851113	0.371747	-0.02809	20.942	9.91	207.5352	881.25	229
-0.59131	0.045311	-2.37932	1.135791	0.365894	-0.05656	20.972	9.8	205.5256	881.88	225
-0.51782	0.044336	-2.42851	0.503645	0.245371	-0.43967	21.02	10.37	217.9774	881.59	224
-0.41151	0.031739	-2.50233	1.237424	0.186573	-0.60915	21.255	10.37	220.4144	882.14	222
-0.2209	0.029877	-2.58625	1.644222	0.230472	-0.67221	21.3	10.4	221.52	882.89	218
-0.05502	0.056009	-2.66756	1.148828	0.342747	-0.53785	21.455	10.4	223.132	882.03	213
0.048819	0.09183	-2.70255	0.844461	0.198014	-0.01425	21.512	10.47	225.2306	881.38	208
0.178362	0.099962	-2.68177	1.306864	0.021353	0.279738	21.762	10.44	227.1953	881.39	205
0.3224	0.093188	-2.65808	0.845259	0.031995	0.092702	21.797	10.44	227.5607	881.22	205
0.320393	0.114596	-2.66828	-0.58452	0.229674	-0.13025	21.882	10.48	229.3234	881.94	207
0.234631	0.146031	-2.67141	-0.57627	0.244041	0.028582	22.022	10.55	232.3321	881.27	207
0.189856	0.171846	-2.66367	-0.35944	0.119261	0.025656	22.342	10.55	235.7081	881.14	206
-0.02153	0.147798	-2.6919	-1.50294	-0.32585	-0.0664	22.555	10.11	228.0311	882.67	207
-0.08447	0.134937	-2.69566	-1.52263	-0.30137	-0.03527	22.592	10.11	228.4051	881.95	207

-0.20966	0.107085	-2.6733	-0.54887	-0.1883	0.357692	22.622	10.13	229.1609	881.82	205
-0.20379	0.109796	-2.62555	0.361305	-0.00312	0.392279	22.682	9.82	222.7372	882.52	206
-0.19011	0.125072	-2.60192	-0.18677	0.083876	0.074876	22.705	9.82	222.9631	882.98	209
-0.25946	0.108705	-2.603	0.064122	-0.02308	0.011821	23.002	9.79	225.1896	882.12	210
-0.24888	0.112418	-2.60448	0.366627	0.153582	0.000114	23.057	9.79	225.728	883.49	211
-0.15996	0.149208	-2.60666	0.87825	0.396757	0.020867	23.082	9.66	222.9721	883.25	210
-0.07145	0.179999	-2.61883	0.659819	0.089463	-0.14089	23.23	9.57	222.3111	882.78	210
-0.04003	0.166261	-2.65734	0.154847	-0.24444	-0.36438	23.425	9.57	224.1773	884.28	209
-0.01694	0.139827	-2.70867	0.393764	-0.17047	-0.40136	23.465	9.23	216.582	884.79	207
0.04832	0.12791	-2.75327	0.621241	-0.00073	-0.31569	23.572	9.23	217.5696	884.15	204
0.076369	0.135439	-2.77805	0.048159	0.068445	-0.10418	23.712	9.38	222.4186	883.52	202
0.059714	0.148264	-2.77514	-0.15324	0.017894	0.145114	23.89	9.03	215.7267	883.94	200
0.053768	0.137182	-2.75903	-0.00213	-0.19601	0.139261	23.955	9.03	216.3137	883.78	201
0.039739	0.095419	-2.75907	-0.21816	-0.37188	-0.08077	24.077	9.08	218.6192	884.79	201
-0.01521	0.045838	-2.78119	-0.54807	-0.39928	-0.19118	24.242	9.08	220.1174	884.72	201
-0.08122	0.018496	-2.79256	-0.48342	-0.13083	0.031243	24.317	8.98	218.3667	885.7	200
-0.10211	0.045519	-2.76177	0.079021	0.370949	0.373123	24.445	9.16	223.9162	885.65	200
-0.08908	0.078907	-2.71953	0.059599	0.259472	0.416756	24.61	9.16	225.4276	884.61	201
-0.10565	0.091093	-2.68551	-0.36502	-0.06006	0.151234	24.717	9.15	226.1606	884.67	204
-0.1642	0.075135	-2.6811	-0.4017	-0.1558	-0.0134	24.78	8.96	222.0288	885.6	206

4		7	4	4	5					
-0.17566	0.075458	-2.68748	0.151654	0.081215	-0.04831	25.022	8.96	224.1971	885.91	206
-0.13957	0.07915	-2.69357	0.38392	-0.01084	-0.03128	25.172	9.09	228.8135	885.47	205
-0.10274	0.067239	-2.70847	0.249828	-0.10768	-0.20448	25.182	9.09	228.9044	884.98	205
-0.07292	0.052223	-2.73235	0.269517	-0.11274	-0.16324	25.395	9.04	229.5708	885.77	204
-0.04297	0.047981	-2.74645	0.272443	0.03439	-0.05629	25.472	9.11	232.0499	884.96	203
0.007204	0.048985	-2.74437	0.459214	-0.00711	0.0935	25.55	9.11	232.7605	886.02	202
0.046635	0.053751	-2.73701	0.225351	0.072436	0.054656	25.592	9.099999	232.8872	885.73	202
0.060102	0.068205	-2.7408	0.060397	0.147729	-0.05203	25.755	9.099999	234.3705	886.54	203
0.03425	0.086458	-2.75131	-0.40387	0.108087	-0.07757	25.853	9.16	236.8135	885.93	202
-0.02633	0.082322	-2.76644	-0.49486	-0.14733	-0.09114	26.173	9.07	237.3891	885.77	202
-0.08557	0.057393	-2.76852	-0.45814	-0.23911	0.02805	26.203	9.07	237.6612	886.69	201
-0.11857	0.030219	-2.76205	-0.11919	-0.17712	0.040023	26.381	9.21	242.969	886.07	201
-0.12605	0.018312	-2.75154	-0.06491	-0.04809	0.087913	26.441	9.21	243.5216	885.52	201
-0.13382	0.018997	-2.74457	-0.09205	-0.02015	0.037894	26.506	9.16	242.795	886.55	202
-0.15154	0.011779	-2.73417	-0.15032	-0.10822	0.100151	26.563	9.2	244.3796	885.49	203
-0.14797	0.003899	-2.72434	0.201939	-0.03957	0.055454	26.768	9.2	246.2656	886.66	203
-0.10692	0.001316	-2.71476	0.387645	-0.01137	0.084188	26.888	9.37	251.9406	886.11	204
-0.06283	-0.002	-2.71999	0.357581	-0.03851	-0.11934	26.973	9.37	252.737	885.51	204
-0.025	-0.00588	-2.74483	0.174269	0.000867	-0.22364	27.153	9.3	252.5229	885.9	203

-0.00123	-0.0047	-2.77135	0.206728	-0.00711	-0.17362	27.216	9.45	257.1912	886.47	202
0.016214	-0.00967	-2.78885	0.144205	-0.05048	-0.10258	27.406	9.45	258.9867	886.29	200
0.042987	-0.01274	-2.7983	0.206195	0.01683	-0.06667	27.468	9.69	266.1649	886.23	199
0.035712	-0.00492	-2.80137	-0.17107	0.072702	0.041885	27.626	9.969999	275.4312	885.73	199
0.011604	-0.00193	-2.79528	-0.17958	-0.0151	0.082059	27.656	9.969999	275.7303	885.68	199
-0.02025	-0.00095	-2.78768	-0.34214	0.003793	0.058913	27.788	10	277.88	886.71	200
-0.09151	-0.0049	-2.78146	-0.70052	-0.06671	0.060775	27.988	10	279.88	887.27	200
-0.15086	-0.01355	-2.76497	-0.24237	-0.1013	0.165867	28.051	10.07	282.4736	885.84	200
-0.13034	-0.00861	-2.74416	0.318737	0.103032	0.140592	28.361	10.29	291.8347	885.52	202
-0.11437	0.01646	-2.73879	-0.06624	0.285546	0.040555	28.361	10.29	291.8347	885.96	202
-0.14691	0.058064	-2.7325	-0.34853	0.318004	0.183692	28.391	10.39	294.9825	885	203
-0.14466	0.091069	-2.7069	0.268984	0.141078	0.273353	28.601	10.39	297.1644	886.05	203
-0.09876	0.095409	-2.68897	0.350929	-0.00525	0.026986	28.631	10.42	298.335	885.92	205
-0.08315	0.100645	-2.70739	0.035122	0.105959	-0.20475	28.831	10.43	300.7073	886.05	205
-0.0717	0.118734	-2.73364	0.220829	0.159702	-0.12786	28.946	10.43	301.9068	886.37	204
-0.03751	0.13324	-2.74853	0.337139	0.14412	-0.09216	29.021	10.58	307.0422	886.26	203
0.001353	0.149217	-2.76231	0.322772	0.155294	-0.09163	29.273	10.58	309.7083	886.19	202
0.017883	0.161387	-2.77932	-0.02017	0.043817	-0.15628	29.348	10.44	306.3931	886.67	201
-0.01524	0.160074	-2.80553	-0.33864	-0.05915	-0.19619	29.468	10.21	300.8683	886.57	200
-0.0494	0.15012	-2.8189	-0.1840	-0.0916	-0.0482	29.528	10.21	301.4809	886.36	198

8		4	6		6					
-0.06597	0.142705	-2.81415	-0.15426	-0.02482	0.081838	29.573	10.22	302.2361	886.79	198
-0.09438	0.142812	-2.79448	-0.35221	0.000716	0.225508	29.683	10.22	303.3603	887	199
-0.1307	0.153539	-2.76494	-0.21067	0.110863	0.255572	29.858	9.91	295.8928	887.28	200
-0.1285	0.172784	-2.74332	0.065763	0.110065	0.145957	29.981	9.83	294.7132	887.59	202

A.2 LANDING FLIGHT

Roll_Speed(rad/s)	Pitch_Speed (rad/s)	Yaw_Speed (rad/s)	Roll (deg)	Pitch (deg)	Yaw (deg)	alt(m)	Ground speed (m/s)	horizontal (m)	Heading (deg)
0.3239237	-0.2187901	-0.3107379	-5.78783	6.869368621	-19.2414296	882.62	7.86	4.56666	340
0.2361257	-0.2592304	-0.1127931	-4.00218	5.075503082	-19.7362933	882.66	7.65	4.44465	340
0.1297037	-0.2807809	-0.03217849	-2.8487	3.025472124	-19.4019323	882.29	7.64	5.12644	340
-0.1368833	-0.2014966	0.04364715	-2.09002	1.223529599	-18.7887872	882.57	7.64	6.27244	342
-0.2512869	-0.2227809	0.1096288	-2.96255	-0.40577736	-17.3302372	882.31	7.57	6.51777	343
-0.2608649	-0.2504506	0.06652787	-4.51146	-2.28245243	-15.8175427	882.1	7.57	7.57757	345
-0.09298421	-0.1376434	0.02661963	-5.74928	-3.58632332	-14.0837552	881.85	7.68	8.37888	346
-0.3569107	-0.00674437	0.001078365	-7.84074	-3.77305141	-13.1309264	881.91	7.75	9.23025	347
-0.901525	-0.03148748	-0.02605923	-13.1131	-3.68624945	-12.6808738	881.34	7.81	10.47321	347
-0.54926	-0.06953	-0.04734	-18.457	-4.03449	-12.4956	880.7	7.81	11.72281	347

83	333	363		435	652				
0.1108138	-0.00674437	-0.2365087	-16.2324	-4.3282458	-12.9974101	880.69	8.059999	14.75786	345
-0.4705161	0.05737485	-0.2718939	-17.3391	-4.85408984	-14.6888846	880.58	8.26	15.37186	344
0.01210746	0.1084574	-0.05771976	-19.5798	-4.42981804	-15.3540256	880.04	8.25	15.84825	346
0.7929786	-0.0956067	-0.1109307	-10.3171	-3.32323485	-13.1664498	879.55	8.25	18.40575	346
0.1297037	0.09355831	-0.1473803	-9.83726	-4.15233801	-15.9070387	879.01	8.7	23.0637	344
0.8637491	0.1685858	0.1801333	-5.44764	-2.88756519	-15.0140038	878.45	8.7	23.0637	346
0.5490062	0.1901362	0.2471791	0.485833	-1.17479553	-12.6357763	878.08	8.78	24.15378	348
-0.3103511	0.1826867	0.1537939	1.163757	-0.22019691	-10.7986444	877.92	8.96	25.09696	352
-0.03684664	0.1898702	0.2266929	0.051393	0.492691622	-8.75476646	872.44	8.96	25.81376	311
0.5194741	0.1105858	0.2769773	2.408872	1.440193016	-6.24742866	871.91	9.02	26.70822	312
-0.1590281	-0.01728065	-0.03969025	0.926281	-0.46357946	-48.6446783	870.96	8.889999	51.14416	313
-0.1161932	0.04337987	-0.09316728	0.20885	-0.43119767	-48.3192612	871.08	9.08	53.87164	314
0.2517607	-0.02499624	-0.01042421	0.768585	-0.36433722	-47.5197845	870.48	9.29	55.11757	315
0.00699019	-0.280675	0.01006201	1.561448	-1.5941886	-46.7459535	870.69	9.29	57.06847	318
-0.5690186	-0.2341154	-0.03436915	-0.25471	-3.51527655	-46.5429946	870.17	9.19	56.72987	319
-0.2133033	-0.02419807	0.058484	-3.16055	-4.57882087	-45.5521157	869.32	9.46	59.34258	319
0.1772653	0.1513982	0.2511077	-3.25567	-3.85434094	-43.264553	869.62	9.46	59.62638	319
-0.2502849	0.03406794	0.1678326	-4.02412	-3.16085747	-40.9967402	868.94	9.48	60.13164	321
-0.6328717	-0.09869344	-0.05299299	-7.20355	-3.58291078	-40.3456597	869.05	9.48	60.70044	323

0.03439385	0.05455417	-0.03011227	-10.3945	-4.07159107	-40.4104612	868.24	9.46	63.88338	325
-0.2553399	0.06386609	0.1268601	-11.3728	-3.50637795	-39.7179328	868.24	9.639999	66.54491	325
0.01843056	0.06493031	0.2013555	-11.666	-2.90758606	-38.0922338	868.08	9.639999	66.83411	324
0.6848981	0.1013798	0.1744839	-8.87666	-2.00107744	-35.802958	867.49	9.75	69.05925	323
0.4105954	0.1088294	0.006869356	-4.92569	-0.99599431	-34.1930727	867.23	9.75	69.74175	322
-0.03318409	0.06173765	-0.2038461	-4.60383	-0.38838122	-34.4451226	867.2	9.76	74.98608	322
0.2655955	-0.04415219	-0.2788736	-3.92235	-0.59366907	-35.7205839	867.25	9.719999	75.26195	329
0.6684027	-0.07155584	-0.2903139	0.359295	-1.34640727	-36.9368071	866.9	9.57	74.48331	333
0.3039074	-0.06250998	-0.208369	3.998011	-2.00194089	-37.5538139	865.87	9.57	74.77041	334
-0.119918	0.02555419	0.121539	3.683812	-2.16195311	-36.9148285	866.02	9.58	75.42334	335
0.3704211	0.1245266	0.5126396	4.223252	-1.84277895	-33.7591775	864.89	9.67	77.09891	338
-0.2806151	0.1162789	0.1952362	7.070505	-1.01117998	-26.2021105	864.39	9.92	81.67136	339
-0.3160004	-0.0281889	-0.09449755	-0.46228	-1.19132364	-24.5920017	864.06	9.74	82.14716	340
0.1679534	0.03167345	0.05209868	-11.4083	-1.79396523	-21.7140863	863.74	9.74	91.88716	339
-0.1962757	0.08594865	0.07763995	-11.7917	-1.15553269	-20.7395023	863.87	9.53	89.90602	338
-0.01243181	0.2035449	0.06407115	-12.6184	0.21746997	-20.2158704	863.28	9.53	90.47782	338
0.2639992	-0.04787696	-0.1809654	-7.92865	1.706798299	-19.9677568	862.9	9.48	95.12232	339
0.272779	0.06253582	-0.2166167	-5.05246	1.608769804	-20.7351764	862.96	9.429999	96.97811	341
-0.02280795	0.1051046	-0.1759103	-3.96255	2.132357545	-21.676632	862.49	9.429999	97.44961	343
0.09452225	0.04604041	-0.03224	-3.77261	2.761548283	-21.3272	862.7	9.28	97.38432	344

		071			997				
0.4590174	-0.06543658	0.1356399	-1.81065	2.653077632	-19.7296069	862.49	9.28	98.96192	345
0.3217331	-0.1678677	0.1321812	0.754471	1.724754797	-17.7515102	861.77	9.38	100.0283	346
-0.07814736	-0.1268953	0.04145649	0.785157	0.746821838	-16.3373128	862.07	9.3	100.0122	346
0.08760483	-0.03351	0.07843812	0.8612	0.257458299	-15.2828356	861.93	9.3	101.3607	346
0.132036	-0.01089533	0.07763995	2.112631	0.127549114	-14.1608009	862.02	9.349999	102.1861	346
-0.1542391	-0.0553265	-0.02026824	2.829407	-0.66520114	-13.3899148	861.83	9.349999	103.8691	347
-0.551459	-0.2067117	-0.1240297	0.039765	-1.9504847	-13.3375694	861.37	9.8	109.1622	348
-0.4724407	-0.3990694	-0.2216718	-3.69441	-4.23447724	-13.4977627	861.34	9.86	112.4927	350
0.02029294	-0.2931796	-0.1479746	-4.95314	-6.95463047	-13.292512	861.15	9.86	112.8871	354
0.04104522	0.0968569	0.03241063	-4.45507	-7.47367867	-12.408186	861.21	10.15	117.5269	356
-0.4455692	0.2458476	0.2452545	-6.91682	-5.77902421	-10.6642572	860.32	10.15	118.6434	355
-0.2133033	0.09047158	0.412337	-10.4803	-4.07199615	-8.05635383	860.25	10.17	119.4873	353
0.4241642	0.1053707	0.2550986	-9.53377	-2.79033311	-4.90715089	859.97	10.16	120.8938	352
0.00406359	0.2735173	-0.01494714	-7.88369	-1.03737848	-3.56905036	860.1	10.05	120.188	349
-0.1843033	0.3855264	-0.3033506	-9.40889	1.294386143	-5.16221623	859.8	10.05	120.8915	348
0.2951276	0.2522329	-0.2802038	-9.35033	3.389559301	-6.60609451	859.93	10.15	122.9064	349
0.6811733	0.0614716	-0.2118278	-5.82287	4.342923829	-7.72723541	859.07	10.15	123.3124	351
0.3669624	-0.1503081	-0.1673966	-2.11543	3.795675223	-9.15483997	859.07	10.46	128.1245	359
-0.2287344	-0.1755833	-0.1806993	-2.0923	2.510134402	-11.0667027	859	10.24	126.1466	298

0.9552098	-0.2263998	0.2487132	2.458124	-2.13688162	-11.4165221	858.23	10.16	130.241	298
-0.04143179	0.1247927	0.3144288	5.608512	-2.54263944	-10.0934136	858.62	10.16	130.5458	296
-0.4104499	0.3887191	0.4729975	3.264891	-1.13370414	-7.91075379	858.41	9.91	128.1264	294
0.4776413	0.4868934	0.364181	11.18433	5.252862168	0.752035754	857.81	9.9	130.0761	295
-0.6858167	0.1157468	-0.1250939	9.271019	6.406166621	-61.1453683	857.89	9.71	127.9681	297
-0.1361473	-0.1423264	-0.3304882	5.996737	6.007645827	-62.4549207	858.3	9.71	130.5024	299
0.7306595	-0.1641429	-0.2724883	8.944295	4.855040382	-64.2854062	857.66	9.599999	129.216	301
0.2384579	-0.08166593	-0.1783048	12.09419	4.230198394	-65.4200346	856.99	9.599999	129.984	304
-0.6520277	-0.06277603	-0.01867191	8.968222	4.045896206	-65.6571818	857.48	9.91	136.3616	309
-0.4144407	-0.309941	0.2388692	4.665248	2.489255247	-64.1691531	857.23	9.889999	136.6798	312
0.3145496	-0.5025647	0.378282	4.735054	-0.94861356	-61.5550332	857.11	9.889999	137.7677	311
-0.1739271	-0.2107026	0.2292912	5.903413	-3.53052239	-59.3466819	856.85	9.83	138.7996	308
-1.167908	0.1939669	0.1976307	0.163638	-3.32623601	-57.4979763	856.71	9.83	139.6843	306
-0.9497431	0.3062421	0.4908232	-7.75043	-0.88986362	-53.7050014	856.95	9.77	139.4179	307
0.1256507	0.1080312	0.4796489	-9.86155	0.993309427	-49.2310834	856.92	10.02	143.6868	308
0.1814571	0.02774776	-0.09935167	-7.85595	1.329117126	-47.2734241	856.29	10.02	146.0916	308
-0.6731112	-0.0544632	-0.571333	-10.1299	0.909416374	-49.4305472	855.95	10.01	146.9468	310
-0.6292121	-0.09463748	-0.435379	-15.3103	-0.5113222	-52.4578499	855.61	10.01	147.2471	313
0.2628698	-0.07574759	-0.09722323	-15.5277	-0.98741942	-53.0894442	855.93	9.8	145.824	316
0.777154	-0.3125364	-0.1001498	-11.6477	-2.49792696	-52.355978	855.6	9.889999	148.1522	315

0.6843008	0.05967434	-0.008893008	-6.24169	-3.49594037	-51.7204246	855.14	9.889999	151.6137	311
0.06891585	0.6040226	0.1347766	-4.24154	-0.85436258	-51.0075104	855.47	9.849999	151.69	309
0.05587916	0.5694355	0.4215838	-4.44216	3.781602807	-48.529021	855.15	9.849999	152.084	309
0.5342458	0.0681881	0.3231435	-1.74698	6.072613511	-45.1949281	854.89	9.42	145.4448	312
0.7292641	-0.3920868	-0.0466728	3.865816	4.482119342	-43.5591164	854.53	9.71	151.9615	313
-0.3737995	-0.3864997	-0.5543055	4.578406	1.671378622	-45.6697955	854.19	9.71	153.6122	315
-0.4770288	-0.1121971	-0.5806449	1.246726	0.032887525	-49.2533428	854.5	9.66	153.111	317
0.1407507	0.03466518	-0.1429847	0.043154	-0.07161961	-50.7324047	853.6	9.66	153.6906	318
0.02129203	-0.08638978	0.1911803	0.587777	-0.2722814	-49.3338319	853.91	9.75	158.2425	318
-0.9093679	-0.2460227	0.1834647	-2.82877	-1.36207652	-47.2544077	853.88	9.67	157.5243	318
-0.9072395	-0.2095732	0.09885922	-9.19266	-2.7883988	-45.9545383	853.17	9.67	158.2012	317
-0.03431344	-0.09197694	0.1153546	-11.6659	-3.71471285	-44.2112111	853.05	9.9	162.162	317
0.1827873	0.02136244	0.04192347	-10.5663	-3.71991817	-42.5301644	852.95	9.9	163.647	316
-0.1138638	0.04903214	-0.06928746	-10.7636	-3.19082545	-41.5841022	852.77	9.96	165.7344	316
-0.1303592	0.06100462	-0.1028104	-12.5097	-2.83767088	-41.8082777	853.32	10.21	173.3658	316
0.4985945	0.04158261	-0.1057337	-10.6956	-2.51863137	-42.0068305	852.9	10.21	173.6721	319
0.65131	-0.0321146	-0.2057736	-5.56217	-2.6659371	-42.3388079	852.61	9.889999	168.5256	324
-0.01675382	-0.1220411	-0.2890488	-3.77198	-3.31875833	-43.0162904	852.81	9.889999	171.6904	329
-0.0893868	-0.3598942	-0.1908745	-4.79753	-5.1692407	-43.780089	852.04	9.8	171.206	330
0.8543099	-0.46578	-0.07354	-1.70377	-8.51280	-43.7494	851.34	10.9	190.423	327

	4	435		065	873				
1.098282	0.2107935	0.1331803	5.886889	-9.64473607	-42.6382128	850.95	10.9	190.75	324
-0.2913225	0.9993801	0.3856664	7.330726	-4.95337827	-39.0592262	851.18	11.2	197.008	328
-1.237414	0.528197	0.6336296	0.181455	0.878124284	-33.7259058	851.83	11.2	198.912	333
0.5762825	-0.5224537	0.3446939	-1.96149	0.664759958	-29.837585	851.19	11.05	198.237	333
0.6773834	-0.3883621	-0.5125349	4.69174	-3.1287111	-30.384416	850.58	10.61	190.8739	330
-1.33745	0.4592887	-0.7208558	0.949217	-2.24976634	-34.6229916	850.33	10.61	191.7227	329
-0.9479459	0.6819767	0.2018224	-8.2488	1.538440381	-35.0020261	850.84	9.809999	179.0325	329
0.7649154	0.3217384	0.7701157	-6.62021	5.079208973	-30.0986074	850.14	9.809999	179.6211	328
-0.08991891	0.07084864	0.1536665	-2.79808	6.29921259	-26.0530785	850.6	10.06	187.0858	325
-1.487239	0.2203715	-0.3550304	-9.63971	6.925558592	-27.5168023	849.84	9.4	174.9998	324
-0.2546069	0.3204081	-0.1581498	-15.8085	8.229209463	-29.7228846	849.43	9.4	175.7518	322
1.188209	0.1924357	0.02196936	-10.7084	10.23890477	-30.0644362	849.47	8.92	168.6772	330
0.3714202	-0.04009624	-0.2643057	-4.52163	10.82530415	-30.436601	848.78	8.92	168.8556	336
-0.5640287	-0.2148943	-0.4329845	-6.50585	9.722486446	-32.8566314	848.47	8.51	162.4559	333
0.1104204	-0.2005273	-0.2116268	-8.59923	7.686927828	-34.5151666	848.12	7.79	149.6459	330
2.50252	-1.729811	-0.6857366	-0.08057	1.622241761	-36.3111716	848.75	7.79	150.5807	330
-2.462064	1.273949	0.7360607	3.158007	0.163452311	-35.2979359	848.64	7.04	136.576	336
-0.06251526	-0.5900316	0.7844827	0.13827	-5.08635204	-27.3566434	848.58	7.04	138.9696	322
1.189805	0.7327932	0.03713449	4.209629	-3.12336827	-23.7491751	848.32	6.51	128.6376	307

0.8367502	0.3893163	-0.6987733	4.149221	-4.00781571	-30.8181221	849.18	6.1	121.268	319
-0.7678267	-0.6932609	0.9845559	5.006553	-5.52770601	-27.1172674	848.44	6.1	121.878	325
-0.1864968	0.9443069	0.5945194	2.846684	-3.91563769	-22.3845386	848.87	5.31	106.8903	339
-1.138441	1.26783	-2.609313	3.459465	-4.94779022	-45.3721554	848.72	5.31	107.7399	337
1.973071	-3.504929	3.846242	11.76096	-8.50021277	-45.9827278	848.94	4.29	87.7305	338
0.5092367	-0.5634261	1.299299	25.59606	-13.4424321	-38.7773653	848.7	4.04	82.7392	341
-0.7675607	2.213123	1.238372	23.42924	-13.2170764	-29.7890727	848.07	4.04	83.4664	343
-3.013064	0.3009861	0.09726289	3.51325	-7.00351523	-18.7908556	848.18	4.13	85.491	345
-0.6390561	1.616894	0.6381525	4.179232	-9.21643293	-21.5803465	848.08	4.13	86.2344	346
1.12675	0.019234	0.214327	11.71079	-7.67830481	-22.0124713	848.5	3.85	80.696	348
-0.5863773	0.1982889	0.3939141	5.694723	-10.1216375	-17.3895326	848.22	3.13	66.6064	349
0.4762459	0.07324314	0.4356847	8.90809	-9.17658372	-15.6197806	848.33	3.13	66.7003	350
0.4076037	0.3060412	0.09806105	8.623966	-9.77911186	-14.7951224	848.37	2.09	44.7051	350
-0.1359464	0.6862336	0.364648	8.826111	-10.2897376	-13.1663982	848.16	2.09	44.7678	350
-0.2181574	0.1650321	0.1456849	7.563856	-10.7445973	-11.2951295	848.77	1.92	41.6448	351
-0.2112399	0.847995	0.2388041	5.904972	-11.2609583	-10.1682877	848.18	1.51	32.7821	351
-0.4818178	0.7977106	0.02329963	6.470229	-10.9354667	-9.14487623	848.26	1.51	33.069	350
0.1769341	-0.5940225	0.1294555	8.644484	-12.0772628	-9.26481922	849	1.21	26.5837	351
0.0691819	0.6271694	0.2643453	9.31367	-11.4541654	-8.4568456	848.61	1.21	26.8741	352
-0.51800	-0.63579	-0.16639	7.680551	-12.1797	-8.55038	848.26	1.03	22.9072	353

12	31	75		305	096				
0.5278605	-0.3838392	-0.2515351	8.46615	-12.1308343	-9.43203695	848.38	1.03	22.9381	355
0.05933788	-0.528839	0.03367577	8.173197	-11.7787002	-8.87219989	848.74	1.01	22.6644	358
0.06678741	-0.324775	0.0653363	8.211723	-11.8802283	-8.56672171	848.87	0.39	8.7789	358
-0.007974	-0.3330227	-0.08046177	8.053386	-11.2759756	-7.35014324	848.63	0.39	8.8647	359
-0.1763867	0.431353	0.4364829	6.498814	-10.0490151	-5.97167554	847.86	1.07	24.3425	359
-0.245561	-0.3918208	0.3210151	5.73289	-11.4087413	-3.98646272	848.41	0.65	14.859	0
-0.211506	-0.1965365	-0.1238287	4.812935	-12.0233131	-1.87563922	848.26	0.19	4.3833	1
0.03486083	-0.04648156	-0.0956269	3.504681	-11.6545173	-0.94733014	848.1	0.19	4.4156	2
0.4562917	0.130711	0.02755651	5.897569	-10.8749739	-0.8536418	848.09	0.2	4.648	2
0.02022781	-0.169665	-0.04214987	7.361299	-11.9235955	-0.20732002	848.39	0.09	2.1042	3
-0.1258363	0.09106882	0.08183171	6.454192	-11.8966321	1.527718622	848.43	0.09	2.13138	3
0.2649983	0.002472541	0.09885922	6.960194	-11.0907727	2.131414457	848.2	0.06	1.42272	4
-0.1617537	-0.00417883	-0.115581	7.155332	-11.1429233	2.572610866	848.25	0.06	1.43124	4
0.0521544	0.02428904	-0.100948	6.870308	-11.0996994	3.05588014	847.59	0.03	0.71802	5
-0.0186162	-0.02067423	0.2055472	7.199083	-11.1059733	3.66059584	848.11	0.11	2.65914	6
0.01889754	0.01311473	0.03074917	6.66374	-10.9812747	3.992669	848.47	0.11	2.66024	6
-0.05533177	-0.0025825	-0.01501227	6.692961	-10.9330603	4.38949212	848.57	0.03	0.73452	7
-0.02792812	-0.00072012	-0.00357191	6.410515	-10.9462785	5.002647488	848.31	0.03	0.73632	7
0.01650304	-0.00018801	0.01771248	6.026674	-10.9085893	5.629231268	848.27	0.01	0.24594	8

-0.02074464	7.80E-05	0.008134504	5.978677	-10.8647867	6.265012739	848.53	0.04	0.98696	9
0.02368652	0.001940432	0.01398771	5.693023	-10.8938586	6.8976269	848.27	0.04	0.99216	9
-0.0210107	-0.00072012	0.009464778	5.553568	-10.8737821	7.519830417	847.94	0.04	0.99576	10
0.01836543	0.001408323	0.01292349	5.426864	-10.8059324	8.121819984	847.95	0.04	1.00256	10
-0.01196483	0.0003441	0.01079505	5.271122	-10.7473819	8.724995573	848.54	0.08	2.01072	11
0.00798929	0.001940432	0.01185927	5.16046	-10.6903554	9.326864818	848.29	0.09	2.28546	12
-0.00105658	0.000610157	0.01185927	4.954139	-10.6727656	9.921898677	847.99	0.09	2.29626	12
-0.00185474	0.001674375	0.01185927	4.824239	-10.6285906	10.51698983	848.32	0.05	1.2787	13
0.00532874	0.001674375	0.01159322	4.650999	-10.5666481	11.09700074	848.49	0.05	1.2812	13
-0.0050474	0.000610157	0.01185927	4.529903	-10.4660711	11.67937796	848.31	0.08	2.06832	14
0.00559479	0.000610157	0.01185927	4.424465	-10.3691152	12.25314362	848.26	0.07	1.80978	14
-0.00158869	0.001408323	0.01079505	4.358448	-10.3438133	12.80996693	847.94	0.07	1.82588	15
0.00080581	0.000610157	0.01185927	4.261519	-10.3083473	13.36719703	847.93	0.08	2.09072	15
0.00187003	0.001674375	0.01185927	4.089471	-10.2585744	13.92060551	848.27	0.08	2.09952	16
-0.00132263	0.001142266	0.01106111	4.006112	-10.2638456	14.46871985	848.51	0.04	1.05736	16
0.00240214	0.001408323	0.01239138	3.922791	-10.2689278	15.00347855	848.23	0.04	1.06576	17
-0.00079052	0.000610157	0.01159322	3.801205	-10.2319662	15.53626054	848.36	0.04	1.06816	17
0.00133792	0.001408323	0.01185927	3.679075	-10.1383736	16.06122739	848.18	0.08	2.13952	18
0.00053975	0.000876213	0.01159322	3.542349	-9.99468724	16.58073396	848.05	0.08	2.14672	18
0.0002737	0.000876213	0.01159322	3.480266	-9.96864	17.09082109	847.94	0.03	0.80802	19

				057					
0.00133792	0.001674375	0.01185927	3.429246	-9.9672712	17.58916259	847.84	0.08	2.17312	19
0.00053975	0.000610157	0.01132716	3.337429	-9.95276964	18.08651861	848.02	0.08	2.17552	20
0.0002737	0.001408323	0.01185927	3.271466	-9.89252886	18.56743646	848.31	0.01	0.27454	20
0.0002737	0.001142266	0.01185927	3.228571	-9.79275399	19.03853955	848.26	0.01	0.27572	21
0.00025613	0.001366466	0.01208347	3.129361	-9.77197854	19.52585734	848	0.04	1.10568	21
0.00052218	0.001632523	0.01208347	3.016828	-9.75255527	20.00271293	847.79	0.12	3.32184	22
0.00025613	0.001366466	0.01261558	2.900552	-9.64772691	20.47611358	848.36	0.12	3.33624	22
0.00025613	0.001366466	0.01208347	2.815844	-9.57621032	20.93251457	848.4	0.16	4.47232	22
0.00052218	0.002430685	0.01208347	2.788672	-9.56412664	21.3729816	847.82	0.16	4.49952	23
0.00025613	0.001366466	0.01234953	2.732707	-9.50883048	21.82101741	847.93	0.04	1.12888	23
0.00105429	0.002164632	0.01261558	2.682255	-9.44649268	22.25594967	848.36	0.04	1.13168	24
0.00025613	0.001632523	0.01261558	2.729779	-9.48768261	22.66841626	847.87	0.04	1.13488	24
0.00025613	0.002430685	0.01234953	2.72173	-9.51017693	23.0828309	848.4	0.05	1.43015	24
0.00105429	0.002430685	0.01181742	2.608952	-9.50620634	23.50396634	847.89	0.05	1.43315	25
0.00105429	0.002164632	0.01261558	2.565798	-9.39569424	23.916834	847.83	0.06	1.72818	25
0.00052218	0.001632523	0.01155136	2.558324	-9.23234397	24.30915539	848.38	0.06	1.73118	26
0.00052218	0.001366466	0.01261558	2.52368	-9.19493556	24.70198098	848.39	0.09	2.61027	26
0.00078824	0.001366466	0.01208347	2.491716	-9.1546337	25.08928899	848.46	0.04	1.17132	26
0.00025613	0.001366466	0.01261558	2.465068	-9.1116676	25.46803701	847.89	0.04	1.17412	27

0.00105429	0.001632523	0.01181742	2.384091	-9.02539734	25.85643937	848.39	0.06	1.76298	27
0.00052218	0.002430685	0.01181742	2.293006	-8.92420154	26.23471757	848.5	0.06	1.76718	27
0.00132035	0.002164632	0.01208347	2.276974	-8.9711497	26.5965576	848.25	0.06	1.78398	28
0.00052218	0.001632523	0.01261558	2.259204	-8.97962948	26.95136172	847.92	0.05	1.49165	28
0.00078824	0.001366466	0.01181742	2.236128	-8.90531685	27.29715321	848.36	0.05	1.49365	28
0.00078824	0.001898576	0.01208347	2.196671	-8.84181594	27.64928161	848.47	0.11	3.29373	29
0.00025613	0.001366466	0.01261558	2.143857	-8.78352894	27.99356622	848.29	0.11	3.31573	29
0.00025613	0.002430685	0.01208347	2.133037	-8.76053614	28.3241686	847.94	0.03	0.90759	29
0.00132035	0.001366466	0.01181742	2.144572	-8.73487337	28.64128928	848.04	0.02	0.60606	30

A.3 TURNING FLIGHT

Roll (rad)	**Pitch (rad)**	**Yaw ()**	**Roll_Speed (rad/s)**	**Pitch_Speed (rad/s)**	**Yaw_Speed (rad/s)**	**Time (s)**	**alt (m)**	**Ground speed (m/s)**	**Horizontal (m)**	**heading (deg)**
0.02814	0.120476	-0.4557315	-1.014997	-0.07063115	0.2355731	0.214	923.61	7.89	1.68846	332
-0.11805	0.105725	-0.4287874	-1.355547	-0.1326219	0.008096121	0.234	924.35	8	1.872	334
-0.25378	0.083036	-0.4036788	-0.8628131	-0.2321265	0.04933463	0.344	923.52	7.74	2.66256	335
-0.29012	0.074304	-0.3807518	-0.04496038	-0.08207152	-0.01584882	0.454	923.88	7.74	3.51396	337
-0.28652	0.065826	-0.3942295	0.0329937	-0.008640368	-0.1150873	0.604	923.77	7.84	4.73536	338
-0.28937	0.059687	-0.4226471	0.05135149	-0.03870457	-0.1773441	0.704	924.27	7.84	5.51936	336
-0.26314	0.048407	-0.4443317	0.4004155	0.03179997	-0.1488762	0.964	923.35	7.87	7.58668	335
-0.19429	0.059089	-0.4686809	0.698397	0.1956898	-0.02223413	0.994	923.27	7.89	7.84266	333

-0.12121	0.099453	-0.4925432	0.5206723	0.3771392	-0.08129832	1.214	923.47	7.89	9.57846	332
-0.07291	0.127795	-0.5155786	0.4025439	0.1565797	-0.04325247	1.364	923.98	7.95	10.8438	331
-0.01864	0.127542	-0.5417443	0.5392962	-0.1089431	-0.1704267	1.444	923.85	7.93	11.45092	329
0.045194	0.102121	-0.5739414	0.4682595	-0.2600622	-0.195968	1.504	923.98	7.93	11.92672	328
0.091509	0.079808	-0.614001	0.3961586	-0.1398054	-0.200757	1.594	923.7	8.01	12.76794	325
0.109069	0.083652	-0.6421301	-0.01276774	0.1246531	-0.1116286	1.744	924.88	8.01	13.96944	323
0.094517	0.09807	-0.65079	-0.1567034	0.09272654	0.1522979	1.894	924.05	7.96	15.07624	322
0.057856	0.106256	-0.637468	-0.4094556	0.0911302	0.2251969	1.934	924.65	7.85	15.1819	322
-0.00607	0.109376	-0.6126323	-0.6890792	-0.01422752	0.3497106	2.024	923.46	7.85	15.8884	324
-0.09229	0.10313	-0.5915303	-0.6826939	-0.0945761	0.2331786	2.295	924.95	7.88	18.0846	325
-0.16097	0.079951	-0.5803589	-0.4906023	-0.162154	0.0807291	2.325	924.24	7.88	18.321	326
-0.21597	0.062653	-0.6027073	-0.2884006	-0.0291266	-0.1422249	2.445	923.72	7.87	19.24215	326
-0.2386	0.058445	-0.6107597	-0.4097216	-0.007310097	-0.08236254	2.615	924.24	7.87	20.58005	325
-0.26547	0.05381	-0.6108809	0.01037904	-0.09404399	0.1876832	2.645	924.81	7.87	20.81615	324
-0.2136	0.047259	-0.5982869	0.751874	-0.05998896	0.1467107	2.755	923.59	7.93	21.84715	325
-0.11697	0.041375	-0.5995344	0.7247364	-0.05573208	0.02671996	2.855	924.12	7.93	22.64015	325
-0.0627	0.042498	-0.6308725	0.3331036	0.1007082	-0.1808028	3.115	924.17	8.02	24.9823	324
-0.02549	0.054694	-0.651653	0.4216999	0.148332	0.004637408	3.325	923.79	8.16	27.132	322
0.068107	0.074529	-0.6473138	1.002764	0.1547173	0.153096	3.355	923.13	8.16	27.3768	322
0.179975	0.095891	-0.6541	0.7851309	0.1613687	-0.1842	3.385	924.02	8.09	27.38465	322

		491			615					
0.226972	0.116232	-0.7139521	-0.05879522	0.05973573	-0.5181605	3.535	923.45	8.01	28.31535	320
0.180676	0.129259	-0.7647652	-0.4847491	0.04191006	-0.4665458	3.605	924.08	8.01	28.87605	317
0.100761	0.130232	-0.7890325	-0.6667306	-0.05892474	-0.1220047	3.805	923.76	8.01	30.47805	314
0.01881	0.093578	-0.7746029	-0.7406939	-0.4396493	0.2073712	3.925	924.35	8.01	31.43925	315
-0.07363	0.034743	-0.7369334	-0.7526664	-0.4699795	0.2028483	3.975	924.17	7.99	31.76025	317
-0.16323	0.004524	-0.6856382	-0.6888131	-0.08792473	0.4143619	4.205	923.87	8.02	33.7241	320
-0.21994	0.038952	-0.6247487	-0.2546116	0.308231	0.5064169	4.385	923.33	8.02	35.1677	323
-0.22895	0.086928	-0.560417	-0.1096117	0.1970201	0.3893527	4.435	923.63	7.96	35.3026	327
-0.23888	0.10044	-0.5216592	-0.0949787	-0.05227337	0.1640043	4.455	923.12	7.96	35.4618	329
-0.20699	0.119011	-0.5094005	0.5653695	0.3098273	-0.04671118	4.635	923.8	7.84	36.3384	330
-0.09581	0.168686	-0.5154411	0.7124979	0.322864	-0.1214726	4.715	924.17	7.86	37.0599	330
-0.01115	0.184097	-0.5297822	0.7510759	-0.09191556	-0.2329496	4.835	923.73	7.86	38.0031	329
0.095012	0.156212	-0.5633965	0.9474244	-0.1829063	-0.3710321	4.985	924.71	7.52	37.4872	328
0.205703	0.148633	-0.5888592	0.8332868	0.04856143	-0.2002248	5.075	923.84	7.55	38.31625	326
0.3135	0.158519	-0.5776109	0.6316172	0.1794604	0.2294538	5.245	924.52	7.55	39.59975	326
0.375583	0.150322	-0.5149143	0.2801587	0.123855	0.6218847	5.565	924.51	7.29	40.56885	329
0.4254	0.117425	-0.4138428	0.3921678	0.1501944	0.9086919	5.605	924.35	7.19	40.29995	335
0.510223	0.078668	-0.2992465	0.436599	0.1847815	0.6905269	5.665	924.23	7.19	40.73135	342
0.485482	0.071853	-0.2455837	-0.7457489	0.2084604	0.1562887	5.745	923.75	7.07	40.61715	345

0.317002	0.062754	-0.2281255	-1.746913	-0.07914492	0.04747224	5.895	925.19	7.07	41.67765	346
0.093484	0.00577	-0.2022291	-1.193253	-0.3771264	0.1517658	6.195	924.66	7.15	44.29425	348
0.008036	-0.04048	-0.1727907	-0.363162	-0.1738604	0.1719859	6.235	925.13	7.32	45.6402	349
-0.11891	-0.04358	-0.1362073	-0.7486755	0.04057978	0.2185455	6.425	924.67	7.31	46.96675	351
-0.1538	-0.04714	-0.1158141	0.1630946	-0.09244766	0.3547656	6.455	924.72	7.31	47.18605	353
-0.08749	-0.06582	-0.08839322	0.5712227	-0.1874292	0.1749125	6.595	924.65	7.31	48.20945	354
-0.06494	-0.07409	-0.09063776	-0.03618057	0.0605339	-0.04165614	6.745	924.14	7.56	50.9922	355
-0.06252	-0.05662	-0.1049792	0.2022046	0.211387	0.1068025	6.915	924.58	7.56	52.2774	354
0.011628	-0.02455	-0.09421061	0.7917823	0.1451394	0.2033804	6.925	924.38	7.52	52.076	354
0.107916	-0.01872	-0.08236877	0.688819	-0.01263119	0.02805024	7.197	924.79	7.52	54.12144	355
0.160993	-0.03372	-0.09422337	0.1050946	-0.103622	-0.1597845	7.387	924.78	7.64	56.43668	354
0.189046	-0.04266	-0.0928267	0.3599751	-0.008374316	0.1507015	7.457	923.88	7.82	58.31374	354
0.253178	-0.04694	-0.05619285	0.7247364	0.08873571	0.3507748	7.467	924.55	7.82	58.39194	356
0.352255	-0.04887	0.0138524	0.6284245	0.2457081	0.385894	7.727	924.82	7.89	60.96603	0
0.391073	-0.04567	0.07712423	-0.0300613	0.2265521	0.3098024	7.747	924.72	8.13	62.98311	3
0.339456	-0.04988	0.1356741	-0.5057674	0.1648274	0.2414263	7.977	923.7	8.13	64.85301	6
0.275342	-0.05153	0.1701422	-0.6648682	0.07915774	0.3457198	7.997	924.19	8.2	65.5754	9
0.159758	-0.06638	0.2277133	-0.7920424	-0.04136512	0.3425271	8.197	924.56	8.42	69.01874	13
0.03403	-0.09283	0.2875325	-0.5757399	-0.0921816	0.3018207	8.347	924.17	8.69	72.53543	16
-0.0181	-0.1073	0.3209488	-0.3256	-0.0860	0.2243987	8.497	924.36	8.69	73.83893	18

5			483	6233						
-0.09207	-0.1344	0.3402644	-0.7321801	-0.1823742	0.1459126	8.577	924.18	8.95	76.76415	19
-0.16036	-0.14278	0.3702455	-0.0678411	0.04004767	0.4300591	8.757	924.24	9.08	79.51356	21
-0.12498	-0.10941	0.4270379	0.5757457	0.2462402	0.6048572	8.817	924.53	9.08	80.05836	24
-0.08568	-0.09122	0.5059074	0.08886523	-0.0320532	0.4814077	9.077	924.53	9.26	84.05302	28
-0.03461	-0.09464	0.542439	0.7875254	0.07064398	0.02751813	9.287	923.33	9.429999	87.57640071	31
0.083322	-0.08978	0.5227079	0.6635438	-0.05945685	-0.2276285	9.327	923.78	9.429999	87.95360067	29
0.063464	-0.11018	0.4703385	-0.6616756	-0.1991356	-0.1746836	9.397	923.53	9.58	90.02326	26
0.027154	-0.11866	0.5089482	0.5009843	0.04031373	0.7799213	9.597	923.6	9.84	94.43448	29
0.1662	-0.11944	0.6360769	1.640497	0.119332	1.088545	9.657	924.38	9.84	95.02488	36
0.334844	-0.13126	0.7332773	0.5291861	0.2603411	0.468105	9.787	923.42	9.929999	97.18490021	42
0.324591	-0.1151	0.7680477	-0.3006391	0.2989191	0.2408941	9.987	923.62	10.28	102.66636	44
0.304609	-0.09814	0.8025115	0.1745349	0.2289466	0.245151	10.197	923.18	10.28	104.82516	45
0.349225	-0.09368	0.8412493	0.2955899	0.1714788	0.1403254	10.267	922.91	10.74	110.26758	48
0.281493	-0.08258	0.8531324	-0.8580241	0.1211944	0.03869243	10.357	923.42	11.12	115.16984	48
0.170515	-0.08207	0.8803326	-0.7308498	0.1360935	0.4226096	10.497	923.93	11.24	117.98628	50
0.135461	-0.0769	0.9636254	0.07210377	0.1039008	0.7102149	10.667	923.24	11.24	119.89708	55
0.111275	-0.07804	1.037213	-0.3589051	0.05920362	0.5742609	10.817	922.8	11.55	124.93635	59
0.042884	-0.07583	1.090022	-0.5007124	0.1709467	0.4811417	10.867	923.26	11.84	128.66528	62
0.049641	-0.05282	1.163938	0.52892	0.2728457	0.5303618	11.147	922.32	11.84	131.98048	66
0.153089	-0.0325	1.203956	0.5866539	0.1810568	0.1584171	11.267	923.42	11.81	133.06327	68

	7									
0.17345	-0.01486	1.184818	-0.1670796	0.1331669	-0.1467478	11.297	923.03	12.33	139.29201	67
0.136287	-0.00636	1.172025	0.02820471	0.1571118	0.1698575	11.547	922.71	12.33	142.37451	67
0.216019	0.002302	1.236995	0.6912135	0.2459742	0.5314261	11.577	923.79	12.33	142.74441	70
0.259151	0.011314	1.288352	-0.04096955	0.177332	0.4037197	11.757	922.36	12.63	148.49091	73
0.195581	0.019636	1.322723	-0.4235565	0.1124146	0.3252335	11.797	923.08	12.63	148.99611	75
0.18807	0.014595	1.377421	0.1995441	0.07144215	0.4013252	11.987	923.43	12.53	150.19711	78
0.176731	0.020099	1.404884	-0.4381895	0.1669559	0.3039491	12.037	922.5	12.7	152.8699	80
0.097684	0.039898	1.433959	-0.547272	0.3095613	0.3619491	12.216	922.94	12.7	155.1432	82
0.066436	0.089151	1.489627	-0.1024282	0.4266254	0.4625179	12.316	922.87	12.83	158.01428	85
0.053159	0.12139	1.529291	-0.2365199	0.2539558	0.2730868	12.486	923.9	12.78	159.57108	88
0.02068	0.131923	1.543439	-0.31474	0.09405681	0.05784838	12.576	923.38	12.78	160.72128	88
-0.00948	0.137579	1.541948	-0.3115474	0.02647888	0.1086649	12.776	924.53	12.71	162.38296	88
-0.04176	0.124184	1.553253	-0.2532814	-0.1807779	0.1791694	12.876	923.47	12.59	162.10884	89
-0.0485	0.075216	1.58794	0.126645	-0.3279062	0.2526006	12.976	924.79	12.59	163.36784	91
0.011751	0.041861	1.626635	0.3437458	0.06824949	0.1855547	13.146	924.51	12.5	164.325	93
0.042176	0.073313	1.65844	-0.002391596	0.3603777	0.2486097	13.296	923.63	12.42	165.13632	95
0.022739	0.099787	1.697128	-0.3618318	0.1709467	0.409839	13.486	923.68	12.42	167.49612	97
-0.00169	0.102729	1.747699	-0.05799707	-0.04695227	0.3819032	13.706	924.04	12.25	167.8985	100
0.004312	0.090072	1.780655	-0.005584254	-0.0567963	0.1546924	13.796	924.46	12.35	170.3806	102
-0.01908	0.086741	1.79328	-0.377529	0.07889169	0.04374747	13.906	923.99	12.35	171.7391	102

-0.06312	0.092477	1.809793	-0.2868043	0.03313025	0.1645364	13.936	924.04	12.36	172.24896	103
-0.09025	0.086037	1.833644	-0.2777584	-0.1302274	0.1839584	14.176	924.12	12.25	173.656	105
-0.1238	0.065252	1.853004	-0.3064923	-0.1485852	0.09296762	14.256	924.08	12.23	174.35088	107
-0.13899	0.05794	1.884581	0.0111772	0.06691922	0.2084354	14.436	924.08	12.23	176.55228	108
-0.10857	0.084767	1.918038	0.2697825	0.2800292	0.3292243	14.456	923.62	12.15	175.6404	110
-0.0798	0.111509	1.946246	0.0548102	0.03206603	0.1163805	14.606	924.16	12.15	177.4629	111
-0.10921	0.100544	1.945965	-0.3487951	-0.08952106	-0.07039007	14.776	925.23	11.95	176.5732	111
-0.17008	0.094863	1.95156	-0.3150061	-0.007044037	0.02938051	14.936	924.44	12.05	179.9788	112
-0.15903	0.091391	1.977606	0.2979844	-0.08473206	0.1882153	15.046	925.62	12.05	181.3043	113
-0.07291	0.075907	2.016352	0.5877181	-0.132888	0.2273254	15.166	925.26	11.92	180.77872	115
0.003502	0.065819	2.044145	0.1859753	0.01450641	0.1230318	15.366	925.16	11.95	183.6237	117
0.025875	0.06264	2.065435	0.2155074	-0.03391558	0.1629401	15.456	924.83	11.94	184.54464	118
0.073074	0.051085	2.103502	0.4475072	-0.0562642	0.2794721	15.576	926.07	11.94	185.97744	120
0.134537	0.035219	2.150787	0.4879475	-0.03604402	0.3983986	15.676	925.37	12.08	189.36608	123
0.201188	0.021647	2.20899	0.5169476	0.04191006	0.5090774	15.966	925.77	12.08	192.86928	127
0.261849	0.007821	2.280369	0.4179751	0.02860731	0.448949	16.036	924.62	12.08	193.71488	131
0.304062	-0.01591	2.334972	0.2474339	-0.02087889	0.2709583	16.116	925.54	12.1	195.0036	134
0.296539	-0.0343	2.375643	-0.2993088	0.0576073	0.3185821	16.386	925.29	12.1	198.2706	136
0.257196	-0.03196	2.451257	-0.0949787	0.3329741	0.6173618	16.416	923.48	12.27	201.42432	141
0.260557	-0.00531	2.56334	0.08753495	0.385919	0.720325	16.586	924.37	12.29	203.84194	147
0.228203	-0.00574	2.650241	-0.4778317	0.02541466	0.3643436	16.736	925	12.45	208.3632	152

0.147539	-0.02904	2.686048	-0.4054647	-0.03444769	0.09057313	16.806	925.24	12.45	209.2347	154
0.119945	-0.0302	2.717001	-0.03352002	0.1946256	0.1953988	16.996	924.97	12.81	217.71876	156
0.110425	-0.01677	2.768977	-0.09231815	0.1709467	0.4199491	17.106	924.23	12.84	219.64104	160
0.1271	-0.01355	2.839456	0.2019386	0.06106601	0.3781784	17.298	924.74	12.84	222.10632	163
0.1217	-0.02609	2.896539	-0.2351896	-0.001988997	0.3239033	17.408	924.05	12.75	221.952	166
0.108075	-0.03021	2.946298	0.06332395	0.1023045	0.3968023	17.458	923.72	12.78	223.11324	170
0.149778	-0.02747	3.02745	0.4288833	0.1571118	0.5000316	17.618	924.21	12.78	225.15804	177
0.196964	-0.02184	3.098741	0.2351954	0.2100568	0.3590225	17.818	923.05	12.78	227.71404	178
0.233337	-0.00883	-3.126166	0.2181679	0.2491668	0.2044446	17.988	924.26	12.49	224.67012	181
0.252034	-0.00571	-3.097575	0.001333173	-0.008906421	0.1991235	18.028	923.63	12.46	224.62888	182
0.243116	-0.02249	-3.077068	0.05933313	-0.001988997	0.2049767	18.138	923.91	12.46	225.99948	184
0.234332	-0.01821	-3.02329	-0.1167952	0.235598	0.4635821	18.488	923.52	12.7	234.7976	188
0.167658	-0.00547	-2.882397	-0.295052	0.1467357	0.4992334	18.658	923.5	12.53	233.78474	195
0.150264	-0.00682	-2.820279	-0.09684108	0.1709467	0.4816738	18.698	923.34	12.53	234.28594	199
0.140711	0.009754	-2.769196	-0.08007962	0.2869466	0.4665087	19.168	923.74	12.52	239.98336	202
0.109659	0.056355	-2.695414	-0.144997	0.5569923	0.5966095	19.238	922.44	11.79	226.81602	149
0.147802	0.114807	2.636956	0.09205788	0.3223319	0.3805729	20.018	923	11.44	229.00592	152
0.225408	0.120376	2.727455	0.7135621	0.05388253	0.8663892	20.058	923.31	11.44	229.46352	158
0.316767	0.090393	2.82153	0.6286906	-0.0379064	0.7115452	20.148	923.08	11.05	222.6354	163
0.383474	0.081156	2.897763	0.2796266	0.2571484	0.5614902	20.188	923.01	11.05	223.0774	167
0.414616	0.110657	2.974441	0.1295716	0.5184144	0.4888573	20.328	922.77	10.69	217.30632	171

0.423398	0.139351	3.04786	-0.1880979	0.3401576	0.3683344	20.328	922.68	10.58	215.07024	180
0.210061	0.182225	3.140029	-0.9285286	0.2728457	0.2954354	20.818	922.16	9.71	202.14278	185
0.111939	0.201497	-3.099262	-0.8660057	0.1219926	0.3747197	20.818	921.89	9.71	202.14278	186
-0.02737	0.184927	-3.032253	-0.426217	-0.08419996	0.1749125	21.028	921.43	9.639999	202.709899	187
-0.08967	0.192593	-3.014345	-0.6020793	0.123855	0.1605456	21.068	921.6	9.639999	203.0954989	189
-0.13124	0.206518	-2.98534	-0.1625566	0.07809352	0.3489124	21.238	921.39	9.37	199.00006	191
-0.09535	0.211652	-2.955672	0.5092319	-0.001190835	0.1826281	21.298	922.02	9.38	199.77524	190
-0.02759	0.216527	-2.95161	0.4927365	0.1438091	-0.05150017	21.438	921.08	9.38	201.08844	189
0.007463	0.236128	-2.97088	0.1436725	0.1438091	-0.1007203	21.698	921.29	8.99	195.06502	189
0.00951	0.235306	-2.980784	0.1130762	-0.07408988	-0.001747909	21.848	921.69	8.99	196.41352	189
0.077174	0.200422	-2.972996	0.7941768	-0.3875025	0.1158483	21.878	921.4	8.96	196.02688	188
0.186596	0.164836	-2.987563	0.8859656	-0.2087136	-0.1499405	21.938	921.19	8.88	194.80944	186
0.234507	0.163715	-3.019672	-0.01409801	0.05680913	-0.2656744	22.158	921.79	8.88	196.76304	185
0.175247	0.180484	-3.040932	-0.7188774	0.1041669	0.007830067	22.3	920.87	8.76	195.348	188
0.089383	0.185335	-3.015422	-0.6129875	-0.01236514	0.3819032	22.3	922.3	8.76	195.348	190
0.070383	0.144599	-2.961455	-0.1064191	-0.4811538	0.4476188	22.47	921.37	8.95	201.1065	190
0.035861	0.084078	-2.954201	-0.5901068	-0.3821814	0.01208694	22.48	921.12	8.99	202.0952	190
-0.08332	0.063407	-2.96203	-1.21374	0.01317613	0.03310528	22.61	921.46	8.99	203.2639	192
-0.20066	0.071368	-2.938855	-0.7635746	0.01823117	0.4699674	22.75	921.23	9.03	205.4325	196
-0.2392	0.082422	-2.8788	-0.0369	-0.0533	0.5694719	22.88	921.42	9.03	206.6064	199

7		06	7873	3759						
-0.21311	0.088109	-2.818163	0.1098836	-0.000924778	0.4667747	23.09	920.7	9.15	211.2735	200
-0.21267	0.102368	-2.793389	-0.106153	0.1134788	0.1828942	23.16	920.94	9.22	213.5352	200
-0.20527	0.117975	-2.788528	0.2958559	0.1951577	0.09403185	23.35	920.35	9.22	215.287	200
-0.12319	0.148169	-2.788435	0.8356813	0.3037081	0.1166465	23.35	921.42	9.11	212.7185	199
-0.03959	0.182608	-2.800366	0.5781401	0.2797631	-0.1190781	23.48	920.89	9.11	213.9028	197
-0.00025	0.191689	-2.827556	0.1920945	-0.02832843	-0.1680322	23.7	920.34	9.01	213.537	195
0.010152	0.187979	-2.861092	0.1615724	-0.001403395	-0.1780888	23.77	921.28	8.99	213.6923	195
0.037097	0.191323	-2.873468	0.2493705	0.1114039	0.01054411	23.91	920.16	8.99	214.9509	196
0.068596	0.203121	-2.863891	0.1879119	0.0858626	0.1935899	23.94	921.04	8.7	208.278	197
0.068727	0.206374	-2.847589	-0.1435925	0.02333971	0.1637917	24.12	920.38	8.7	209.844	198
0.036693	0.195118	-2.830386	-0.4793538	-0.1056969	0.2300394	24.26	920.45	8.65	209.849	199
-0.02344	0.19255	-2.807382	-0.5389501	0.02227549	0.3034705	24.3	920.84	8.52	207.036	201
-0.08007	0.189763	-2.772026	-0.5511886	-0.03944924	0.3282136	24.43	920.63	8.52	208.1436	202
-0.12645	0.178174	-2.745524	-0.3420695	-0.1397519	0.247599	24.62	920.59	8.38	206.3156	202
-0.16021	0.174736	-2.749807	-0.2287301	0.1068809	-0.08363932	24.68	920.38	8.38	206.8184	200
-0.2068	0.188454	-2.773054	-0.5011703	0.1616882	-0.05756595	24.78	921.14	8.26	204.6828	200
-0.25917	0.195905	-2.785155	-0.2383081	0.015092	-0.004887076	24.94	920.27	8.349999	208.2489751	200
-0.24288	0.18078	-2.785781	0.3946365	-0.1293758	-0.01286872	25.02	921.2	8.349999	208.916975	198
-0.1726	0.157122	-2.802782	0.5816731	-0.1291097	-0.1679787	25.2	920.26	8.16	205.632	196

-0.14364	0.143987	-2.842673	0.115811	0.08027545	-0.2970153	25.35	921.09	8.16	206.856	196
-0.12454	0.164916	-2.86044	0.2727833	0.2580001	0.1084523	25.38	921.42	8	203.04	197
-0.0581	0.189549	-2.846739	0.7139024	0.1036883	0.2417458	25.5	921.5	7.92	201.96	197
0.032258	0.183845	-2.836918	0.639141	-0.1166052	0.02836978	25.65	920.15	7.92	203.148	195
0.067325	0.156601	-2.85638	-0.005510043	-0.2669261	-0.1025292	25.73	921.35	7.81	200.9513	194
0.029264	0.131837	-2.887436	-0.3471245	-0.1913666	-0.1405751	25.86	920.74	7.81	201.9666	194